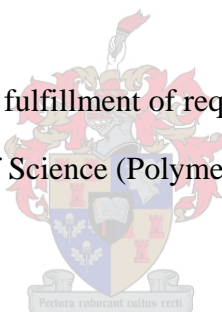# Co-crystallization in polyolefin blends studied by various crystallization analysis techniques

By

Muhamed Sweed

Thesis presented in partial fulfillment of requirements for the degree of

Master of Science (Polymer Science)

at the

University of Stellenbosch

Study Leader: **Stellenbosch**
Dr.P.E.mallon   April 2006

DECLARTION

I, the undersigned hereby declare that the work contained in this thesis is my own original work and has not previously, in its entirety or in part, been submitted at any university for a degree

Opsomming

In die proses van ko-kristallisasie kristalliseer polimeerkettings met verskillende kristalliseerbaarhede by dieselfde temperatuur. Ko-kristallisasie kom dikwels voor in mengsels van verskillende tipes poli-etileen. Daar word aanvaar dat ko-kristallisasie 'n gevolg is daarvan dat die termodinamies mengbare dele van twee komponente in die mengsel vergelykbare kristallisasietempos het.

Hiedie studie ondersoek die verskynsel van ko-kristallisasie in poli-etileenmengsels en die verandering in die ko-kristallisasiegebied met verandering in kristalisasietoestande.

Gedurende hierdie studie is van drie verskillende kristallasie-analisetegnieke gebruik gemaak. Preparatiewe temperatuurstygingseluering-fraksionering (prep-TREF) is gebruik om die polimere en mengsels te skei (fraksioneer). Elkeen van die prep-TREF fraksies is bestudeer m.b.v. differensieëlskandeerkaloriemetrie (DSC) en diekristallisasie-analise-fraksioneringstegniek (CRYSTAF) om te bepaal of die afsonderlike fraksies beide komponente bevat. Daar is bewys dat die verskil in die kristallisasie-fraksionerings-meganismes tussen TREF, CRYSTAF en DSC gebruik kan word om die ko-kristallisasie-effekte in polietileenmengsels te bestudeer.

Resultate het getoon dat deur die verhittings- en afkoelprofiele in DSC en CRYSTAF te verander kan die ko-kristalisasiefraksies óf as enkel fraksies óf as twee afsonderlike fraksies voorkom. Daar is verder beskryf hoe die ko-kristallisasiearea geillustreer kan word deur van 'n unieke 3-dimensionele diagram gebruik te maak. Hier word data van die prep-TREF skeidings, die DSC en CRYSTAF saam gebruik om 'n 'kristallisasiekaart' van die mengsel op te stel. Hierdie grafieke gee 'n visuele voorstelling van enige potensiële ko-kristalisasiegebiede in die mengsels, asook hoe die kristalisasiekondisies die kristalliniteit van die mengsel beinvloed.

Abstract

Co-crystallization is the phenomenon by which chains of different crystallizabilities crystallize at the same temperature. Co-crystallization is frequently observed in the blends of different types of polyethylene. It is believed that co-crystallization can occur due to the thermodynamically miscible parts of two components in the blends having similar crystallization rate.

The study focused on the phenomenon of co-crystallization in polyethylene blends and how by varying the crystallization conditions the co-crystallization region will change.

Three techniques have been used in this study. TREF was used to fractionate the polymers and blends. Each of the TREF fractions was studied using both DSC and CRYSTAF to determine whether the fraction contained both types of materials. It is shown that the difference in the crystallization fractionation mechanisms between TREF, CRYSTAF and DSC can be utilize to study co-crystallization effects in polyethylene blends.

Results also shows that by varying the heating and cooling rate profiles in DSC and CRYSTAF the co-crystallization fractions will appeared as a single fraction or as two separate fractions. Further, it was demonstrated how the co-crystallization area could be illustrated using a unique 3-dimensional plot where the data from the prep-TREF fractionation, and the DSC and CRYSTAF, were combined to give the "crystallization map" of the blend. These plots give a quiche visual illustration of any co-crystallization regions in the blends as well as how much the crystallization conditions effect the blend crystallization

This thesis is dedicated to my mother and father, for their unwavering confidence in me over the years, to my wife for her support, and to my family

Acknowledgments

I would like to extend my heartfelt thanks to the following people and companies for their help in making this project possible:

Chapter 1: General introduction and objectives

Chapter 2:   Historical and theoretical background

Chapter 3: Experimental

List of Abbreviations

BPE	branch polyethylene
CCD	chemical composition distribution
CRYSTAF	crystallization analysis fractionation
DSC	differential scanning calorimetry
2-D	two dimensional
3-D	three dimensional
EPDM	ethylene-propylene-diene monomer
EVA	ethylene–vinyl–acetate
FTIR	fourier transform infrared spectroscopy
FWHM	full width at half maximum
ΔG	Gibbs free energy change
GP	gutta percha
GPC	gel permeation chromatography
ΔH	enthalpy change
HDPE	high density polyethylene
HIPS	high-impact polystyrenes
IR	infrared
LPE	linear polyethylene
LCB	long-chain branching

LDPE	low density polyethylene
LLDPE	linear low density polyethylene
LMWPE	low molecular weight polyethylene
NC	nitrocellulose
NMR	nuclear magnetic resonance spectra
NR	natural rubber
PE	polyethylene
PC	polycarbonate
Plastomer	Plastomer – Dow PL1881
PMMA	polymethyl methacrylate
PP	Polypropylene
ΔS	entropy change
SBR	styrene-butadiene rubber
SCB	sort-chain branching
SCBC	sort-chain branching content
SCBD	sort-chain branching distribution
SEC	Size exclusion chromatography
TEM	transmission electron microscopy
ΔT	temperature range
T_c	crystallization temperature
$T_{c\ (CRYSTAF)}$	CRYSTAF crystallization temperature at peak maximum

$T_{c\ (TREF)}$	TREF crystallization temperature at peak maximum
TCB	trichlorobenzene
T_m	melting temperature
TREF	temperature rising elution fractionation
UHMWPE	ultra-high molecular weight polyethylene
Unfr	unfractionated
VLDPE	very low density polyethylene
W_i	weight fraction
$W_i\%$	weight fraction percentage
$\Sigma W_i\%$	sum of weight fraction percentage
ZN	Ziegler Natta catalysts

List of Tables

Chapter 2

List of Appendices

Appendix B

Appendix C

Appendix D

Appendix E

CHAPTER 1

General introduction and objectives

1.1 Introduction

Blending of two or more different polymers is often used to develop new polymeric materials, which allows the combination of desirable properties of different polymers with advantages over those of other polymeric materials. Among those systems, blending an amorphous polymer with a crystalline polymer is a convenient way of improving the impact strength, toughness, ductility and other physical properties.

The properties of polymer blends (such as mechanical strength, surface bonding, and resistance) are a strong function of the blend morphology. This morphology and the associated phase behavior strongly depend on the co-crystallization between the components of the blend. Thus, a fundamental understanding of the co-crystallization between the components in the blend is crucial for end applications.

Blending of different branch contents of polyethylene such as HDPE, LLDPE and LDPE allows for the production of a broader range of materials with a variety of different properties.

Considering that they all are derived from the ethylene monomer though different polymerization techniques and/or incorporating a small amount of comonomer, namely, octene and hexane (in this study is octane) and that the resulting polymers are almost structurally similar, it is difficult to understand their causes of incompatibility. Incompatibility arising out of the amorphous phase sounds unrealistic because of the looseness of its construction, and it can accommodate entanglements, chain ends, and pendent groups. In the absence of any major compulsive force among chain segments in the amorphous phase, the compatibility among polyethylenes may be viewed as the extent of accommodativeness of their chain segments in the crystalline phase. As the crystalline phase is considered to be very ordered and selective in accommodating linear

chain segments, a slightest variation in chemical structure of the polyethylene segments partaking in crystallization is rejected by the crystalline phase and results in the formation of individual crystalline phase and/or segregation to its constituents. When the polyethylene chain sequences of both the constituents undergo crystallization in a single crystalline entity, co-crystallization results [1]. Furthermore, the occurrence of co-crystallization ought to have an effect on the structural conformation of crystallites.

1.2 Objectives

The overall objective of this study was to study co-crystallization in polyolefin blends by using various crystallization analysis techniques, specifically crystallization analysis fractionation (CRYSTAF), temperature rising and elution fractionation (TREF), and differential scanning calorimetry (DSC).

Specific objectives were the following:

1 Select polyolefin blends with which to examine the co-crystallization effect.
2 Use various crystallization analysis techniques to examine co-crystallization.
3 Investigate factors that influence co-crystallization, such as cooling rate and profile.
4 Consider different crystallization mechanisms and how this difference can be utilized to study potential co-crystallization.
5 Use preparative fractionation to isolate potential co-crystallization fractions.
6 Determine the effects of variables on the analyses.
7 To investigate three dimensional plots as a way to present analytical data.

1.3   Outline of the thesis

This manuscript comprises five chapters.

Chapter 1: Introduction and objectives

Chapter 2: Historical and theoretical background

Chapter 3: Experimental

Chapter 4: Results and discussion

Chapter 5: Conclusions

1.4   References

1.   A. Gupta, S. Rana, and B. Deopura. Journal of Applied Polymer Science, 1992, 42,719 - 720.

Chapter 2

Historical and theoretical background

2.1 Polyolefins

2.1.1 Introduction

Polyolefins are the largest class of synthetic polymers. In 2001 about 50 million metric tons of polyolefins were produced worldwide, and this is projected to increase to 90 million metric tons by 2010. These materials have enjoyed such great success because of their combination of useful properties such as light weight, low cost, high chemical resistance, low dielectric constant and losses [1].

Polyolefins have the simplest chemical structure of all polymers, yet they vary due to branch concentration and distribution, which provides a diversity of chain structure, and this is reflected in their morphology and miscibility [2, 3].

In the worldwide production of synthetic materials, polyolefins hold first place (55%), for two reasons: 1) their specific properties (high chemical and mechanical resistance, easy processability, low specific gravity), which are highly recommended for a large range of applications, and 2) the low quantity (about 7-8%) of extracted oil consumed for their manufacture. Therefore the analysis of polyolefins has become increasingly important in polymer science [4].

Over the past two decades the polyolefins fields has seen great growth, particularly in the use of metallocene catalysts, advancing from academic interest to industrial applications.

Polyolefins are often produced and used as blends of several different types. Sometimes these materials are blended in the melt, after polymerization, such as the blends of polypropylene with ethylene-propylene copolymers that are known as thermoplastic olefins. Many polyolefins are blended as they are made in polymerization reactors, because of the presence of multiple catalyst species. A good example of this type of polyolefin is linear low-density polyethylene, which is often a blend of several different ethylene-α-olefin copolymers that differ in ethylene content.

There are several paths that a polyolefin blend can follow when it cooled from the melt. These are shown in Figure 2.1. If the components are immiscible in the melt then the two phases will continue to be immiscible on cooling and so they will crystallize independently. This is because polyolefins are expected to exhibit upper critical solution behaviour. If the compounds are miscible in the melt then they may become immiscible on cooling and again crystallize independently. Alternatively, they may continue to be miscible, but crystallize independently, or they may co-crystallize. Because of the dispersity of the branches, mixtures of the above behaviours may occur. When a polyolefin blend forms two phases then each phase will consist of a mixture of each component, according to the phase rule. Therefore, even if the blend crystallizes as two phases the morphology of each phase will be different to that of the respective polymers in the blend [1].
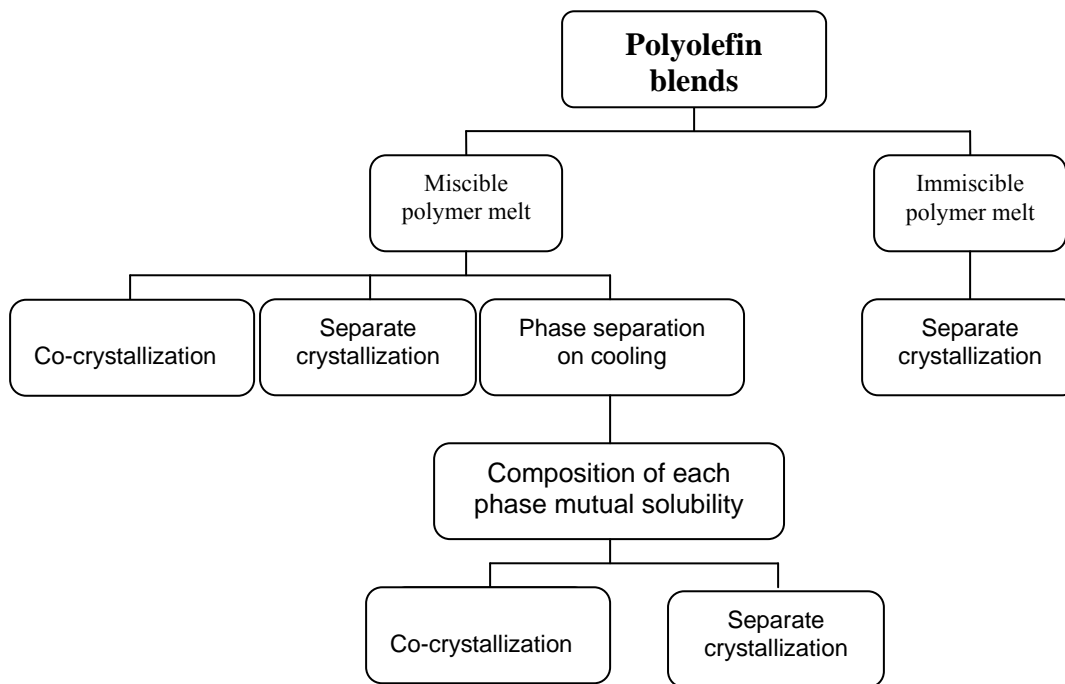
Figure 2.1 Time-temperature miscibility and morphology of polyolefin blends.

2.1.2 Commercial importance

Polyolefin blends, which can economically combine the characteristics of the individual polymers, have found applications in almost all areas of polymer uses. Major commercial blends of polyolefins include the blends of low molecular weight polyethylene (LMWPE) with ultra-

high molecular weight polyethylene (UHMWPE) to improve processability, and blends of LLDPE with LDPE to produce thinner-gage blown films with improved tensile and tear strength for packaging. Impact modification of polypropylene (PP), achieved by blending it with ethylene-propylene rubber (EPR), makes it possible to develop inexpensive bumpers for automobiles, automotive trim, and appliance parts. The addition of an ethylene copolymer to polyethylene has been used to improve toughness, impact resistance, and chemical resistance in films and other plastic forms.

Sometimes thermoplastic elastomers are improved by adding polyethylene for thermoplastic processesability and strength. The addition of ethylene-propylene-diene monomer (EPDM) to PE produces an increase in modulus. Blends of styrene-ethylene-styrene block copolymer with PE have improved flexibility and impact strength.

2.2 Polyethylene

Polyethylene is synthesized from the polymerization of ethylene monomers and has a very simple chemical structure, as shown in Figure 2.2.
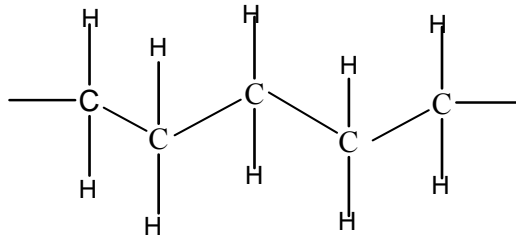
Figure 2.2 Structure of polyethylene.

The basic structure of polyethylene is the chain $-(CH_2-CH_2)n-$, which has no subsistent groups, i.e. branches on the backbone. Polyethylene is the most widely used polymer nowadays. It is distinguished by some peculiarities that make it a unique polymer.

Polyethylene was first prepared in low molecular weight form from diazomethane by von Pechmann in 1894 [5]. In the late 1930s free radical processes operating at high pressures and high temperatures were used to produce branched ethylene polymers, which are now known as

LDPE [6-8]. By the early 1940s the polymers had soon found use as highly efficient electrical insulating materials and played an important role in establishing reliable and practical airborne radar systems [9].

PE has an extremely high crystallization rate, arising from its high chain flexibility, mostly from a perfect chain structure. This is particularly true in the case of HDPE. For this reason PE is not commonly available in a completely amorphous state, and therefore many characteristics of amorphous PE are derived via extrapolation of semi-crystalline samples.

Polyethylene plastics generally have the advantageous properties of toughness, high tensile strength, and good barrier properties to moisture. A particularly important property of PE plastics, which is due to their relatively low melting point ranges, is the ease with which PE packaging can be heat-sealed.

In commercial PE, n (the repeat unit) may range from about 400 to above 50,000. Alkyl substituents, called short-chain branches, are usually present on the chain backbones [10].

Polyethylene is prepared by polymerization of ethene, by radical polymerization, anionic polymerization, or cationic polymerization. This is because ethene does not have any substituent groups that influence the stability of the propagation head of the polymer. Each of these methods results in a different type of polyethylene (LDPE, or HDPE, or LLDPE) [6].

$$n \ H_2C{=}CH_2 \longrightarrow \left[-\underset{H_2}{C}-\underset{H_2}{C}- \right]_n$$

PE is produced in different forms, each of which has different properties that result from variations in structure. HDPE is mainly linear and it may contain very little branching, with density in the range 0.940 to 0.965 g/cm^3 and a high crystallinty of 70 %. LDPE contains short-chain branches (SCB) as well as long-chain branches (LCB), with density in the range 0.910 to 0.925 g/cm^3.

Short chains are formed by what is called a 'backbiting" reaction, which tends to give branches only four carbon units long. This happens when a growing polymer chain reacts with itself,

pulling a hydrogen atom off the backbone chain and generating a radical site, which can then add more monomer units. This is illustrated below [10].
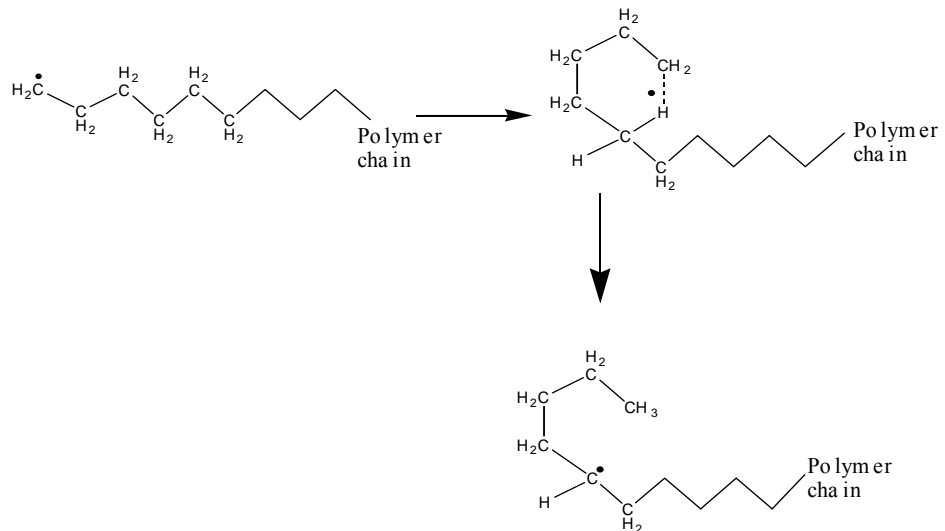
Figure 2.3 The mechanism for short-chain branching in polyethylene (the 'backbiting' reaction).

LLDPE is produced by copolymerizing ethylene with α-olefins, such as 1-butene, 1-hexene or l-octene. It has a wide range of branch contents, depending on the catalyst used and the concentration of added comonomer. The density of conventional LLDPE is in the range 0.900 to 0.935 g/cm^3 [11].

The structure of Low Density Polyethylene (LDPE).

The structure of High Density Polyethylene (HDPE).

The structure of Liner Low Density Polyethylene (LLDPE).
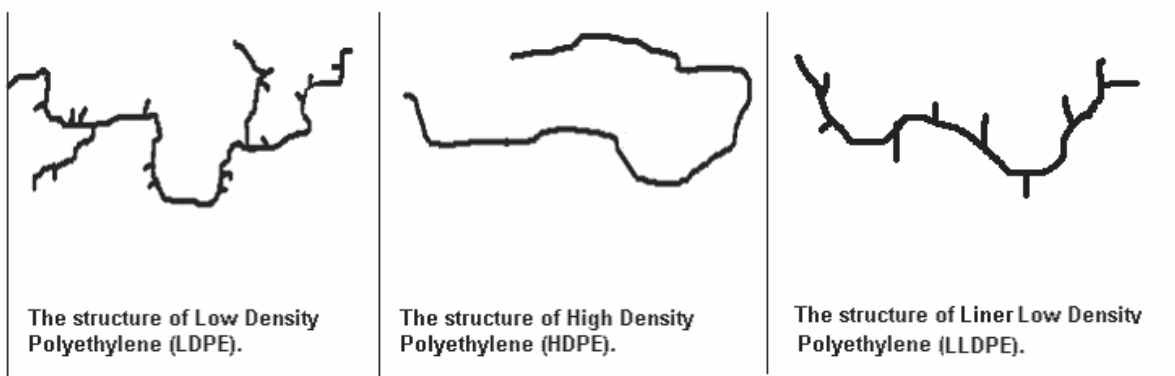
Figure 2.4 Structure of LDPE, HDPE and LLDPE.

2.2.1 Low-density polyethylene

Low-density polyethylene is an economical option for many applications requiring low-temperature flexibility, toughness and durability. LDPE has gained wide acceptance in transporting air, water and chemicals. LDPE has a polymethylene-like structure which contains alkyl substituents, or short-chain branches, on the chain backbone [10].

LDPE is manufactured from ethylene monomer using high pressures, ranging from 100 to 135 MPa, at temperatures in the range 150°C to 300°C, in the presence of a small amount of oxygen or an organic peroxide [6]. Both stirred autoclave and tubular reactor processes are used. The density/crystallinity of the resulting polymer is determined by the reaction temperature (the lower the reaction temperature, the higher the density). Other important polymer characteristics, such as molecular weight and molecular weight distribution, are controlled by the pressure used in the process and by the concentration of chain transfer agents. Molecular weights are typically in the range 10,000 to 50,000.

2.2.2 Linear low-density polyethylene

Linear low-density polyethylene is substantially a linear polymer, as the name implies, but it has side chains, the lengths of which depend on the comonomer used in the manufacture [12]. The density is controlled by the amount and type of comonomer, which typically ranges from 2.5 to 3.5 mole %.

LLDPE is usually manufactured in either gas-phase or slurry-reactor processes by co-polymerizing ethylene with one or more of the α-olefin monomers under low pressure conditions, typically 2 to 7.5 MPa, and at temperatures of up to 250°C in the presence of a catalyst, such as the Ziegler Natta (ZN) type. The type of comonomer (1-butene, 1-hexene or 1-octene) also influences other characteristics of the polymer produced. Molecular weights range from 50,000 to 200,000.

2.2.3 High-density polyethylene

High-density polyethylene has also been claimed to be an accidental discovery, made at Phillips Petroleum in the early 1950s [3, 13]. Phillips researchers found that a polyethylene polymer with

a high degree of crystallinity and a relatively high density was produced under low pressures, ranging from 3 to 4 MPa, and at temperatures ranging from 70°C to 100°C, with catalysts containing chromium oxide supported on silica (Phillips catalyst) [10, 14]. In 1953 Ziegler produced polyethylene polymers with similar crystallinity and density with a catalyst system based on titanium halides and alkylaluminium compounds (Ziegler catalysts), and under even milder conditions of atmospheric pressure and at temperatures ranging from 50°C to 100°C [13]. The polymers produced with both the Phillips and the Ziegler catalysts were substantially linear, with only short side chains, mainly ethyl. They were the forerunners of the high-density range of polymers. The HDPE polymers manufactured today are also substantially linear polymers.

HDPE is manufactured as the homopolymer using a reaction processes, catalyst systems, and pressure and temperature conditions similar to those used for the manufacture of linear low-density polyethylene [15]. Small quantities of comonomer can be used to produce polymers at the lower end of the density range. The type of catalyst used determines the molecular weight distribution, whereas the molecular weight is controlled by the proportion of hydrogen included. Molecular weights of HDPE are as high as 250,000.

LLDPE and HDPE polymers can be manufactured with metallocene catalysts, which produce polymers with uniform structures, both in terms of molecular weight distribution and comonomer incorporation.

2.3 Metallocene catalysts and polyolefins

Metallocene catalyst systems were discovered by Kaminsky and Sinn in 1980 [16]. They are generally viewed as the next generation of catalysts for olefin polymerization. Several different transition metals have been used in the preparation of metallocene catalysts, including zirconium (i.e. zirconocene), titanium (i.e. titanocene), and hafnium (i.e. hafnocene). The order of metallocene activity is generally Zr>Hf>Ti. Metallocenes can be used to obtain extremely uniform polymers with narrow molecular-weight distributions.

Ethylene was the first olefin to be polymerized using metallocene catalysts [16]. Metallocenes can also be used to copolymerize ethylene with propylene, butene, hexene and octene. Compared with ZN catalysts, metallocenes are more expensive but can be more productive in terms of the

quantity of polymer produced per quantity of catalyst. Figure 2.5 shows a typical metallocene catalysts for olefin polymerization.
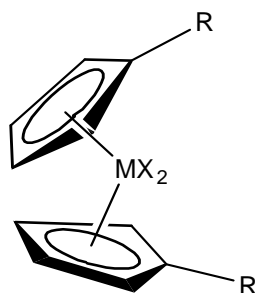
Figure 2.5 Typical metallocene catalyst for olefin polymerization (e.g. LLDPE, HDPE, α - PP, and ethylene-cycloalkene copolymers).

Metallocenes consist of a bent Ti, Zr or Hf complex with two cyclopentadienyl ligands and two halide or alkyl ligands. The metallocene is often combined with a cocatalyst. The metallocenes consist of a single active site for polymerisation, which offers some distinct advantages over the multi-site Ziegler catalysts [17]. The most important feature of the metallocene catalysts is thus the control of polymer structure and properties that can be achieved by variation of catalyst structure, allowing the production of new polymers, otherwise not possible using Ziegler catalysts. Metallocene technology is currently very important for industry; and new polyolefins with controlled molar mass distribution, stereostructure and comonomer distribution can be prepared [17].

The catalyst plays a very big role in the case of PE [18]. It has long been recognized that one of the major differences between LLDPE prepared by metallocene catalysts and ZN catalysts is the distribution of the comonomers along the backbone of the molecule [19]. In particular, LLDPE prepared by Ziegler-Natta catalysts has a more uneven comonomer distribution. However, LLDPE synthesized by metallocene catalysts is claimed to possess a relatively uniform distribution. It is generally believed that this difference in comonomer distribution is mainly attributed to the difference in the number of active sites available in the two catalysts and manifests itself in the mechanical properties of the polymers as well as their melt miscibility with HDPE [20].

PE is available in different grades and can be used in different applications, either as pure resin or blended with other polymers. The main distinguishing feature of all of these commercial grades is the type of comonomer, branch content, and composition distribution. The details of branching strongly influence the processing and the properties of the final product. Also, the branching can affect molecular conformations and dimensions, which again affect solution and melt properties of LLDPE.

2.4 Polymer blends

2.4.1 History

The individual members of the polyolefin family offer a fairly broad spectrum of structures, properties, and applications. This spectrum can however be broadened even further by blending individual polyolefins with other polymers [21]. When two or more polymers are intimately mixed into a single continuous solid product, the composition is referred to as a polymer blend.

Polyolefin blends have been studied extensively, with a view to improve the properties and processability of the polymers involved. They are also of interest in terms of recycling plastic waste where polymers of different types are mixed and there is a need to produce materials with acceptable properties [22]. The advantages of the blends include, for example, improvements in impact strength, optical properties, low-temperature impact strength, rheological properties and overall mechanical behaviour.

Blending is a natural way to widen the range of polymer properties. This has been well illustrated by the history of polymer blends. In 1846 when only natural rubber (NR) and gutta percha (GP) were available, these were blended [23, 24]. Once nitrocellulose (NC) was invented, its blend with NR was patented in 1865, three years before commercialization of NC.

In the 1960s the principal reason for blending was modification of a specific resin for a specific type of behaviour, in most cases the improvement of impact strength. During the next decade blending was used for economic reasons; expensive engineering resins were diluted with commodity ones. During the 1980s the processability of high-temperature specialty resins was improved by blending. Currently, blending is used to prepare materials with specific properties

for envisaged applications [25]. Table 2.1 shows the improvements achieved in the field of commercial blends over time.

Table 2.1 Brief overview of historical developments of polymer blends

Year	Event	Reference
1911	**First patent on dissolution of styrene in rubber, then polymerization into SBR.**	**[24]**
1951	**Discovery of crystalline polypropylene (i-PP), followed by work on low temperature impact improvements by blending with PE or co-polymerizing with ethylene.**	**[25]**
1958	**LDPE were blended with LLDPE for improved stiffness, abrasion resistance and reduced water permeability.**	**[26]**
1962	**Utilizing chemical reactions in the production of high-impact polystyrenes (HIPS)**	**[27]**
1988	**Preparing homogenous blends of polycarbonate (PC) and polymethyl methacrylate (PMMA)**	**[28]**
1991	**Engineering polymers were blended with low-temperature inorganic glass or ceramic glass.**	**[29]**

1997	Detecting co-crystallization in LDPE/HDPE blends using DSC and TREF.	[30]
2003	Study the effects of the cooling rate and co-crystallization on CRYSTAF and TREF for ethylene/1-olefin copolymers	[31]
2005	Nanostructured polymer blends prepared via anionic ring opening polymerizations	[32]

2.4.2 Developing commercial blends

The field of polymer blends, or alloys, has experienced enormous growth in size and sophistication over the past two decades in terms of both the scientific base and technological and commercial development. The properties of polymer blends (such as mechanical strength, surface bonding, and resistance) are a strong function of the blend morphology. This morphology and the associated phase behaviour strongly depend on the miscibility between the components of the blend. Thus, a fundamental understanding of the miscibility of the components in the blend is crucial for end applications.

Among the great variety of polymeric mixtures, much attention has been focused on those involving one crystalline polymer. However, blends involving two crystalline components are more complicated, and provide the opportunity to study how the crystallization of one component affects the crystallization behaviour of the other [33].

The reasons for blending can be separated between those that are related to products, and those related to the producers. The following material-related reasons are often given [24]:

• developing materials with a full set of desired properties

• extending engineering resins performance by diluting them with low-cost polymers

- improving a specific polymer property, e.g. impact strength, rigidity, ductility, barrier properties, abrasion resistance, flammability, gloss, etc.

- adjusting the material performance to fit customer specifications at the lowest possible cost

- recycling industrial and/or municipal plastics waste.

The following advantages of blending technology for the producer have been identified [24]:

- better processability can be achieved, thus improving product uniformity and scrap reduction

- products can be tailored to specific customer needs, thus creating better customer satisfaction

- quick formulation changes can be made, thus plant flexibility and high productivity.

- blending reduces the number of grades that need to be manufactured and stored, thus savings in space and capital investment are achieved

- recyclability of blends is achieved by control of morphology, thus improving the economics

Industrially, the blending process is almost always carried out in the molten state. At equilibrium, the amorphous components of both polymers may exist as a single homogeneous phase that would, in turn, mean that the two polymers are miscible; that is, the two materials are compatible. In most cases, however, the amorphous components of the two polymers will separate into distinct phases consisting primarily of the individual components. Further, if there exists sufficiently long uninterrupted blocks of one repeat unit on both copolymers, then the two blocks can co-crystallize [34].

It is believed that co-crystallization occurs due to the thermodynamically miscible parts of two components in the blends having similar crystallization rates. This means that the miscibility of the components in the melt plays an important role in the co-crystallization phenomenon,

although it is a kinetic process. The miscibility of the blend melt and the crystallization rate strongly depend on the molecular structure of the polymers, such as branch content, molecular shape and molecular weight [35].

2.4.3 Reasons for blending

The main reason for blending, compounding and reinforcing is economy. If a material can be generated at a lower cost with properties meeting specifications, the manufacturer should use it to remain competitive. The blending strategy has the anticipated outcome of producing a material that has better balance of properties than either of the respective blend components or perhaps, through synergistic effects, a material with some novel properties. Tailoring properties for familiar and new applications through polymer blending is usually quicker and less capital intensive than producing a totally new polymer [13].

As indicated earlier, the major advantages of blending are to increase the following properties of polymers: impact resistance, modulus, heat deflection temperature, flammablily, solvent resistance, elongation, glass-transition temperature, dimensional stability, processability and thermal stability.

2.4.4 Miscibility of blends

The mixing of structurally different polymers is an easy and economical way to obtain new polymeric materials with a desirable combination of properties. It is well known that most polymer blends are immiscible. This is due to the small contribution of combinatorial entropy in mixing high molecular mass chains as well as to the endothermic heat of their mixing. The term "miscibility" was chosen to describe polymer-polymer mixtures having behaviour similar to that exhibited by a single-phase system. However, it does not imply ideal molecular mixing but suggests that the level of molecular mixing is adequate to yield macroscopic properties expected of a single-phase material [13].

Miscibility has been shown to be achieved if there is a favourable specific attractive intermolecular interaction, such as hydrogen bonding, between the two components of a binary polymer blend [36].

Blend miscibility is of major importance since it affects the physical properties of the blend and consequently determines the field of its applications and uses.

The kinds of factors that affect polymer-polymer miscibility are as follows: (i) entropy of mixing, (ii) dispersion forces, (iii) specific interactions (Lewis acid-base or electrostatic), and (iv) free-volume differences.

Miscibility of the components in a melt plays an important role in the co-crystallization phenomenon, although it is a kinetic process. The miscibility of the blend melt and the crystallization rate strongly depend on the molecular structure of the polymers, such as branch content, molecular shape and molecular weight. Among these factors, the branch content of ethylene copolymers may be the most important one. As a result, when one of the components is composed of a series of fractions with different branch contents, i.e. the intermolecular composition distribution is non-homogeneous, the composition distribution may have a great influence on co-crystallization [35].

2.4.5 Thermodynamic miscibility

For two polymers to be completely miscible down to the molecular level, the mixing must produce a decrease in free energy (ΔG).

According to elementary thermodynamics, the change in free energy of the mixing process is as follows:

$$\Delta G = \Delta H_{mix} - T \Delta S_{mix}$$

and

$$\Delta G = \Delta H - T \Delta S \leq 0$$

where: ΔG is the free energy change for mixing

ΔH is the enthalpy change for mixing

ΔS is the entropy change for mixing.

Enthalpy (ΔH) depends on the attraction between the two polymers and, since unlike molecules usually repel each other, ΔH is generally positive. Entropy (ΔS) results from the randomization that occurs upon mixing. Since large polymer molecules produce very modest randomization upon mixing, this is not enough to overcome the repulsion between unlike molecules ($+\Delta H$). Thus most polymer blends lack thermodynamic microphases [37].

2.5 Polyethylene blends

Polymer blends have attracted considerable interest both in the research community and in industry. Blends of HDPE, LDPE and LLDPE are widely used in industry. However, as mentioned earlier, various PEs exhibit different characteristics and properties. Therefore, different types of PE are often blended together to meet various kinds of requirements of processing and final product properties. For example, LLDPE has better characteristics such as flexibility, resistance so the environment, shear strength, and thermal properties compared to HDPE. However, LLDPE has disadvantages in yield stress, melt strength, and hardness. In order to modify these latter properties, the LLDPE is usually blended in small quantities with HDPE to improve flexibility and reduce extruder backpressure [24]. Thus, miscibility studies of PE blends in the liquid state have both industrial and scientific significance. The polyethylene melt processing industry is concerned about the miscibility of the components because miscibility affects the melt rheology.

2.6 Fractionation and characterization of polyolefins

Crystallization analysis fractionation is a powerful new technique for the analysis of short-chain branching in LLDPE and the analysis of polyolefin blends.

CRYSTAF is an analytical technique for determining the distribution of chain crystallizabilities of semicrystalline polymers [38]. After only approximately a decade since it was developed, CRYSTAF has become one of the most important characterization techniques in polyolefin characterization laboratories because it provides fast and crucial information required for a better understanding of polymerization mechanisms and structure-property relationships. In the polyolefin industry it has been established as a very important tool for product development and product quality monitoring [39].

The distribution of crystallizable fractions of polyolefins is usually measured by either CRYSTAF or TREF. Both techniques are based on the fact that semicrystalline polymers in solution at high temperatures will crystallize and precipitate as the solution temperature is decreased [40]. In the case of LLDPE the chains with fewer comonomer units will precipitate at higher temperatures, whereas the chains with more comonomer units will precipitate at lower temperatures. The main difference between these two techniques is that CRYSTAF monitors the concentration of polymer in solution during the crystallization process, whereas TREF measures the concentration of polymer in solution during the dissolution step that takes place after all the polymer has been crystallized from solution. Consequently, the CRYSTAF analysis time is significantly shorter than that required by TREF [41]. In addition, TREF is generally easier to use for preparative fractionation since the respective fractions to be collected are in solution, whereas in CRYSTAF the fractions to be collected are in the solid state, which requires the solution to be first filtered then recovered.

Fractionation by differential scanning calorimetry (DSC) is based on the same principle of separation as in TREF, but it does not physically separate the fractions. Therefore, thermal fractionation by DSC can separate molecules differing in both intermolecular and intramolecular branching because segments of molecules can be part of different crystals, whereas TREF can only separate molecules differing in intermolecular branching because it is a physical separation technique [42].

2.6.1 Temperature rising elution fractionation (TREF)

2.6.1.1 Historical background

Fractionation of polyethylene according to composition, by using an extraction technique with a single solvent at increasing temperature, was first described by Desreux and Spiegels in 1950 [43]. Shirayama *et al.* [44, 45] first coined the term temperature rising elution fractionation to describe the method used to fractionate LDPE according to the degree of short-chain branching. In the 1970s Wild *et al.* [43] developed the analytical TREF, which soon became established as an analytical technique for polyolefins.

TREF is a separation technique for fractionating crystallizable polymers based on crystallinity. There are two important points that should be remembered with TREF. First, TREF only

fractionates semicrystalline polymers; it is not applicable to amorphous polymers because TREF is mainly sensitive to differences in polymer crystallinity/solubility. Secondly, the TREF technique fractionates polymer chains according to the molecular structure, which affects crystallinty/solubility. Distinct molecular structures of semicrystalline polymers are reflected in their different crystallinities/solubilities, and TREF is sensitive to these differences [46].

The TREF process is a two-step process, comprising precipitation and elution steps. In the first step, polymer chains are crystallized and precipitated from a dilute solution at a constant cooling rate in a column loaded with an inert support. In the second step, a solvent flows through the column while the temperature is increased; this elutes the polymer precipitated in the first step. The concentration of the polymer being eluted at each elution temperature is usually monitored with a mass-sensitive detector [47].

2.6.1.2 Fractionation setup

The experimental setup used for separation by TREF is shown in Figure 2.6. The process of TREF can be divided in to the following two steps:

Step 1. The sample is dissolved in a suitable solvent at high temperature and mixed with an inert support (e.g. sea sand, glass beads, silica gel, etc). The mixture is then slowly cooled to room temperature over about 1-3 days. When the temperature gradually decreases the polymer fractions will precipitate from the solution by deposition of layers of decreasing crystallinity or increasing branch content. This step is usually carried out at very low crystallization rates. A slow cooling rate is essential in this process. At faster cooling rates different types of crystallization of fractions will occur. At slower cooling rates the polymer fractions precipitate in an orderly manner. The slow cooling rate also provides an optimal crystallizabillity separation, which is free from significant influence of molecular weight.

Step 2. A second temperature cycle is required to quantify or collect these fractions. In this step the precipitated polymer is eluted with solvent at increasing temperatures (continuously or stepwise). At lower temperatures the fractions with less crystallinity (outermost layer) dissolve. As the temperature increases so the crystallinity will increase, in other words, there will be a decrease in branch content. These fractions are then collected (in preparative TREF) or analyzed

by a detector. From the separation mechanism of TREF one can see that TREF has two features compared with other fractionation methods.

Firstly, the polymer is pretreated (crystallizing slowly from the solution) and the effect of the previous crystallization history of the polymer on fractionation is eliminated. In other fractionation methods, such as extraction with solvents, badly crystallized samples may be extracted out at a lower temperature than the same well-crystallized sample, thus the supermolecular structure also exerts an effect on the extraction results. Secondly, the polymer fractions have been arranged regularly before fractionation. This reduces the effect of entanglement among polymer chains to a lesser extent and facilitates the following separation [48].
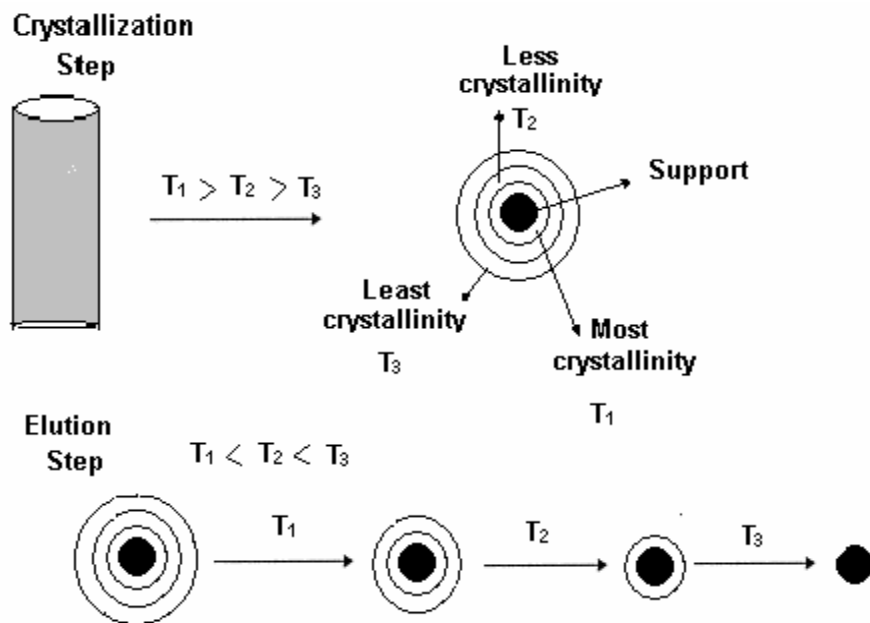
Figure 2.6. Schematic separation mechanism of TREF.

There are two kinds of experimental TREF apparatus: analytical TREF and preparative TREF (prep-TREF).

2.6.2 Preparative and analytical TREF

2.6.2.1 Preparative TREF

Prep-TREF is used to obtain relatively large quantities of polymer fractions. These fractions can be characterized off-line by different analytical methods, such as nuclear magnetic resonance spectroscopy (NMR) and DSC, yielding much information about the microstructure of the fractions. Prep-TREF requires large columns in order to obtain the required large quantities of samples required for analysis [43].

2.6.2.2 Analytical TREF

Automatic analysis of polymer fractions is achieved by coupling TREF with other analysis methods such as size exclusion chromatography (SEC) and infrared spectroscopy (IR). The structure of polymer fractions can then be determined on-line [43]. Chemical composition and stereoregularity distribution can be obtained from analytical TREF elution-temperature profiles by using calibration curves. Most calibration curves for comonomer content in LLDPE are nearly linear, but it is still not possible to obtain a universal calibration curve for all polyalkene types. Short-chain branches, chain crystallinity, comonomer sequence length and stereoregularity are factors that will have the effect on calibration curve, so it is necessary that the standards used for calibration have a similar microstructure to those of the samples being analyzed. The standards are obtained by prep-TREF and analyzed off-line to study short-chain branches or stereoregularity. Standards obtained at narrow elution temperature intervals with prep-TREF generally elute with broader profiles than in analytical TREF. The analytical TREF peak temperature of each standard is used to determine the elution temperature for creating the calibration curve [43].

2.6.2.3 Comparison of preparative and analytical TREF

See Table 2.2

Table 2.2 Comparison of preparative and analytical TREF

Preparative TREF (prep-TREF)	Analytical TREF (A-TREF)
- The different fractions are collected at different temperatures in a stepwise manner.	- Fractions are collected continually, by gradually increasing the elution temperature.
- Information on macromolecular structure is obtained off-line by other analytical methods [49].	- Information about macrostructures is obtained on-line.
- Large columns and large sample sizes are required.	- Smaller columns and smaller sample sizes are required.
- More time is required to weigh and dry the samples before analysis.	- It is faster than prep-TREF, but provides less information about the polymer.

2.6.3 Effects of various experimental conditions on the TREF process

2.6.3.1 Solvent

The incorporation of an IR detector in analytical TREF equipment leads to the requirement for special solvents which are transparent in the IR region at the measuring wavelength (around 3.5 μm) [50]. An important factor in choosing a solvent is the temperature range of the TREF operation. TREF equipment used for crystalline polymers must often operate at sub-ambient temperatures, hence a solvent that neither solidifies nor boils in the range of elution temperatures is required. The common solvents used in TREF are trichlorobenzene (TCB), o-dichlorobenzene (ODCB), xylene (X) and α-chloronaphtalene (ACNT) [51]. It does not appear to be too important which solvent is used in the separation but it will shift the elution temperature, depending on solvent power; the better the solvent the lower the elution temperature [48].

The solvent flow rate has an effect on the TREF profile; the TREF profile becomes broader when the solvent flow rate is low. This may be because the solvent will spend more time in the column, and so broader ranges of polymer molecules are eluted per pass of solvent at a lower flow rate [52].

2.6.3.2 Column

Columns commonly used in analytical TREF are 6-9 mm wide and 10-15 cm long. The cooling step usually takes place outside the column, without or with a support, and this is called 'off-column crystallization' [47]. At the end of the cooling step the mixture of polymer and support is injected to the column. The advantage of using off-column crystallization is to decrease any influence of packing material in the cooling or elution step. On the other hand, in 'on-column crystallization' the cooling stage takes place inside the column in the presence of a support. In the elution step the column is kept in a programmable oven, or may be kept in an oil bath. An air oven is preferable because it is then easier to change the column. Also, the temperature of an air oven system can reach room temperature much faster than an oil bath system can [43]. In prep-TREF a large column may be necessary in order to collect the large amount of fractionations required for analysis by off-line analytical techniques, such as ^{13}C NMR, FTIR spectroscopy, DSC and GPC, which give extensive information about the polymer fractionation [43].

2.6.3.3 Sample size

The samples size required depends on the type of separation method to be used. In prep- TREF a sample size of between 2 and 200 mg is required, however in analytical TREF the sample size is between 0,02 and 10 grams. In general, the lower the concentration (sample size) the better, in order to decrease co-crystallization and the entanglement effect [43].

2.6.3.4 Cooling rate of crystallization

The cooling step in the TREF processes is the key to the entire separation according to the crystallizability, and is usually carried out at very low cooling rates (about 1.5 $^{\circ}$C/h). Those rates are necessary to avoid many effects that will otherwise happen such as co-crystallization and molecular weight influences [53]. If the cooling process is too fast then the species with different molecular structures will not have enough time to separate and fractionation will be inefficient.

When the crystallization step is carried out in a stirred vessel in the absence of a support, the stirring speed should be keep low because a high stirring speed leads to chain scission. The latter can be important in the case of the determination of the molecular weight for prep-TREF fractions. The probability of polymer oxidation in this step can be avoided by carrying out the crystallization step under an inert atmosphere or by adding an antioxidant [43].

2.6.4 CRYSTAF

CRYSTAF is a relatively new technique for the analysis of the composition of polyolefin blends. After approximately only a decade since it was developed, CRYSTAF has become one of the most important characterization techniques in polyolefin characterization laboratories because it provides fast and crucial information required for the proper understanding of polymerization mechanisms and structure–property relationships [53, 54]. Figure 2.5 illustrates the CRYSTAF technique.
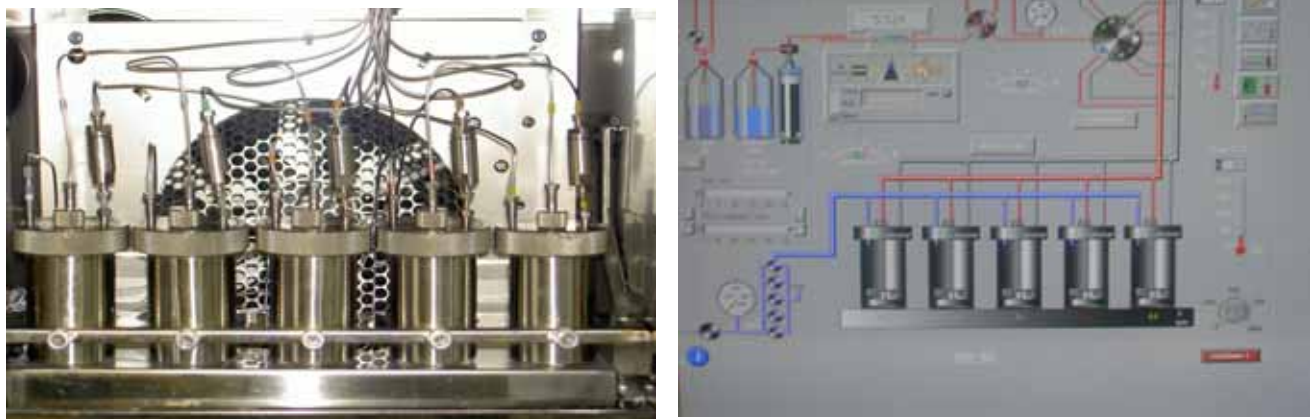
Figure 2.5 Schematic representation of the CRYSTAF setup.

CRYSTAF fractionates blend components of different crystallizabilities by slow cooling of a polymer solution. During the crystallization step the concentration of the polymer solution is monitored as a function of temperature. Different from DSC, blends of polyolefins are separated into the components and quantitative information can be obtained directly from the crystallization curves. Even very low quantities of one component in polyolefin blends can be quantified with good accuracy.

CRYSTAF was developed as an alternative to TREF. The two techniques are based on similar fractionation mechanisms and provide comparable results, but TREF operation is more time consuming because it involves two fractionation steps: crystallization and elution, whereas CRYSTAF requires only a single crystallization step [55].

Deviations from the predicted profile are a measure of the extent of co-crystallization taking place during the analysis.

When the blend comprises polymers with very different crystallizabilities, co-crystallization is minimal and does not have a significant effect on CRYSTAF profiles. However, co-crystallization can be significant when the components of the blend have similar crystallizabilities. In this case, co-crystallization can be so dramatic as to distort the shape of the measured CRYSTAF profile for the blend and completely mislead its interpretation.

2.6.3 Thermal analysis by DSC

Thermal analysis refers to a variety of techniques in which a property of a sample is continuously measured as the sample is programmed through a predetermined temperature profile. Among the most common of such techniques is DSC.

In a DSC experiment the difference in energy input to a sample and a reference material is measured while the sample and reference are subjected to a controlled temperature programme. DSC requires two cells equipped with thermocouples, in addition to a programmable furnace, recorder, and gas controller. A thermal analysis curve is interpreted by relating the measured property versus temperature data to chemical and physical events occurring in the sample. It is frequently a qualitative or comparative technique. In DSC the measured energy differential corresponds to the heat content (enthalpy) or the specific heat of the sample [56].

Morgan *et al.* [57] studied blends of linear and branched PE by DSC and TEM, and both were found to be miscible in the melt. They report that the degree of phase separation increased when the cooling rate decreased and that the morphology was different from that of blends that exhibited phase segregation in the melt.

2.7 Crystalline polymer blends

2.7.1 Introduction

Crystallizable polymers are different from normal crystalline solids in that they possess amorphous segments and are therefore generally semi-crystalline. The crystallinity of polymers is governed by the extent of branching (number and type), type and composition of comonomers and by tacticity (isotactic, syndiotactic, atactic) (Figure 2.6). For example, polymers with long-chain branching or atactic polymers are usually non-crystalline. On the other hand, isotactic and syndiotactic polymers or copolymers of ethylene with small amounts of propylene have the ability to crystallize. The degree of crystallinity as well as the T_g determines the brittleness or toughness of the polymer. In addition, the size and the spatial arrangement of the crystallites profoundly influence the physical and mechanical properties of the polymer.
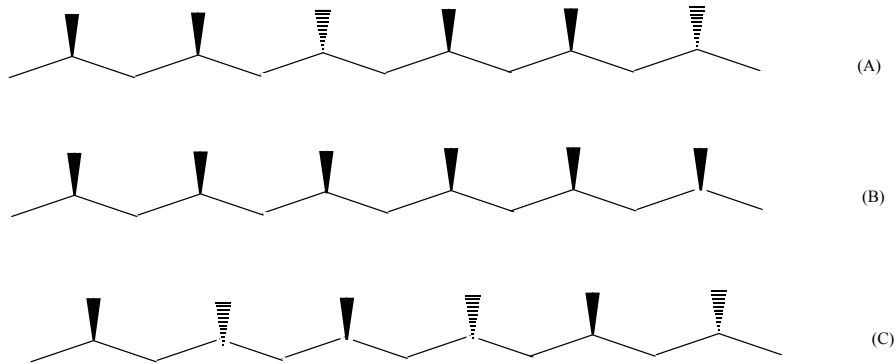
Figure 2.7 Polypropylene with different tacticities: (A) completely amorphous atactic PP, (B) semi-crystalline isotactic PP, (C) semi-crystalline syndiotactic PP.

In fact, roughly half to two thirds of all useful polymers are crystalline or crystallizable. Consequently, mixtures containing crystalline polymers are also commonplace, and growing numbers of commercial materials are also blends of two or more polymers in which at least one of the components is a crystalline polymer.

The drive towards crystallization in polymers can be understood from the thermodynamics of the process. In the molten state the polymer chains are in the random coil configuration and are entangled, which is an entropy driven process. However, when the melt is cooled slowly, the polymer molecules arrange themselves in a regular fashion to attain a state of minimum free

energy. There are a number of factors that influence the rate of crystallization and the resulting degree of crystallinity such as: the rate of cooling from the melt, presence of nucleating agents, molecular weight and molecular weight distribution of the polymer, the amount of branching, etc. If the cooling rate is very fast then the polymer may not crystallize at all, leading to a completely amorphous polymer.

2.7.2 Co-crystallization

Co-crystallization of different polymers in polymer blends is a very rare phenomenon. The necessary conditions for co-crystallization of two different polymers are thought to be: miscibility in the melt, similarity in the molecular structures, similarity in the crystalline lattice structures, and similarity in the crystallization rates. The first and fourth conditions are for kinetic accessibility to form co-crystals, while the second and third conditions are requirements for thermodynamic stability of co-crystals. The thermodynamic requirements are quite tough. Additionally, even if the similarity in the structures ensures the co-crystallization in the equilibrium state, immiscibility and difference in the crystallization rate between the component polymers preclude the crystallization at the same time and at the same place. It is very difficult to acquire polymer pairs fulfilling all the above conditions simultaneously, and that is a possible reason why only a few co-crystal pairs have been reported in the literature [58].

Certain crystallizable polymers are thermodynamically miscible and truly miscible in the melt but, upon cooling, each polymer separates and forms its own unique crystal structure. Rarely do two polymers have such similar isomorphous crystal structures that both can enter the same crystal lattice and co-crystallize, thus forming a single homogeneous solid product. The term co-crystallization as used here refers to crystallization of two crystalline polymers in the same lamellar crystals. For this process to occur, the polymers must exhibit at least a measure of melt miscibility, and their repeat unit chemistry must be similar. As a result of these restrictive criteria, true co-crystallization is a rare phenomenon: co-crystallization has been relatively well established in only a small number of polymer blends. In addition, co-crystal formation is influenced by crystallization kinetics: the more rapid the solidification, the greater the probability of co-crystallization.

Co-crystallization is slightly favoured in mixtures of unfractionated, polydisperse ethylene copolymers. The polydispersity of the linear component, or that of the long-chain branched polyethylene, does not seem to affect the co-crystallization to a measurable degree [59]. The co-crystallization phenomenon is frequently observed in the blends of different types of polyethylene. It is believed that co-crystallization is produced due to the thermodynamically miscible parts of two components in the blends having similar crystallization rates [34].

Polyethylenes may be immiscible in the melt, although they do have similar crystalline structures. The ability to co-crystallize requires first that the polyethylenes in the blend are miscible. They then must have similar segment lengths between branches since branches are excluded from the crystal. In the portions of the branch distribution where they are similar they co-crystallize, while in other portions they crystallize independently. In segments where they do not have similar branch distribution the crystallization of one polyethylene can still be modified by the other. In this way polyethylene blends can modify the transparency, elasticity and gloss of films.

The degree of co-crystallization in polyethylene blends was first studied in the 1960s, using differential thermal analysis techniques [60]. More recent studies have used further techniques: electron microscopy, both small and wide angle X-ray scattering, small angle light scattering, infrared spectroscopy and neutron scattering. In general LPE and BPE have been found to separate upon crystallization, to varying degrees. It is expected that some segregation will occur in all systems at slow enough cooling rates [60].

For the blends of LDPE with HDPE, it is often observed that the linear part of LDPE is incorporated into the crystals of HDPE and co-crystallization occurs in HDPE crystals, leading to the decrease in the melting temperatures of both LDPE and HDPE. However, co-crystallization can also occur in other forms. For example, co-crystals may segregate from both HDPE and LDPE and exist as separate parts (showing a third intermediate melting peak between the melting temperatures of two pure components) [34].

Recently, Wignall *et al.* reported that co-crystals can also occur within the LDPE lamellae by incorporating HDPE molecules [61]. Wild *et al.* first fractionated a LLDPE/LDPE blend and then Kelusky [62] reported the TREF of an ethylene-vinyl-acetate (EVA)/LLDPE blend. Both found

that TREF profiles of the blends and the individual components agreed quite well, indicating that co-crystallization has a negligible effect on the fractionation. As Monrabal [49] points out: co-crystallization can also occur in CRYSTAF at higher concentrations and slow crystallization rates.

Maria *et al.* [59] reported that a key factor that governs the extent of co-crystallization is the closeness of crystallization rates of each component. Increasing the copolymer concentration reduces the crystallization rate of a blend and progressively moves it closer to that of the copolymer. Consequently, under these conditions a greater amount of co-crystallization will be achieved. The amount of co-crystallization is favoured at the lowest isothermal crystallization temperatures and is maximized under quenching conditions.

Chen *et al.* [63] found that the approximate distributions of short-chain branches of polyethylene blends can indeed be obtained if every component in the blend has the same comonomer and the type of comonomer is known. Therefore, thermal fractionation by DSC is a powerful tool to characterize branched polymers and their blends [63].

The amount of SCB seems to be an important factor. This factor, together with the crystallization conditions, more or less determines whether or not and to what extent co-crystallization occurs. Tashiro *et al.* [64, 65] reported co-crystallization for all blend compositions in blends of LPE with a commercial LLDPE, containing 3.4 mol % ethyl SCB. By increasing the content of SCB to 8.2 mol %, separate crystallization of the two components is found to be the dominant mechanism. Alamo *et al.* [66] also support the importance of the branching content.

In some cases complete co-crystallization has been reported in blends of HDPE with LLDPE [64, 67], but it should be noted that LLDPEs are very broad in intermolecular branch distribution and so they will contain both material prone to co-crystallization with the HDPE and material prone to segregation.

2.8 References

1. R. Shanks, J. Li and F. Chen. Journal of Applied Polymer Science, 2000, 18, 263-270.

2. C. Chung and P. Deslauriers. Polymer 2004, 45, 2657-2663.

3. H. Krivheldorf. Handbook of Polymer Synthesis; 1991, Marcel Dekker: New York, 11-15.

4. C. Vasile and R. Seymour. Handbook of Polyolefins; 1998, Marcel Dekker: New York, 126-128.

5. L. Utracki and A. Leszek. Polymer Alloys and Blends:Thermodynamics and Rheology; 1989, Hanser: New York, 5-8.

6. M. Mishra and Y. Yaggi. Handbook of Radical Vinyl Polymerization; 1998, Marcel Dekker: New York, 305-307.

7. O. Olabisi. Handbook of Thermoplastics; 1997, Marcel Dekker: New York, 1-8.

8. J. Brydson. Plastics Materials; 1999, Biddles Ltd: Oxford, 206-208.

9. H. Mark and F. Bikales. Encyclopaedia of Polymer Science and Engineering; 1985, John Wiley & Sons Inc: New Jersey, 384-385.

10. A. Peacock. Handbook of Polyethylene; 2000, Marcel Dekker: New York, 1-50.

11. R. Bradley. Radiation Technology Handbook; 1998, Marcel Dekker: New York, 95-97.

12. G. Olah and A. Molnar. Hydrocarbon Chemistry; 2003, John Wiley & Sons Inc: New Jersey, 771-773.

13. C. Vasile and R. Seymour. Handbook of Polyolefins; 1993, Marcel Dekker: New York, 780-790.

14. Y. Imamoglu. Metathesis Polymerization of Olefins and Polymerization of Alkynes; 1995, Kluwer Academic Publishers: Noweel: 390-398.

15. L. Spain and J. Paauwe. High Pressure Technology; 1977, Marcel Dekker: New York: 102-105.

16. B. Krentsel, V. Kleiner and L. Stotskaya. Polymers and Copolymers of Higher α-Olefins; 1997, Hanser: New York, 11-15.

17. G. Benedikt and B. Goodall. Metallocene Catalyzed Polymers: Materials, Processing and Markets; 1998, William Andrew Inc: USA, 1-10.

18. A. Shenoy and D. Saini. Thermoplastic Melt Rheology and Processing; 1998, Marcel Dekker:New York, 5-10.

19.   E. Karbashewski, L. Kale and A. Rudin. Journal of Applied Polymer Science, 1993, 47, 1143-1154.

20.   E. Karbashewski, A. Rudin and L. Kale. Journal of Applied Polymer Science, 1993, 33, 1370.

21.   A. Quental and M. Felisberti. European Polymer Journal, 2005, 41, p. 894-902.

22.   A. Andrady. Plastics and the Environment; 2003, John Wiley and Sons Inc: New Jersey, 771-773.

23.   P. Hiemenz. Polymer Chemistry; 1984, Marcel Dekker: New York, 2-15.

24.   L. Utracki. Commercial Polymer Blends; 1998, Springer-Verlag: USA, 80-90.

25.   J. Hogan and R. Banks. 1953, US Patent 333,576.

26.   P.Canterino and R. Martinovich. 1963, US Patent 3,086,958.

27.   G. Shonaike and G. Simon. Polymer Blends and Alloys; 1999, Marcel Dekker: New York, 622-623.

28.   T. Kyu and J. Saldanha. Journal of Polymer Science, 1988, 26, 33

29.   W. Bahn and H. Beal, 1991, US Patent 5,043,369.

30.   A. Claudia and I. Harrison. Thermochimica Acta,1998, 313, 37-41.

31.   S. Anantawaraskul and P. Wood-Adams. Polymer Science: Part B: Polymer Physics, 2003, 41, 1762-1778.

32.   T. Alam, J. Otaigbe, D. Rhoades, G. Holland, B. Cherry and P. Kotula. Polymer, 2005, 46, 12468-12479.

33.   L. Chaoxu, K. Qingshan, Z. Jun , Z. Delu , F. Qingrong and X. Yanzhi. Materials Letters, 2004, 58, 3613- 3617.

34.   P. Nutthakan, S. Nathaporn and V. Worakanya. Journal of Applied Polymer Science, 2004, 91, 2216-2222.

35.   X. Junting , X. Xurong , C. Linsen and F. Linxian. Polymer, 2001, 42, 3867-3874.

36.   M. Coleman, P. Painter and J. Graf. Specific Interactions and the Miscibility of Polymer Blends; 1991, Technomic Publishing Company Inc: New Holland, 3-24.

37.   I. Lipatov, A. Nesterov and Y. Lipatov. Thermodynamics of Polymer Blends; 1997, Technomic Publishing Company Inc: Holland, 2-9.

38.   R. Sanderson, H. Pasch, I. Meisel, C. Kniep, S. Spiegel and K. Grieve. Developments in Polymer Synthesis and Characterization; 2001, International Union of Pure and Applied Chemistry Conference, Stellenbosch, 94-96.

39.   P. Soares and S. Anantawaraskul. Journal of Polymer Science: Part B: Polymer Physics, 2005, 43, 1557-1570.

40.   B. Monrabal. Journal of Applied Polymer Science, 1994, 52, 491.

41.   J. Nieto, T. Oswald, G. Blanco and J. Soares. Journal of Polymer Science: Part B: Polymer Physics, 2001, 39, 1616-1628.

42.   F. Chen, R. Shanks and G. Amarasinghe. Polymer International 2004, 53, 1795-1805.

43.   B. Monrabal. Encyclopaedia of Analytical Chemistry; 2000, John Wiley and Sons Inc: Vienna, 8074-8094.

44.   K. Shirayama, T. Okada and S. Kita. Journal of Applied Polymer Science, 1965, 3, 907.

45.   L. Wild. Advances in Polymer Science. Vol. 98. 1990, Springer-Verlag: USA, 1-47.

46.   J. Soares and A. Hamielec. Polymer, 1995, 36, 1639-1654

47.   B.Monrabal, J. Blanco, N. Nieto and J. Soares. Journal of Applied Polymer Science 1999, 37, 89.

48.   J. Xu and L. Feng. European Polymer Journal, 2000, 36, 867-878

49.   C. Gabriela and D. Lilgeb. Polymer 2001, 42, 297-303.

50.   L. Britto, J. Soares and A. Penlidis. Journal of Polymer Science: Part B: Polymer Physics, 1999, 37, 553-560.

51.   R. Petherick and J. Dawkins. Modern Techniques for Polymer Characterisation; 1999, John Wiley and Sons: USA, 13-30.

52.   K. Russell, D. Mcfaddin, B. Hunter and R. Heyding. Polymer Science, 1996, 34, 2443-2447.

53.   J. Tomba, M. Carella and J. Pastor. Journal of Polymer Science: Part B: Polymer Physics, 2005, 43, 3083-3092.

54.   J. Soares. Polymer Reaction Engineering V: Macromolecular Symposia, 2004, 206, 57-58.

55.   L. Britto, J. Soares, A. Penlidos and B. Monrabal, Journal of Polymer Science: Part B: Polymer Physics, 1999, 37, 539-552.

56.   N. Cheremisinoff. Polymer Characterization - Laboratory Techniques and Analysis. 1996, William Andrew Inc: USA, 19-21.

57.   R. Morgan, M. Hill and P. Barham. Polymer, 1999, 40, 337-348.

58.   N. Yoshie, A. Asaka and Y. Inoue. Macromolecules, 2004, 37, 3770-3779.

59.   J. Maria, L. Mandelkern and R. Alamo. Polymer, 1998, 39, 5105-5119.

60.   T. Sato and M. Takahashi. Journal of Applied Polymer Science, 1969, 13, 2665.

61.   G. Wignall, J. Londono, J. Lin, R. Alamo, M. Galantt and L. Mandelkern. Macromolecules, 1995, 28, p. 3156.

62.   C. Kelusky, T. Elston and R. Murray. Polymer Engineering, 1987, 27, p. 1562.

63.   F. Chen, R. Shanks and G. Amarasinghe. Polymer, 2001, 42 p. 4579-4587.

64.   K.Tashiro, R. Stein and S.Hsu. Macromolecules, 1992, 25, p. 1809-1811.

65.   K. Tashiro, K. Imanishi, Y. Izumi, M. Kobayashi, M. Satoh and R. Stein. Macromolecules, 1995, 28, 8477.

66.   R. Alamo, R. Glaser and L. Mandelkern. Journal of Applied Polymer Science, 1988, 26, 2169.

67.   S. Hu, T. Kyu and R. Stein. Journal of Applied Polymer Science, 1987, 25, 71-73.

Chapter 3

Experimental

3.1 Introduction

This chapter describes all the materials, the instrumentation and parameter settings used in this study. Detailed information will be given on the specifications of each polymer used. In addition, information on the working profiles of certain techniques is given since they are not standard profiles used in routine analyses.

3.2 Materials

3.2.1 HDPE and LDPE and plastomers

The LDPE that was used in this study was a Sasol polymer (XHF 77/50), prepared in an autoclave reactor using free radical polymerization. This LDPE had a melt flow index (MFI) of 1 g/10 min and a density of 0.922 g/cm^3. The commercial product contains an added anti-oxidant medium slip and anti-block agent. It is mainly used in the film-blowing industry.

The plastomer that was used was from the Affinity range of DOW Chemicals. Plastomer (PL1881) had a MFI of 1 g/10 min and a density of 0.904 g/cm^3. The plastomer consisted of ethylene, with octene as comonomer. The percentage comonomer content was 9.4 %.

The HDPE that was used was BP Solvay polyethylene, it had a MFI 0.3 g/10 min and a density 0.959 g/cm^3. Table 3.1 shows the physical properties of the plastomer, LDPE and HDPE.

3.2.1 Solvents

Xylene (Aldrich, 99% purity) was used as the solvent in all TREF reaction procedures. It was recycled (distillation) and re-used.

3.2.3 Stabilizers

Irganox 1010 and Irgafos stabilizer mix (Sasol) were used in the TREF procedures to inhibit thermal degradation as high temperatures are used in the crystallization (cooling) step. These are amine-based stabilizers.

Table 3.1 Physical properties of the plastomer (PL1881), LDPE and HDPE used

Physical Properties	PL1881	LDPE XHF 77/50	HDPE
MFI (g/10ml)	1	1	0.3
Density (g/cc)	0.9035	0.922	0.959
DSC melt. pt. (°C)	212 / 100	-	235/100
Tensile yield (psi /MPa)	1170 / 8.1 1040 / 7.2	10	25
Clarity	83	-	-
Gloss, 20°C	112	61	-
Haze %	3.2	8.9	-

3.2.4.1   Preparation of blends

In this study the following three blends were used. The blends were prepared using solution blending (All the percentage by mass).

A) 80% HDPE + 20% LLDPE
B) 80% HDPE + 20% LDPE
C) 50% LDPE + 50% LLDPE

Figure 3.1 shows a plan of this project.
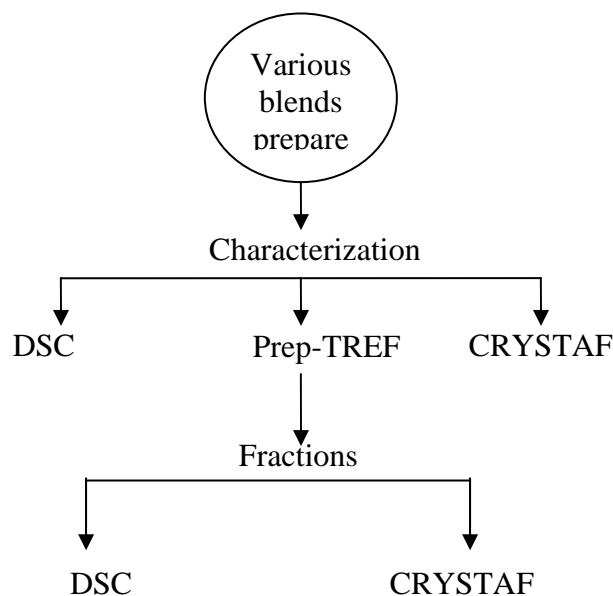
Figure 3.1 Flow diagram showing the project plan.

3.3   Fractionation

3.3.1 CRYSTAF

The CRYSTAF apparatus had five, stirred stainless steel crystallization vessels placed inside a temperature-programmable oven, which meant that up to five samples could be analyzed simultaneously. Figure 3.2 shows the CRYSTAF setup. The crystallization vessels are connected to a nitrogen line, a waste line, and a sampling line attached to an in-line filter. The sampling line is connected to an on-line detector cell used to measure the polymer solution concentration as a function of the crystallization temperature.

In this study, CRYSTAF was carried out using a CRYSTAF commercial apparatus, model 200, manufactured by Polymer Char S.A. (Valencia, Spain). Before the fractionation, about 20 mg of sample is dissolved at 130 ℃ in a good solvent inside a crystallization vessel (volume 60 mL). 1,2,4-Tricholobenzene was used as solvent in this study [1].

Figure 3.2 CRYSTAF setup showing stainless steel crystallization vessels inside a temperature-programmable oven.

The dissolution step is followed by the stabilization period, during which the temperature of the polymer solution is kept a few degrees above the initial crystallization temperature. During the crystallization step, the temperature of the solution is decreased at a constant cooling rate, typically in the range of 0.1–0.2 ℃/min. This allows the polymer chains with the highest crystallizabilities to precipitate first at high temperatures, followed by the chains with lower crystallizabilities. A slow cooling rate is essential to minimize undesirable crystallization kinetics and co-crystallization effects. The concentration of the polymer in the solution as a function of the crystallization temperature is monitored through the on-line infrared detector and recorded by the data acquisition software.

3.3.2 TREF

Temperature rising elution fractionation, which separates semi-crystalline polymer chains is based on the relative crystallizability of molecules [2].

The polymer is dissolved in a solvent (xylene) at high temperatures (135°C). A heated inert support is added, and the mixture then slowly cooled, allowing polymer molecules to crystallize on the support according to their respective crystallizabilities. Decreased crystallinty is reflected in a lower crystallization temperature [3]. After crystallization the temperature is raised

continuously, with solvent flowing through the column. As a result, at the lower temperatures the fractions with less crystallinity dissolve. With increasing elution temperature the fractions of higher crystallinity dissolve. Figure 3.3 illustrates the TREF process.
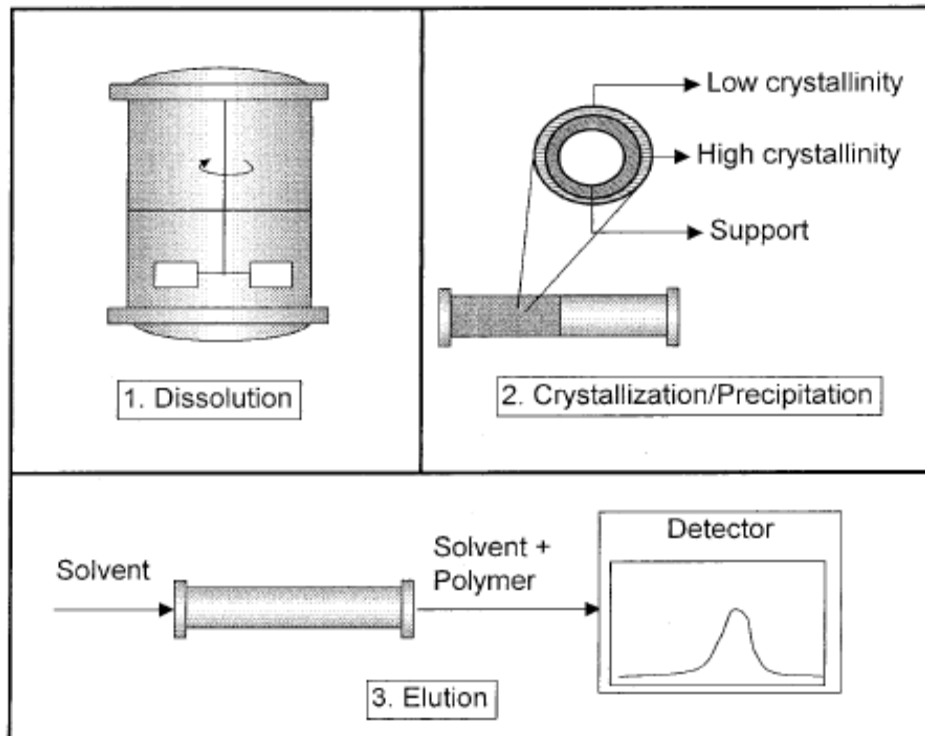
Figure 3.3 Schematic representation of the TREF process [1].

3.3.2.1 Prep-TREF

In this study preparative TREF was used to fractionate the polymers and the blends. The general procedure is described below.

The operation of prep-TREF is divided into two steps.

1.   About 2 g of polymer is dissolved in 200 mL of xylene, followed by the addition of 3 mg of an anti-oxidant. The solution is heated to $135^{\circ}C$ to ensure that the whole sample is dissolved. This solution is then placed in a 1-L round bottom flask and placed into a preheated oil bath with attached temperature profiler. A dilute solution of polymer is mixed with an inert support (for example, sea sand or glass beads). The amount of the support will depend on the initial amount of polymer and xylene used (2-3 kg of support). This mixture is slowly cooled to room temperature.

As the temperature gradually decreases the polymer fractions precipitate from the solution and coat the support in layers of different crystallinity. The most crystallizable fraction precipitates first, as is shown in Figure 3.3. On the other hand, the fraction with the least crystallinity precipitates last and deposits on the outermost layer. This step can be performed in a stirred vessel or directly in the TREF column [2].

2.   In the second step the precipitated polymer is eluted with a solvent using increasing or stepwise temperatures. As a result, chains which crystallize with difficulty are eluted first (at lower temperatures). As the temperature rises, less defective and more perfect chains are eluted [4].

In this study, two temperature profiles in prep-TREF were used.

1.   In the normal TREF (profile A) the polymer was dissolved in xylene at 130 ℃. A heated inert support was added (sea sand), and the mixture then slowly cooled at a cooling rate of 1 ℃/h, allowing the polymer molecules to crystallize on the support according to their crystallizabilities. After cooling, the sample was transferred to a metal elution column which was placed in a gas chromatography (GC) oven for the elution step. A stepwise heating was applied, with solvent flowing through the column. As a result, chains which crystallized with difficulty were eluted first (at lower temperatures). As the temperature increased, less defective and more perfect chains were eluted.

2.   In quench TREF (profile B), the solution was rapidly crystallized prior to elution, as opposed to slow crystallization. In quench TREF the polymer was dissolved in a solvent at high temperatures. A heated inert support was added, and the mixture then quench cooled by putting it in an ice bath. In the elution step a stepwise heating was applied, with solvent flowing through the column.

3.4   Analyses

3.4.1 DSC measurements

The melting and crystallization properties of samples were determined on a DSC instrument, in a nitrogen atmosphere, using the following method. Approximately 4-5 mg of each sample was used for analysis. All the experiments were performed after heating the samples to 180 °C at a

rate of 10°C/min to eliminate the thermal history. The crystallization curves were obtained by cooling the sample from the melt to -40 °C at a rate of 10 °C/min. The melting curves were obtained on reheating the sample to 180 °C at the same scanning rate. The data were only stored on the second run. The instrument used was a TA Instrument Thermal Analysis DSC standard cell. Data was baseline zeroed and normalized whenever 3-D plots were created.

3.4.2 NMR measurements

^{13}C NMR spectra of the polymers were recorded at 100 ^{0}C on a Varian VXR 300 instrument, in a 9:1 mixture of 1,2,4-trichlorobenzene/C_6D_6 as a solvent, using C_6D_6 at 127.9 ppm as internal secondary reference. The pulse angle was 45 degrees and the repetition time 0.82 s.

3.4.3 HT-SEC measurements

Molecular weights were determined using size exclusion chromatography. A PL-GPC 220 high temperature chromatograph was used at flow rate of 1 ml/min at 160 oC with a differential refractive index detector. Columns packed with a polystyrene/divinylbenzene copolymer (PL gel MIXED-B [9003-53-6]) from Polymer Laboratories were used. The length and diameter of these columns were 300 mm and 7.5 mm, respectively. Particle size was 10 µm. The concentration of the samples was 1.5 mg/ml. 1,2,4-trichlorobenzene(TCB), stabilized with 0.0125% 2,6-di-tert-butyl-4-methylphenol was used as solvent. The calibration was done with monodisperse polystyrene standards (EasiCal from Polymer Laboratories).

3.5 References

1.   S. Anantawaraskul and P. Wood-Adams. Polymer Science: Part B: Polymer Physics, 2003, 41, 1762-1778.

2.   J. Soares and A. Hamielec. Polymer, 1995, 36(8), 1639-1654.

3.   J. Xu and L. Feng. European Polymer Journal, 2000, 36, 867-878.

4.   A. Claudia and I. Harrison. Thermochimica Acta,1998, 313, 37-41.

Chapter 4

Results and discussion

In this chapter the following applies:

quench TREF: profile B, and normal TREF: profile A.

4.1 Prep-TREF

4.1.1 Prep-TREF of polymers

Table 4.1 shows the raw data of the prep-TREF of HDPE obtained after fractionation by TREF profile A.

Table 4.1: Raw data for the prep-TREF fractionation of HDPE at profile A

Elution temperature (ºC)	Mass recovered from 2 g sample (g)	Weight fraction, W_i	Weight fraction,% W_i (%)	Sum of the weight fraction %, $\Sigma W_i\%$	ΔT (ºC)	$W_i\%/\Delta T$
50	0.10	0.05	5.00	5.00	n/a	-
60	0.01	0.01	0.40	5.40	10	0.04
70	0.02	0.01	1.05	6.45	10	0.10
80	0.06	0.03	3.11	9.56	10	0.31
85	0.11	0.05	5.00	14.56	5	1.01
90	0.21	0.10	10.01	24.56	5	2.01
95	0.54	0.27	27.01	51.57	5	5.40
100	0.38	0.19	19.01	70.58	5	3.80
110	0.59	0.29	29.41	100	10	1.20

where:

W_i is the mass of each fraction/total mass recovered

W_i (%) is the mass/total (2g) $\times$ 100

ΔT is the elution temperature range between each fraction

$W_i\%/\Delta T$ is the weight fraction percentage divided by the elution temperature range between each fraction.

Figure 4.1 shows the weight fractions of preparative TREF fractions for HDPE at profile A (described in Section 3.3.2.1). The figure shows a relatively narrow peak which has peak maximum at 98 ℃, corresponding to the majority of the HDPE, and a small shoulder on the lower temperature side.
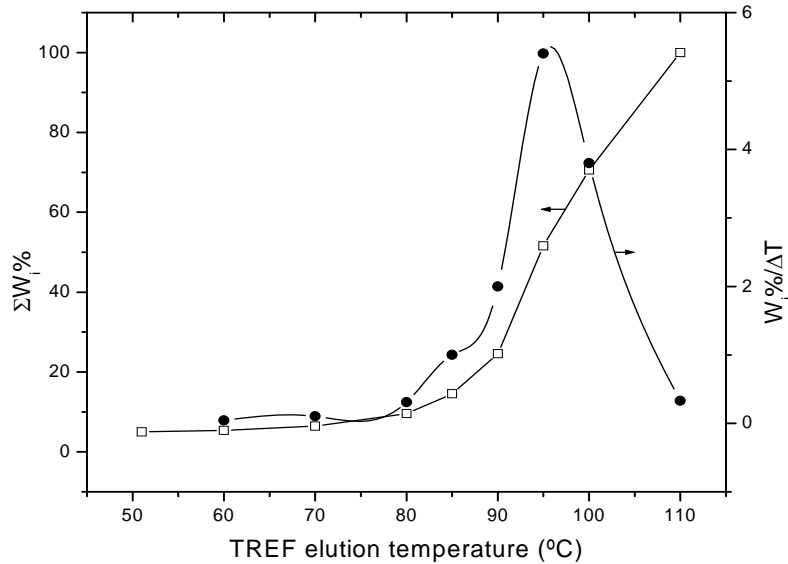

Figure 4.1 The $\sum W_i$ % and $W_i\%/\Delta T$ vs TREF elution temperature for HDPE at profile A.

The raw data of the LDPE obtained after fractionation by TREF profile A are shown in Appendix A1. Thirteen fractions were collected for this polymer.

The weight fraction of the preparative TREF fractions for LDPE at profile A is shown in Figure 4.2. The data used to produce this plot can be found in Appendix A1. The figure shows two distinct peaks, one at 77 ℃ and one at 100 ℃. This indicates that there are some crystalline chains at the lower temperature (at about 77 ℃), which may be due to the high amount of chain branching. The second peak (at about 100 ℃) may be due to the chains which have few branches, causing them to crystallize at a higher temperature, or the possibility of high molecular weight chains. The shoulder at 65 ℃ indicates that the polymer chains contain a very high number of branches, which reduces the ability of the chains to crystallize.

Figure 4.2 The $\sum W_i$ % and $W_i\%/\Delta T$ vs TREF elution temperature for LDPE at profile A. (See also Appendix A1.)

Figure 4.3 presents the weight fraction of prep-TREF fractions for LLDPE at profile A. The data used to produce this plot can be found in Appendix A2. Thirteen fractions were collected for this plastomer.

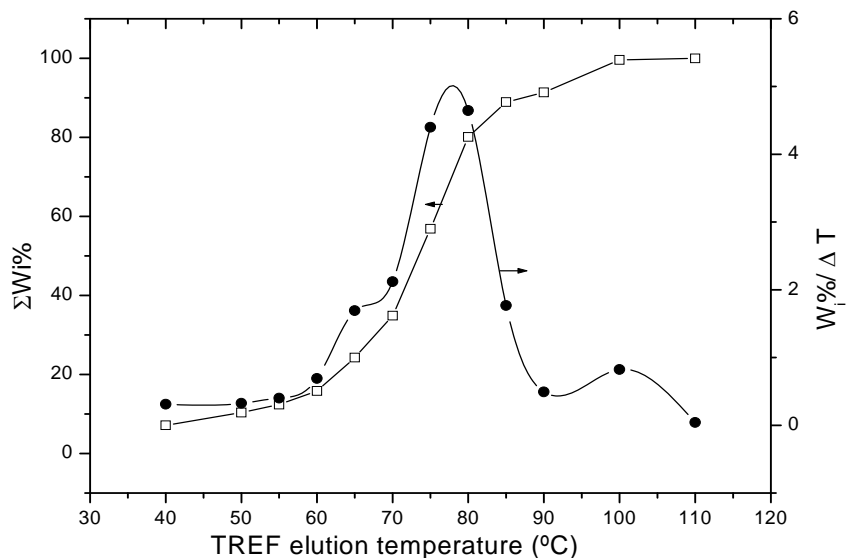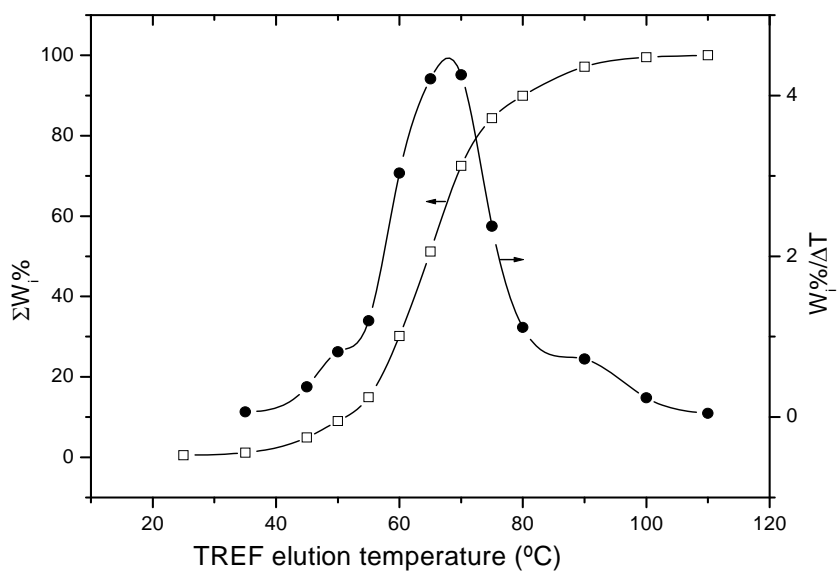**Figure 4.3 The $\sum W_i$ % and $W_i\%/\Delta T$ vs TREF elution temperature for LLDPE at profile A. (See also Appendix A2.)**

45

The figure shows a broad peak with a peak maximum at 68 ℃, which corresponds to the majority of the LLDPE. The broadness of the peak is due to crystallization of the polymer chains with different amounts of octane comonomer and therefore different degrees of short-chain branching.

4.1.2 Prep-TREF of the blends

4.1.2.1 HDPE-LDPE blend

The raw data of the HDPE-LDPE blend obtained after fractionation by TREF profile A are tabulated in Appendix A3. Fourteen fractions were collected for this blend. As the table shows, very small quantities were collected, especially in the middle fractions, which made it difficult to carry out many analyses on these fractions.

Figure 4.4 illustrates the weight fraction of preparative TREF fractions for the HDPE-LDPE blend at profile A. It shows two distinct peaks, at 75 ℃ and 95 ℃. The peak at 75 ℃ corresponds to the same temperature as the peak maximum of LDPE. The region between this peak and the peak at 95 ℃ could be associated with the effect of co-crystallization, where there are some HDPE chains incorporated with LDPE which are crystalline at lower temperatures. The second peak at about 95 ℃ is due to the HDPE chains, which have few branches and therefore elute at higher temperature.
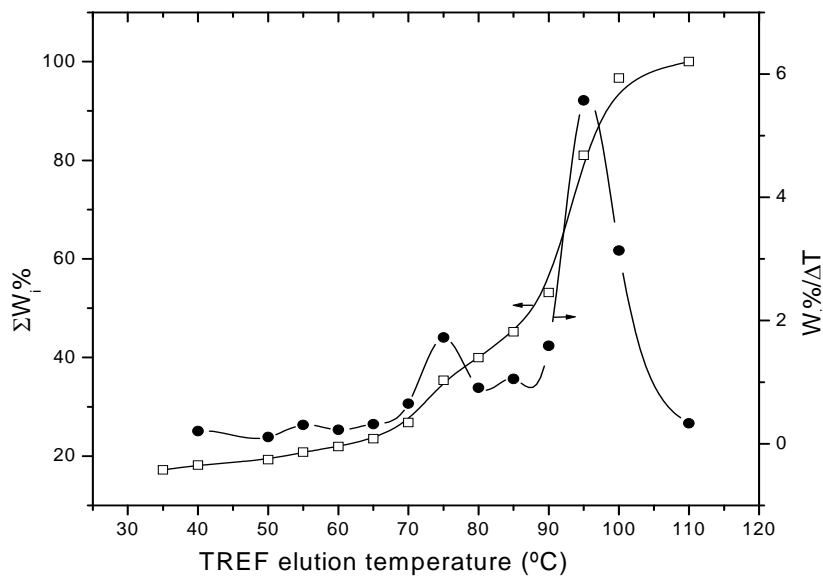

Figure 4.4 The $\sum W_i$ % and W_i%/ΔT vs TREF elution temperature for a HDPE-LDPE blend at profile A. (See also Appendix A3.)

4.1.2.2 HDPE-LLDPE blend

The raw data of the HDPE-LLDPE blend obtained after fractionation by TREF profile A are tabulated in Appendix A4. Fourteen fractions were collected for this blend.

Figure 4.5 illustrates the weight fraction of prep-TREF fractions for a HDPE-LLDPE blend at profile A. If we compare this figure with Figure 4.1 we see that the peak maximum at about 98 ºC corresponds to HDPE. However, there is a broad peak in the range between 60º C and 70 ºC, which corresponds to LLDPE. The shoulder at about 80 ºC may indicate the effect of co-crystallization. It is expected that some of the HDPE chains are incorporated in the LLDPE chains and crystallize at a lower temperature.

Figure 4.5 The $\sum W_i$ % and W_i%/ΔT vs TREF elution temperature for a HDPE-LLDPE blend at profile A. (See also Appendix A4.)

4.1.2.3 LDPE-LLDPE blend

Appendix A5 shows the raw data of the LDPE-LLDPE blend obtained after fractionation by TREF profile A. Fourteen fractions were collected for this blend.

The weight fraction of prep-TREF fractions for the LDPE-LLDPE blend at profile A is presented in Figure 4.6. The figure shows clearly a very broad peak, between 55 ºC and 85 ºC. When this

figure is compared with Figures 4.3 and 4.2 we see that the first peak corresponds to the crystallization of LLDPE chains and the second peak corresponds to LDPE. Because the blending ratio used was 50% LDPE and 50% plastomer, and the crystallization temperature (T_c) for both the polymer and the plastomer is very similar, there is a large overlap between the two elution peaks. This indicates that in this blend there is a relatively large fraction where co-crystallization can be expected.
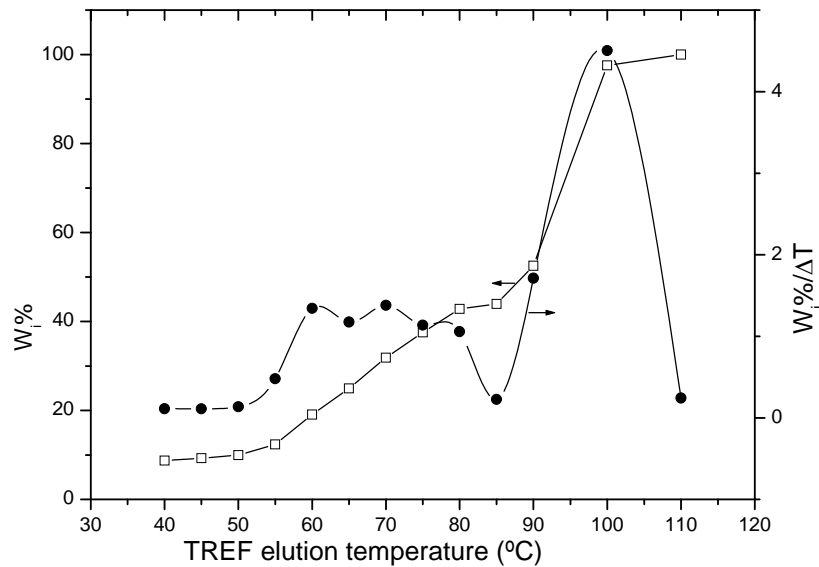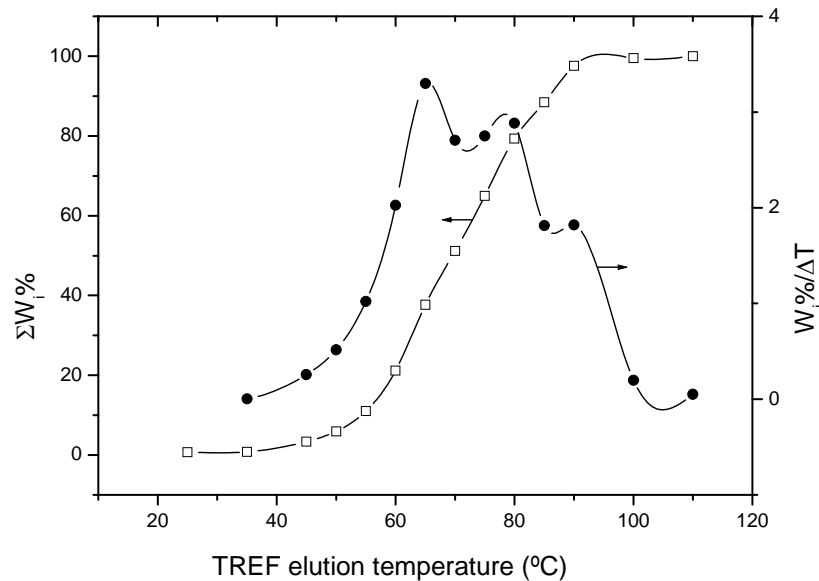

Figure 4.6 The $\sum W_i$ % and $W_i\%/\triangle T$ vs TREF elution temperature for a LDPE-LLDPE blend at profile A. (See also Appendix A5.)

4.1.3 Quench prep-TREF of blends HDPE-LDPE, HDPE-LLDPE and LDPE-LLDPE

4.1.3.1 HDPE-LDPE blend

Figure 4.7 shows the weight fraction of prep-TREF fractions for the HDPE-LDPE blend where the samples were quench cooled. This was done to try to force the co-crystallization and therefore co-elution in TREF. Two peaks are seen, at 75 ºC and 95 ºC respectively. Once again, the first peak corresponds to LDPE, where there is a high amount of branching, which allows it to crystallize at low temperature. The areas in between the two peaks indicates the region of possible co-crystallization, where some HDPE chains may be incorporated into the crystalline

structure with some LDPE chains and crystallize at the same time due to the quench-cooling profile. The second peak represents HDPE where there is a limited amount of chain branching.
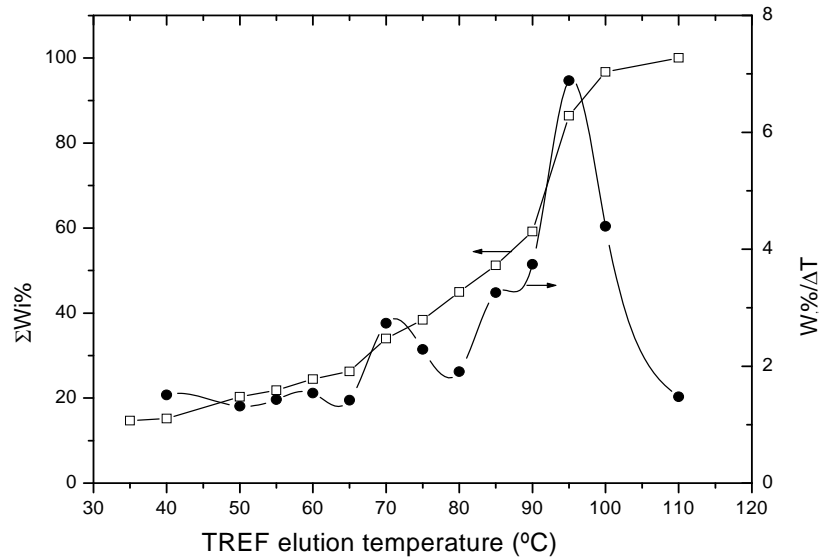

Figure 4.7 The $\sum W_i$ % and $W_i\%/\Delta T$ vs quench TREF elution temperature for a HDPE-LDPE blend. (See also Appendix A6.)

The raw data of the HDPE-LDPE blend obtained after fractionation by TREF profile B is illustrated in appendix A6. Twelve fractions were collected for this blend.

When Figure 4.7 is compared to Figure 4.4 it can be seen that, in both cases, the main two peaks of LDPE and HDPE appeared, but the peak of the LDPE is shifted to lower temperature in the case of the quenched profile. This is expected, since there is not enough time for the chains to crystallize. It can also be seen that the co-crystallization region is much larger in the case of the quench cooling than the normal TREF. This is expected, since the fast cooling rate is more favourable for co-crystallization.

4.1.3.2 HDPE-LLDPE blend

The raw data of the HDPE-LLDPE blend obtained after fractionation by TREF profile B is illustrated in appendix A7. Thirteen fractions were collected for this blend.

The weight fraction of prep-TREF fractions for a HDPE-LLDPE blend from quench TREF profile is shown in Figure 4.8. There are two main peaks, one at 65 ℃ and one at 100 ℃. The first peak corresponded to LLDPE and the second peak to HDPE, where there is a limited amount of chain branching. The shoulder at about 85 ℃ indicates the possible co-crystallization effect, where the linear part of LDPE is incorporated into the crystals of HDPE and co-crystallization occurs in HDPE crystals.
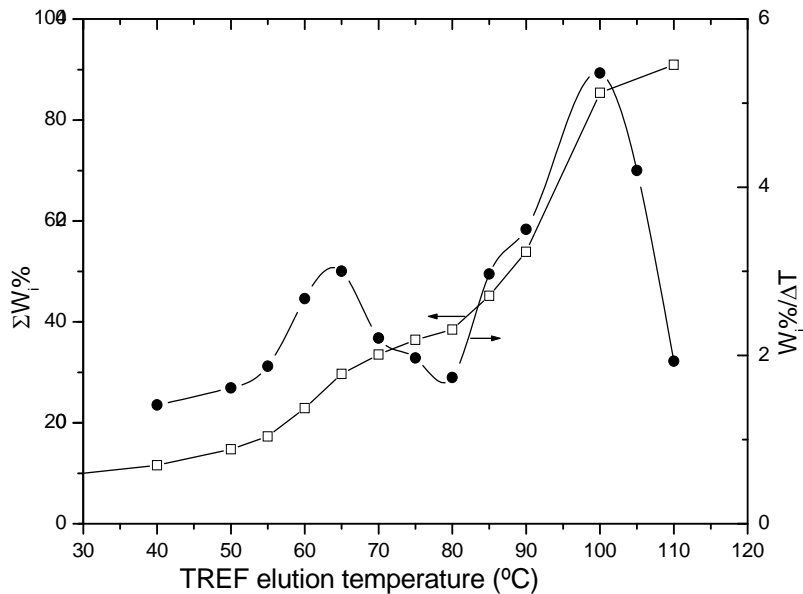

Figure 4.8 The $\sum W_i$ % and W_i%/ΔT vs the quench TREF elution temperature for a HDPE-LLDPE blend. (See also Appendix A7.)

When Figures 4.5 and 4.8 are compared it can be seen that two peaks appear in both cases but the co-crystallization region has changed significantly.

4.1.3.3 LDPE-LLDPE blend

The raw data of the LDPE-LLDPE blend obtained after fractionation by TREF profile B is presented in Appendix A8. Fifteen fractions were collected for this blend.

Figure 4.9 shows the weight fraction of prep-TREF fractions for a LDPE- LLDPE blend where the sample was quench cooled. A very narrow peak was detected at 72 ℃, and a slight shoulder at lower temperature, which may be due to a high branch content. A comparison between the

quench TREF and normal TREF profiles for the LDPE-LLDPE blend (Figures 4.6 and 4.9) indicates that the same peaks are present in both cases but there is a significant change in the peak width. In the case of the quench-cooled sample there is a narrow peak with a small shoulder, and a very broad peak in the case of the normal TREF. This is due to the difference in the crystallization cooling rates.

Indications are that quench cooling has a significant effect on each of the TREF blend profiles, most notably in the possible co-crystallization regions.
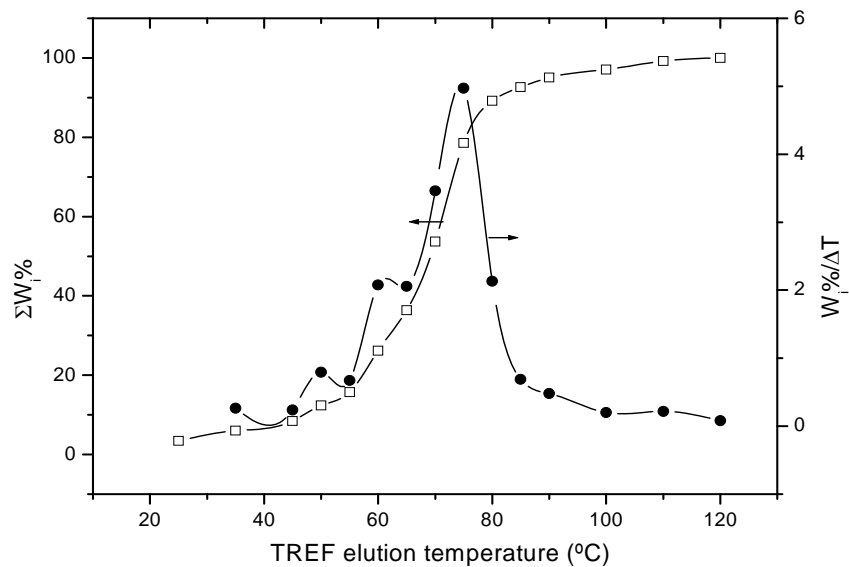
Figure 4.9 The $\sum W_i$ % and W_i%/ΔT vs quench TREF elution temperature for a LDPE-LLDPE blend. (See also Appendix A8.)

In the following section the analysis of the blend fractions, using CRYSTAF and DSC, will be discussed. This was done in order to identify any potential co-crystallization in each fraction.

4.2 CRYSTAF results

CRYSTAF is a very powerful fractionation technique that generates information equivalent to that obtained with TREF. There are however differences between the two techniques, and these have been used here to study possible co-crystallization in the TREF fractions.

CRYSTAF relies on the measurement of the concentration of dissolved polymer during crystallization following dissolution at high temperature; the temperature is decreased at a controlled rate. During the crystallization process, aliquots of a sample are filtered and the concentration of polymer in solution is determined. The main difference between CRYSTAF and TREF is that CRYSTAF analysis is done by monitoring the decrease in concentration of the polymer as it crystallizes (out of solution), while in TREF analysis the polymer is eluted by a melt-dissolution process after being crystallized onto a support.

Here we have utilized this difference in the crystallization mechanism to analyze the preparative TREF fractions. In addition, the cooling rate in CRYSTAF was varied in order to study what effect this would have on the CRYSTAF profile and any potential co-crystallization fractions.

CRYSTAF was done using three different cooling rate profiles to investigate the effect of the cooling rate on the CRYSTAF profiles.

1- CRYSTAF at profile A, where the cooling rate was 0.25 °C /min.
2- CRYSTAF at profile B, where the cooling rate was 0.15 °C /min.
3- CRYSTAF at profile C, where the cooling rate was 0.1 °C /min.
4- CRYSTAF at profile D, where the cooling rate was 0.08 °C /min.

4.2.1 CRYSTAF results for unfractionated blends

Figure 4.10 illustrates the unfractionated HDPE-LDPE blend CRYSTAF trace, followed by the CRYSTAF traces for LDPE and for HDPE. The unfractionated HDPE-LDPE blend CRYSTAF trace has two peak maxima, at 67 °C and 90 °C respectively. This is to be expected, since the first peak corresponds to the crystallization of LDPE. The broadness of this peak may be due to a co-crystallization effect. The second peak corresponds to HDPE. The second curve shows the unfractionated LDPE CRYSTAF trace, which indicates one peak at 67 °C for LDPE. The third curve shows the unfractionated HDPE CRYSTAF trace, which indicates one peak at 90 °C for HDPE.
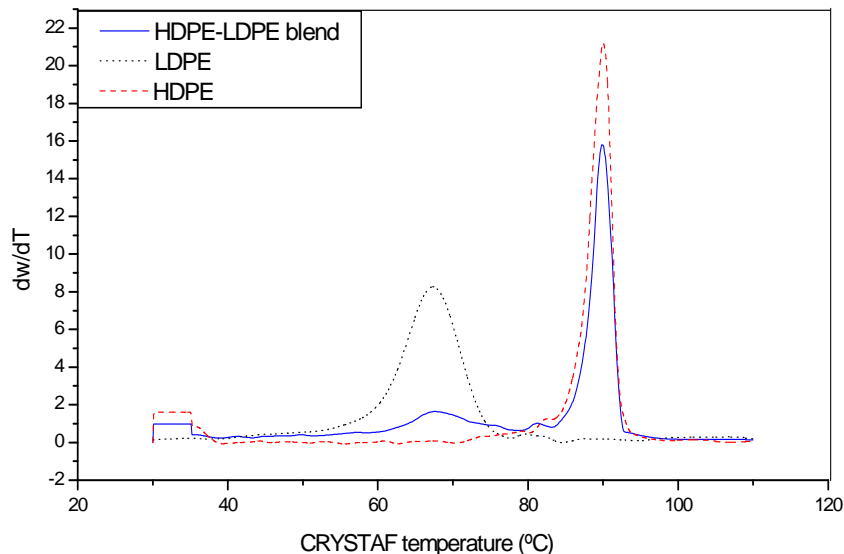
Figure 4.10 CRYSTAF traces for the unfractionated HDPE, LDPE and HDPE-LDPE blends at profile C.

The CRYSTAF trace of the unfractionated HDPE-LDPE blend in comparison with the weight fraction percentage divided by the fraction temperature range, obtained from the preparative TREF, is shown in Figure 4.11. The figure shows that in both cases there are two peaks, which correspond to LDPE and HDPE respectively. However, there is a significant difference in terms of the peak maxima; the peak maimum is much higher in the case of prep-TREF (100 ºC) than CRYSTAF (90 ºC). This shift is the result of the under-cooling effect. There is also a difference in the broadness of the peaks; the prep-TREF peak is much broader than the CRYSTAF peak. A similar result was reported by Britto *et al.* [1] and Gabriela and Lilgeb [2], who pointed out that the shift between CRYSTAF and TREF profiles is due to the super-cooling effect, since CRYSTAF curves are measured during crystallization, while TREF is measured during the melt dissolution process [3]. Therefore, the most crystalline polyethylene peaks in CRYSTAF and TREF are located at about 90 °C and 100 °C, respectively.
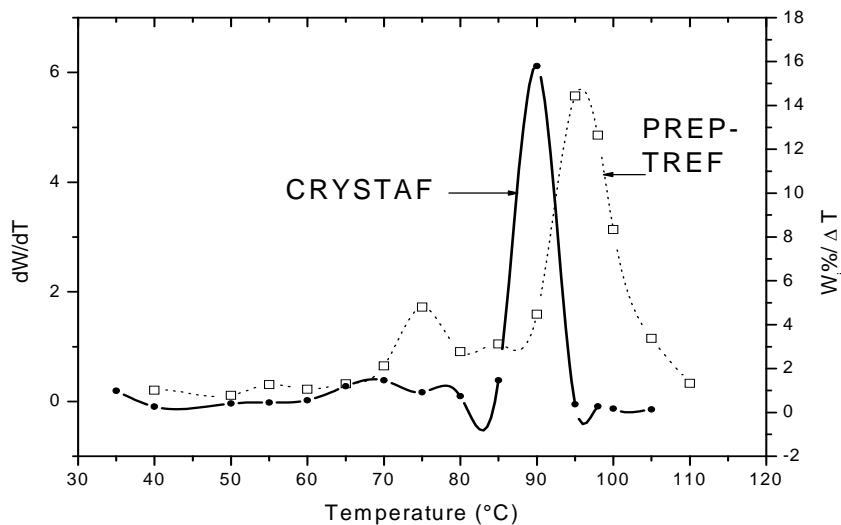
Figure 4.11 Schematic representation of the CRYSTAF trace of the unfractionated HDPE-LDPE blend in comparison to the weight fraction percentage divided by the fraction temperature range collected from the prep-TREF.

Figure 4.12 shows the unfractionated HDPE-LLDPE blend CRYSTAF trace, followed by the CRYSTAF traces for LLDPE and for HDPE. The first curve presents the CRYSTAF trace of the unfractionated HDPE-LLDPE blend, which has two peak maxima at 57 ℃ and 90 ℃ respectively. The first broad peak corresponds to the crystallization of LLDPE, and the second peak corresponds to HDPE. The second curve shows the unfractionated LLDPE CRYSTAF trace, which indicates one peak at 57 ℃ for LLDPE.

Figure 4.13 illustrates the CRYSTAF trace of the unfractionated HDPE-LLDPE blend in comparison with the weight fraction percentage divided by the fraction temperature range, obtained from the prep-TREF. In both cases there are two peaks, which correspond to LLDPE and HDPE respectively. Once again, we see a shift between the prep-TREF profile and the CRYSTAF profile due to the under-cooling effect and the TREF peaks appear to be broader.
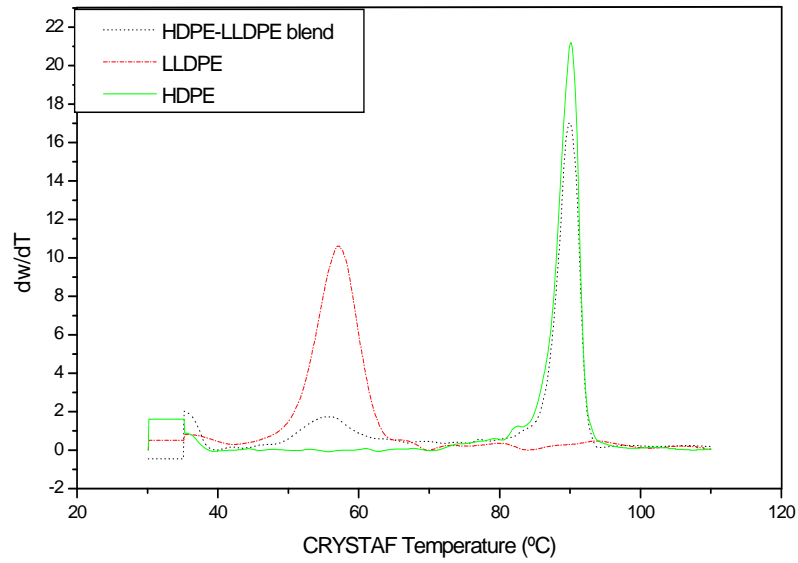
54

Figure 4.12 The CRYSTAF traces for the unfractionated HDPE and LLDPE, and HDPE-LLDPE blend at profile C
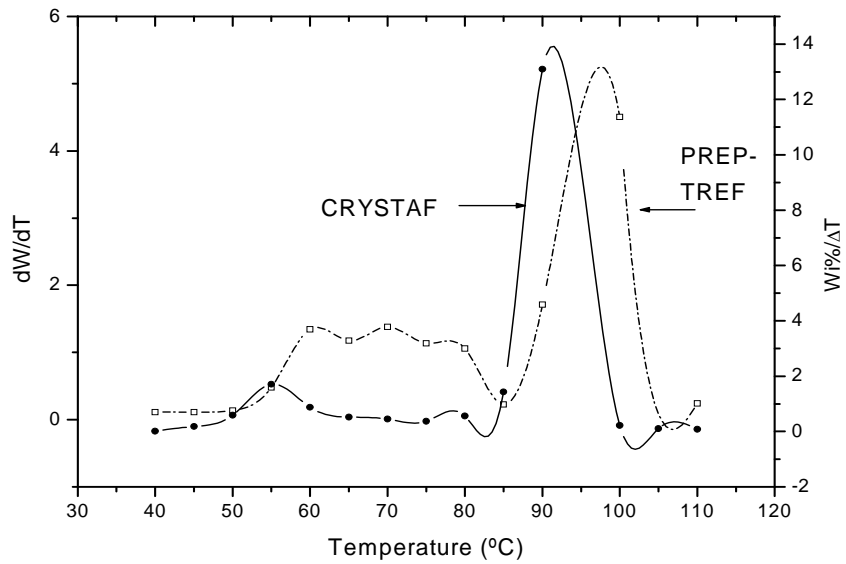

Figure 4.13 Schematic representation of the CRYSTAF trace of the unfractionated HDPE-LLDPE blend in comparison to the weight fraction percentage divided by the fraction temperature range collected from the prep-TREF.

4.2.2 CRYSTAF results for unfractionated blends and unfractionated polymers at different profiles

CRYSTAF traces for the HDPE-LLDPE blend at different cooling profiles are shown in Figure 4.14. In all cases there are two crystallization peaks, in the range of 55 ºC and 85 ºC, which correspond to LLDPE and HDPE respectively. However, there is a significant shift in those peaks with a change in cooling rate. There is a progressive shift in the peak to a lower temperature as the cooling rate is increased. This is in agreement with the findings of Anantawaraskul *et al.* [4]; they noted that a slow cooling rate permits the polymer molecules to crystallize at higher temperatures.
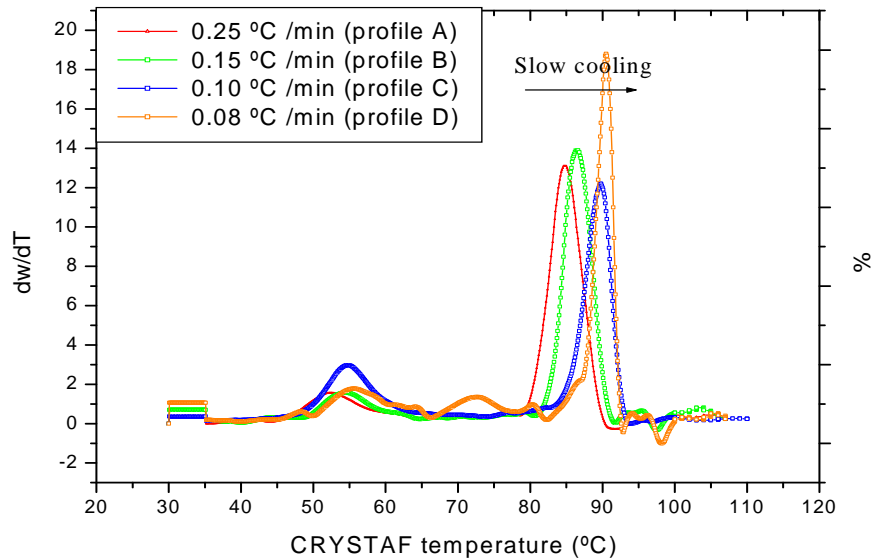
Figure 4.14 The CRYSTAF traces for the unfractionated HDPE-LLDPE blend at different profiles.

The broadness of the peaks also increases with an increased cooling rate. In order to quantify the broadness of the HDPE peak the CRYSTAF data was fitted using a simple Gauss function, from which the full width at half maximum (FWHM) could be determined. This value allows for the quantification of the peak broadness. The results of this analysis of the CRYSTAF traces are summarized in Table 4.2.

Table 4.2: Broadness of the HDPE crystallization peaks calculated by Gauss function for the HDPE-LLDPE blend

CRYSTAF cooling rate (ºC/min.)	FWHM for CRYSTAF peak of HDPE
0.08	2.10 (± 0.09)
0.10	3.21 (± 0.07)
0.15	3.84 (± 0.03)
0.25	4.44 (± 0.03)
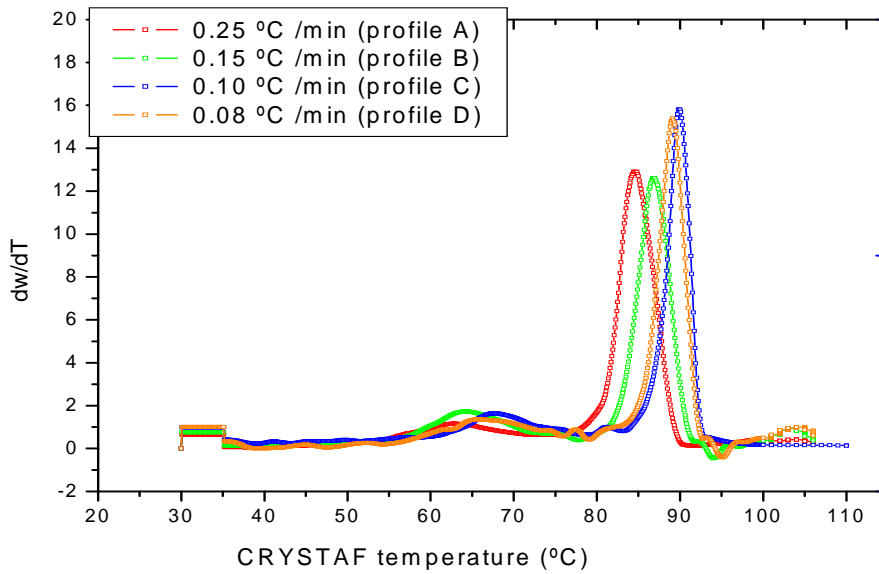
Figure 4.15 CRYSTAF traces for the unfractionated HDPE-LDPE at different profiles.

Similarly, in the case of the HDPE-LDPE blend, as shown in the Figure 4.15, the peak in the range of 55 °C can be attributed to the crystallization of LDPE, which occurs in the normal range of temperatures, and the peak in the range of 85 °C can be attributed to HDPE. There is also a shift in crystallization peaks with different cooling rates. Similar to the HDPE-LLDPE blend, the broadness of the crystallization peak increased with an increasing cooling rate, as shown in Table 4.3. However, at a cooling rate of 0.1 ºC/min the broadness of the peak decreases.

Table 4.3: Broadness of the crystallization peaks calculated by Gauss function for the HDPE-LLDPE blend

CRYSTAF cooling rate (ºC/min)	FWHM for CRYSTAF peak of HDPE
0.08	2.88 ($\pm$ 0.07)
0.10	2.34 ($\pm$ 0.06)
0.15	3.65 ($\pm$ 0.04)
0.25	4.01 ($\pm$ 0.05)

It can be concluded that changing the cooling rate has a significant effect on the crystallization temperature, as well as the broadness of the crystallization peaks. At a faster cooling rate the polymer appears to crystallize over a large temperature range, leading to peak broadening; this is due to less time that each polymer has to crystallize at a different temperature. Significantly, the blends used in this study show that although the cooling rate affects the broadness of each of the peaks in the blend, these peaks still appear as separate peaks.

4.2.3 CRYSTAF results for fractionated blends at different profiles

The fractionated CRYSTAF trace for each of the nine TREF fractions collected for the HDPE-LLDPE blend, and the unfractionated HDPE and unfractionated LLDPE CRYSTAF traces, are presented in Figure 4.16.

The CRYSTAF traces for each of the fractions show that prep-TREF was successful in fractionating the sample according to crystallizability. The maxima in the first derivative of the concentration curve from CRYSTAF moves progressively to a higher temperature with an increase in the TREF fraction temperature. The broad shoulders on the middle-temperature fractions are due to co-crystallization, which occurs during the TREF crystallization step, causing these fractions to co-elute and giving the two distinct peaks in the CRYSTAF trace.
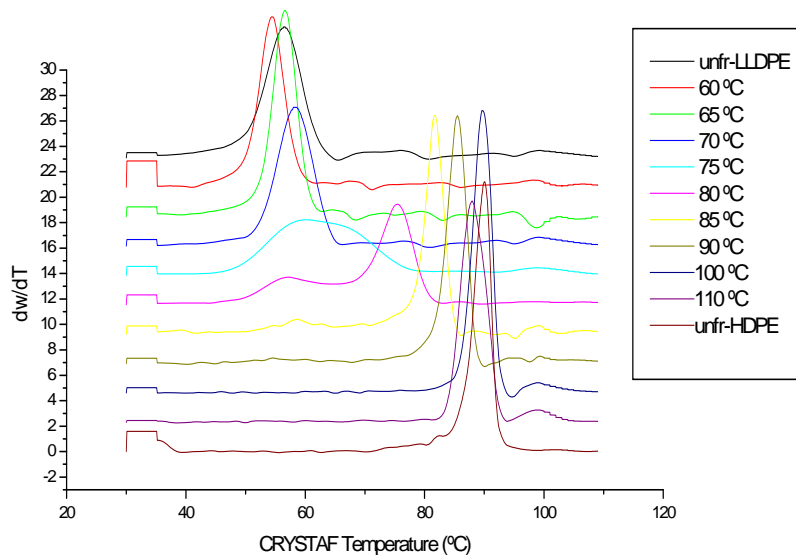
Figure 4.16 The fractionated HDPE-LLDPE blend CRYSTAF trace, and unfractionated HDPE and unfractionated LLDPE CRYSTAF traces.

In order to more clearly illustrate the co-crystallization behaviour, three dimensional (3-D) TREF-CRYSTAF plots for the fractionated HDPE-LLDPE blend were created. These were created by using a matrix to replace the x-axis of conventional graphs with a 3-D plot, and presenting the data of three variables. This graph was created using the normalized, baseline corrected and unweighted prep-TREF fractions. This type of plot allows for the easy visual representation of the heterogeneity with respect to the TREF and CRYSTAF data and to obtain the CRYSTAF crystallization map, as shown in the Figure 4.17.

The CRYSTAF crystallization map clearly shows two peaks, at 68 °C and 96 °C respectively. The first peak corresponds to the crystallization of LLDPE and the second peak corresponds to the crystallization of HDPE. In addition, the CRYSTAF crystallization map shows the co-crystallization region in between the two peaks. The box in the figure represents the area where the co-crystallization occurred during the prep-TREF fractionation. In this blend the TREF fractions between 75 °C and 90 °C contained significant amounts of each polymer. This results clearly illustrates the difference in components that co-eluted in TREF fractionation. It should also be noted the shift between the two temperature axes due to the so-called "under cooling" effect discussed earlier.
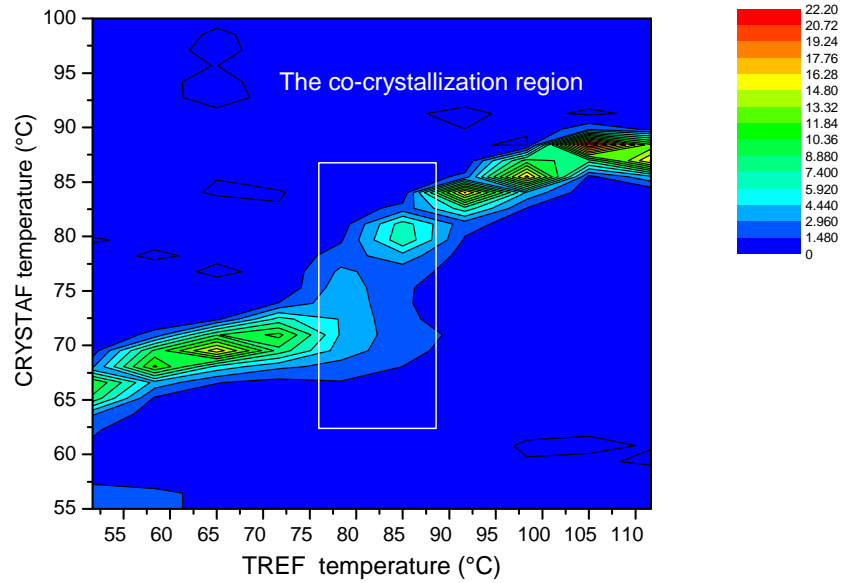
Figure 4.17 CRYSTAF crystallization map for the fractionated HDPE-LLDPE blend at profile C.

Figure 4.18 CRYSTAF crystallization map for the fractionated HDPE-LDPE blend at profile C.

Figure 4.18 presents a CRYSTAF crystallization map for a HDPE-LDPE blend. The two peaks were at 60 °C and 96 °C respectively. The first peak corresponds to the crystallization of LDPE and the second peak corresponds to the crystallization of HDPE. The area in the range of 75°C to 90 °C presented the co-crystallization region in between the two peaks.

To investigate the effect of changing the cooling rate in CRYSTAF, CRYSTAF crystallization maps were created for different cooling profiles (B and D) for the fractionated HDPE-LLDPE blend, as shown in the two figures below. On comparing Figure 4.17 above with Figures 4.19 and 4.20 below, it can be concluded that changing the cooling rate influences the crystallization temperature; it can be shifted from a higher to a lower temperature, and vice versa. In addition, changing the cooling rate in CRYSTAF affected the co-crystallization region. It is however significant that, regardless of the CRYSTAF cooling rate, the co-crystallization area for the TREF fractions between 75 °C and 95 °C is observed in all cases. This clearly shows that those are in fact co-crystallization fractions and the two CRYSTAF peaks in these fractions are not an artifact of the CRYSTAF cooling rate or technique.

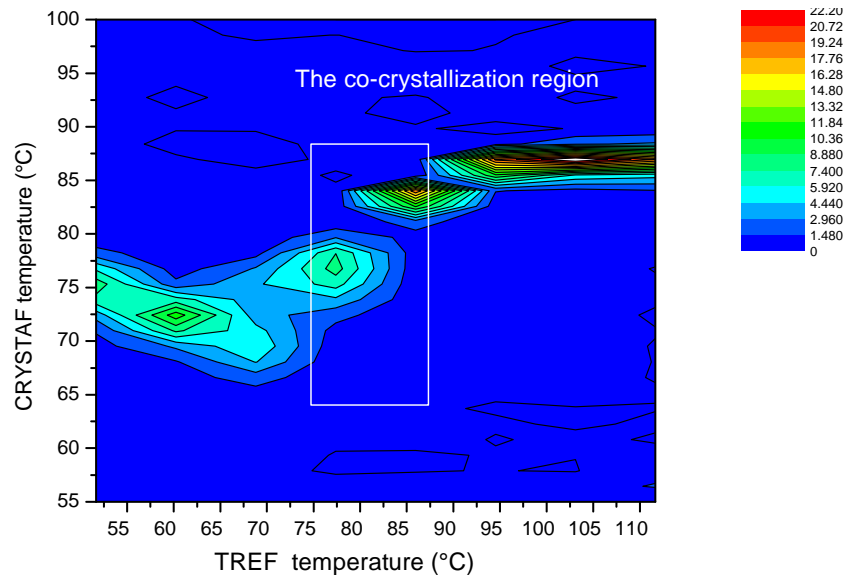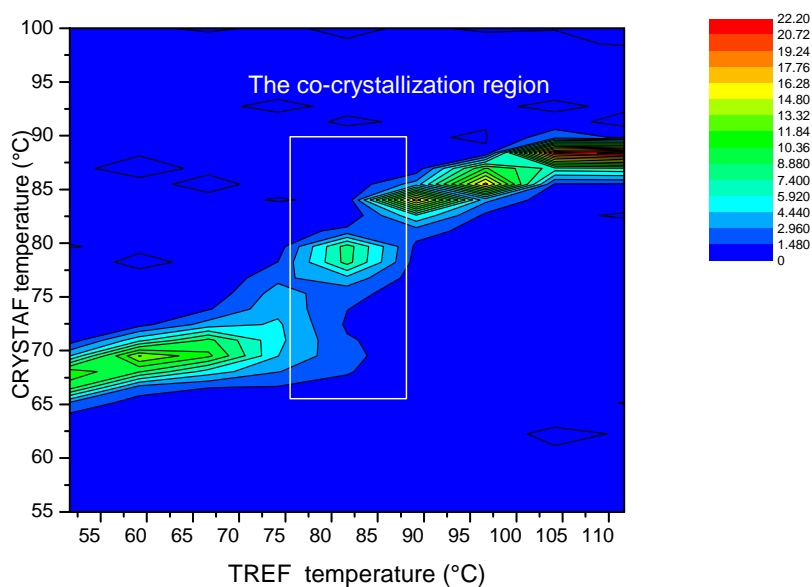**Figure 4.19 CRYSTAF crystallization map for the fractionated HDPE-LLDPE blend at profile B.**
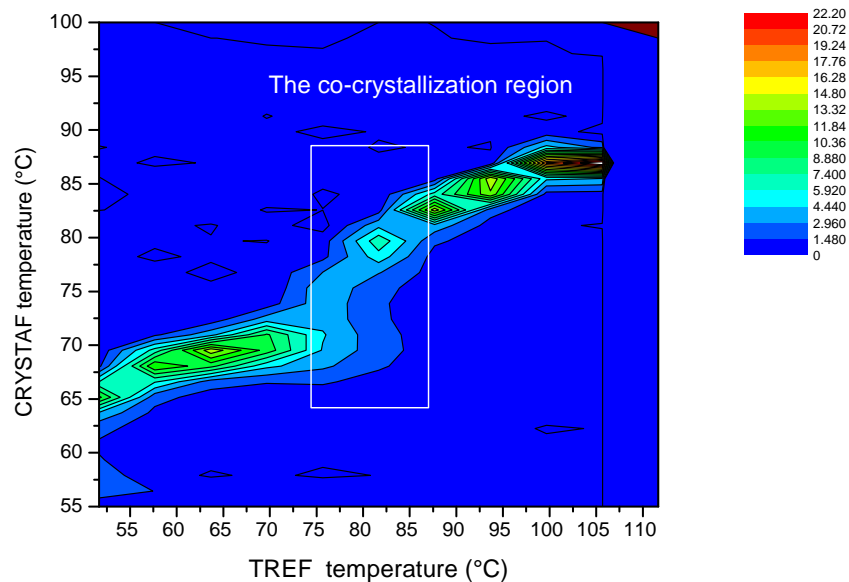
Figure 4.20 CRYSTAF crystallization map for the fractionated HDPE-LLDPE blend at profile D.

Figure 4.21 shows the CRYSTAF crystallization map of the quench cooled HDPE-LLDPE blend. When this figure is compared to the normal (or slow cooled) map in Figure 4.17, it can be seen that in the case of the quench cooling the co-crystallization fractions shift to a lower temperature on the TREF axis with a significant co-crystallization fraction between 65 °C and 80 °C. It is also seen that there is a clear distinction between the two components in the TREF co-crystallization fractions. This is most probably due to the fact that the extremely fast cooling rate force part of the material to co-crystallize that is not the case in the slower cooling rate.

It should be noted that the results presented in this section clearly indicate the presence of both types of polymer in the so-called "co-crystallization" fractions. This does not prove *per se* that co-crystallization has occurred as it is possible that the two separate materials may have simply co-eluted in the TREF fraction. Nevertheless the presence of both materials in these fractions presents strong evidence for the existence of co-crystallization.
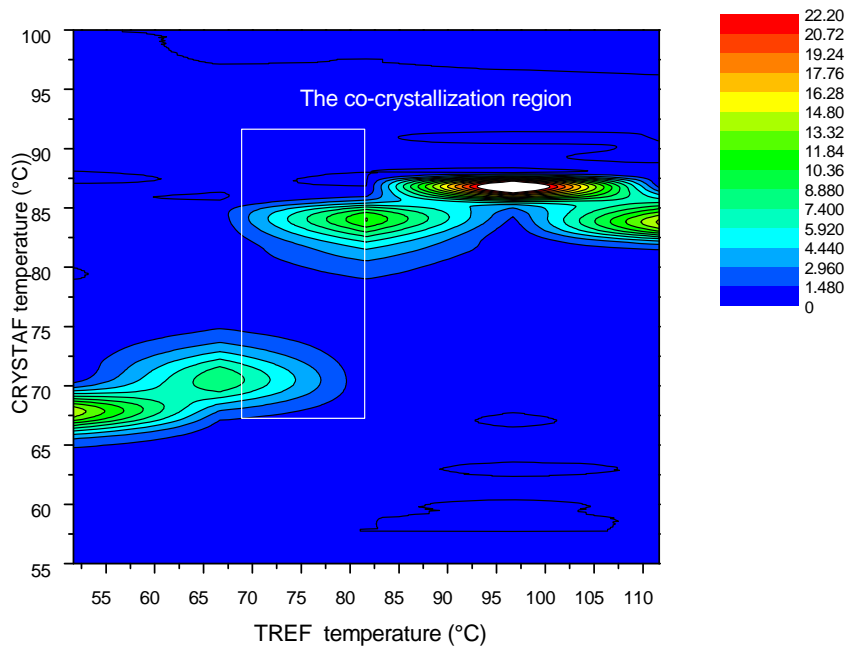
Figure 4.21 CRYSTAF crystallization map for quench TREF fractions of the fractionated HDPE-LLDPE blend

4.3 Differential scanning calorimetry (DSC) results

DSC measures the temperatures and heat flows associated with transitions in materials as a function of time and temperature. Such measurements provide quantitative and qualitative information about physical and chemical changes that involve endothermic or exothermic processes, or changes in heat capacity. DSC can be performed with relative speed and is therefore widely used to determine the percentage of crystalline material in semi-crystalline resins as well as to identify first- and higher-order phase transitions

In this study DSC was used to study the melting behaviour of the blends and the pure components as well as the respective fractions obtained from prep-TREF. Four different temperature profiles were used in this study. In the first the fractionated polymers and blends were measured using the standard polyolefin profile, where the samples were heated to 180 °C at 10 °C/min and then cooled from the melt to -40 °C at 10 °C/min and, lastly, reheated to 180 °C at 10 °C/ min.

In the second profile, the samples were heated to 180 °C at 10 °C/min and then cooled from the melt to 103 °C (above the crystallization peak) and held isothermally there for 15 min, then cooled to -40°C at 10 °C/min, and lastly reheated to 180 °C at 10 °C/ min.

63

In the third profile, the samples were heated to above the melt temperature and cooled at the TREF cooling rate of 1 °C/ h; this was done by placing the DSC samples in test tubes which are placed in TREF cooling bath. Once the samples reached room temperature they were removed and placed in the DSC. They were heated at 10 ºC/min and the melt curve was measured on the first heat.

In the third profile, crystallization occurred from the solid state. In the last profile, samples were dissolved in xylene and placed in test tubes in the TREF cooling bath. Samples were then cooled at 1 ºC/h to room temperature. Once room temperature was reach the solution was filtered to remove the solid crystallized polymer. The solid polymer was dried and place in the DSC were the melt curve was determined at a heating rate of 10 ºC/min. All the profiles are summarized below:

1- DSC at profile A, where the cooling rate was 10 ºC/min (normal profile for polyolefins)
2- DSC at profile B, where the same cooling rate (as in 1) was applied, but the temperature was held isothermally above the crystallization peak (103 ºC) for 15 minutes
3- DSC at profile C, where normal TREF fractions were introduced at a cooling rate of 1 ºC/h, and then DSC was applied, to measure the first heat melt curve.
4- DSC at profile D, where unfractionated blends in solution were cooled at a cooling rate of 1 ºC/h, filtered to remove the crystallized polymer, and then DSC was applied, to measure the first heat melt curve.

In order to achieve a better fractionation for individual polymers, careful selection of experimental parameters, such as crystallization temperature and isothermal time is very important.

4.3.1 DSC results for the fractionated polymers and plastomer

Figure 4.22 illustrates the DSC crystallization peaks for the fractionated HDPE. This figure shows the increase of the DSC T_c (crystallization peak maxima) with the increase in the prep-TREF elution temperature. These DSC results confirm that the HDPE was fractionated according to crystallizability. The crystallization peaks become progressively narrower as the fractionation temperature increases.
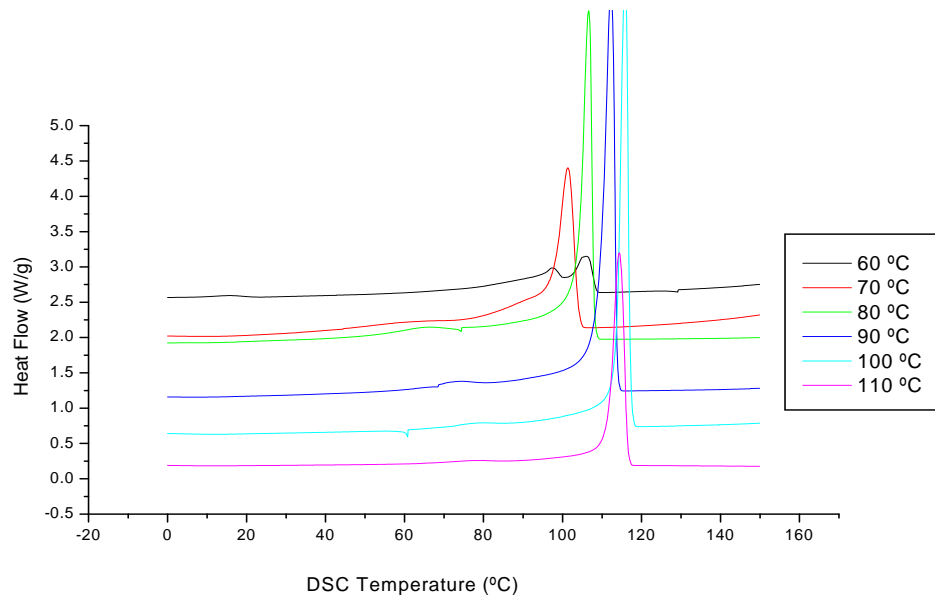
Figure 4.22 DSC crystallization peaks for fractionated HDPE, normal prep-TREF traces at profile A.

Figure 4.23 shows the DSC melting peaks for the fractionated HDPE. The figure shows the gradual increase of the T_m (DSC melting peak maxima) with an increase in the prep-TREF elution temperature for the polymer. The melting peaks also become gradually narrower for each of the higher temperature fractions.
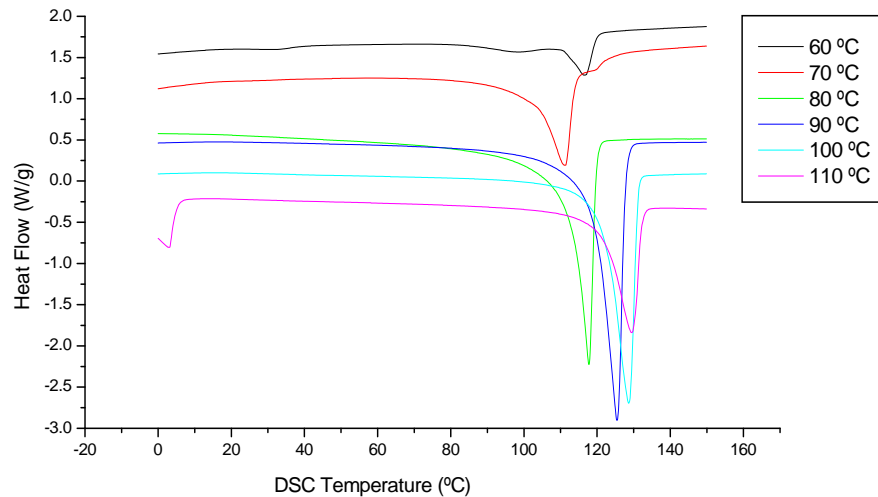

Figure 4.23 DSC melting peaks for fractionated HDPE, normal prep-TREF traces at profile A.

Similar to Figure 4.22, Figure 4.24 shows the DSC crystallization peaks for the fractionated LDPE. This figure shows an increase in the DSC T_c (crystallization peak maxima) with an increase in the prep-TREF elution temperature.
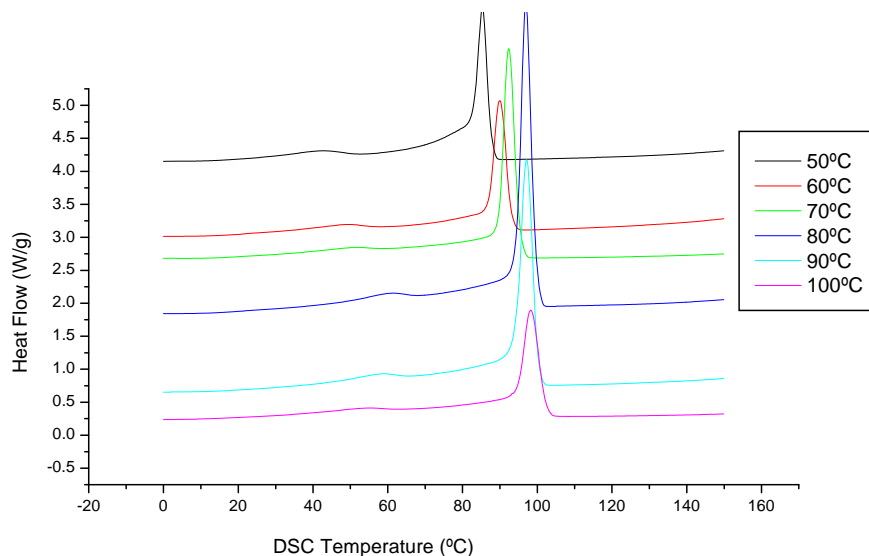

Figure 4.24 DSC crystallization peaks for fractionated LDPE, normal prep-TREF traces at profile A.
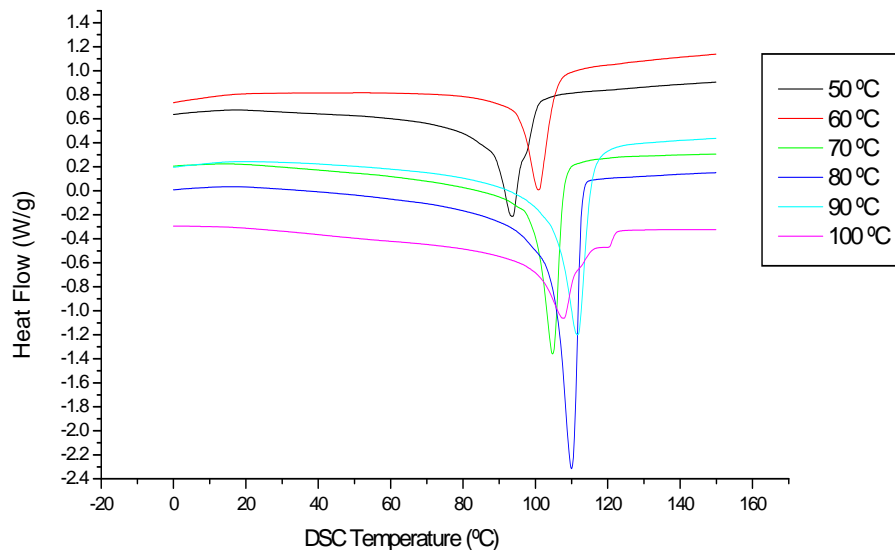

Figure 4.25 DSC melting peaks for the fractionated LDPE,normal prep-TREF traces at profile A.

Figure 4.25 shows the DSC melting peaks for the fractionated LDPE. The figure shows the expected increase of the T_m (DSC melting peak maxima) with an increase in the prep-TREF elution temperature for the polymer.

Once again, Figure 4.26 shows the DSC crystallization peaks for the fractionated LLDPE. This figure shows a slight increase in the DSC T_c (crystallization peak maxima) with an increase in the prep-TREF elution temperature.

Figure 4.27 shows the DSC melting peaks for the fractionated LLDPE. The figure shows a slight increase in the T_m (DSC melting peak maxima) with an increase in the prep-TREF elution temperature for the polymer.
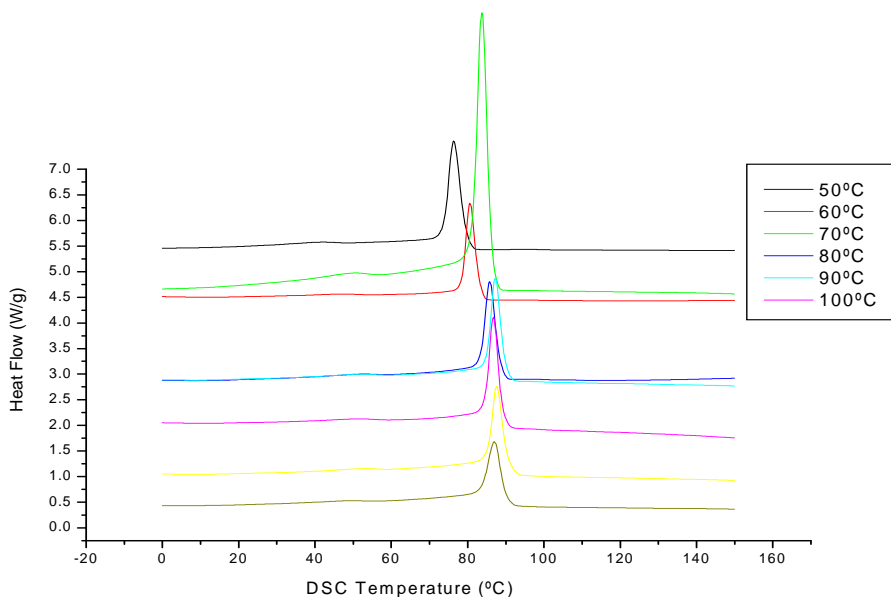

Figure 4.26 DSC crystallization peaks for the fractionated LLDPE, normal prep-TREF traces at profile A.
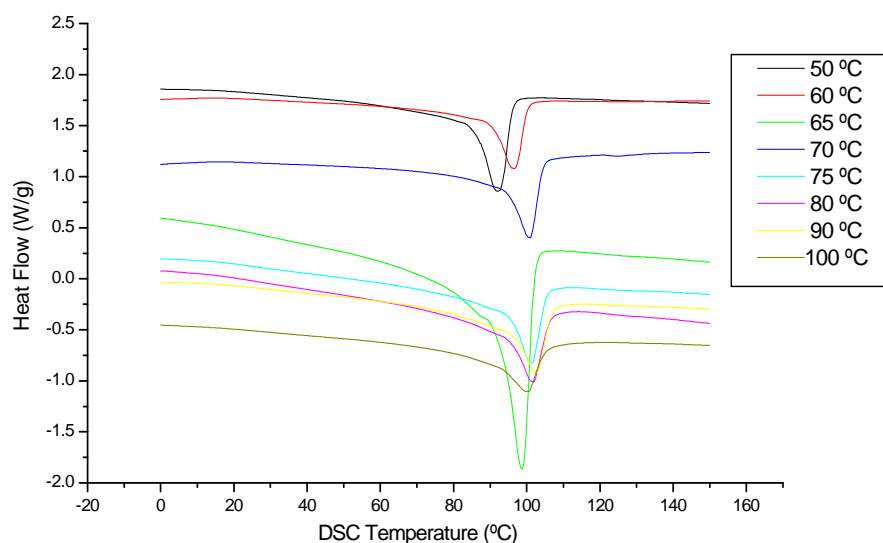
Figure 4.27 DSC melting peaks for the fractionated LLDPE, normal prep-TREF traces at profile A.

4.3.2 DSC results for the unfractionated polymers and fractionated blends at profile A

DSC analysis was done for the entire range of fractions in both cases, i.e. normal TREF fractions and quench TREF fractions.

4.3.2.1 DSC results for the unfractionated polymers and fractionated blends from normal TREF

Figure 4.28 shows the DSC crystallization peaks for the unfractionated and fractionated HDPE-LLDPE blend at profile A (cooling rate 10 °C/min). The peak maxima show an increase in the T_c(crystallization peak maxima) with a increase in the prep-TREF fraction temperature.

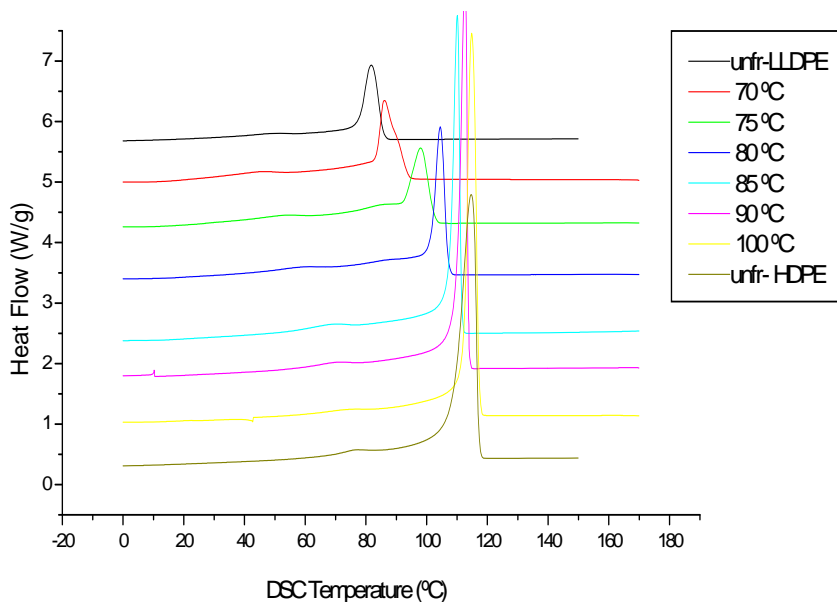**Figure 4.28 DSC crystallization peaks for the unfractionated polymers and fractionated HDPE-LLDPE blend, normal prep-TREF traces at profile A.**

Figure 4.29 shows the DSC melting peaks for the unfractionated and fractionated HDPE-LLDPE blend. The figure shows the gradual increase of the T_m (DSC melting peak maxima) with an increase in the prep-TREF elution temperature for the blend. The figure also shows a slight shoulder on the left side of the melting peaks which may be due to the crystallization of a small number of HDPE chains at lower temperature because of the incorporation of those chains with LLDPE chains. This behaviour can be interpreted as being due to the co-crystallization effect.

The percentage crystallinity in each fraction was calculated using the heat of fusion for 100 % crystallinity for polyethylene and observed heats of fusion in DSC. Table 4.4 gives the percentage crystallinity in each fraction of the HDPE-LLDPE blend.
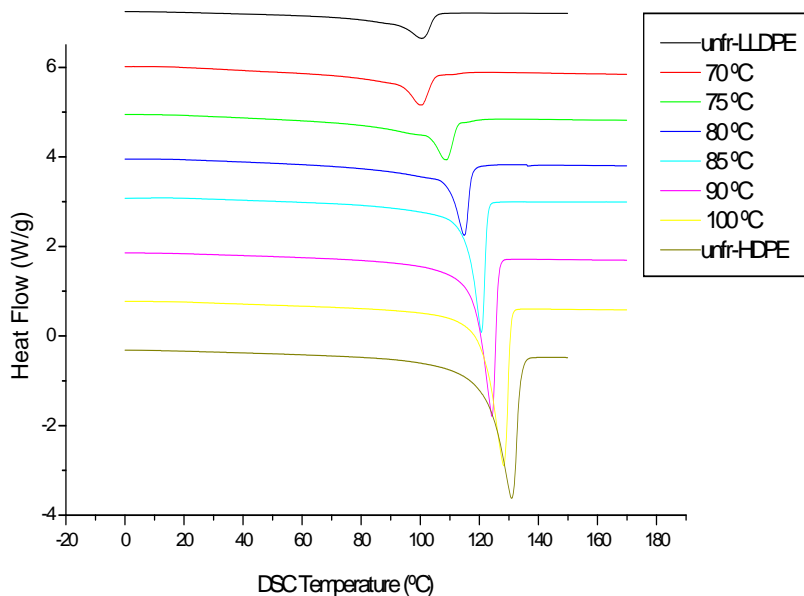
Figure 4.29 DSC melting peaks for the unfractionated polymers and fractionated HDPE-LLDPE blend, normal prep-TREF traces at profile A.

Table 4.4: The percentage crystallinity in each TREF fraction of the HDPE-LLDPE blend

Fraction temperature (ºC)	T_m (ºC)	T_c (ºC)	ΔH_m (J/g)	% Crystallinty
50	90.5	76.6	24.2	8.2
60	96.3	80.9	42.6	14.5
65	99.9	83.6	63.3	21.5
70	100.4	86.1	63.8	21.7
75	108.7	97.9	87.7	29.8
80	114.8	104.4	90.1	30.6
85	120.7	110.1	121.2	41.2
90	124.2	112.5	151.2	51.5
100	128.2	114.8	170.6	58.1
110	127.7	114.4	190.9	65.0

where: $\Delta H^o_{f,c}$ 100 % crystallinty for polyethylene is 293.6 J/g [5, 6].

Overall, the table shows that the percentage crystallinity in the fractions generally increases as the TREF fractionation temperature increases. Evidently, increasing crystallinity and melting temperature increase with the increase in the TREF elution temperature. In particular, the linear relationship can be verified from the plots of crystallinity and melting temperature against elution temperature. These results are in accordance with those of Hosoda [7] and Mirabella [8].

From the data in Table 4.4 it is possible to plot TREF fractionation temperature against the percentage crystallinty. Figure 4.30 shows that the percentage crystallinity increases as the TREF fractionation temperature increases, which proves that TREF fractionates the blends according to their crystallizability. A similar result was reported by Soares and Hamielec [9], namely that TREF is a powerful technique for fractionating and characterizing semicrystalline polymers, and that TREF is regulated by the crystallinity of the polymer samples.
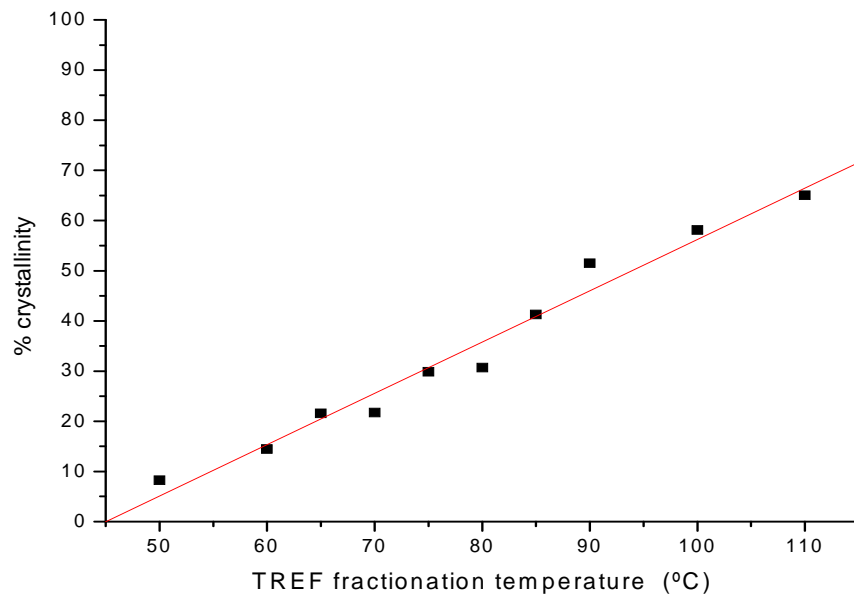

Figure 4.30 Percentage crystallinty present in each TREF fraction of the HDPE-LLDPE blend.

The co-crystallization behaviour is better shown in Figure 4.31. It shows a three-dimensional (3-D) TREF-DSC for the fractionated HDPE-LLDPE blend. Only the TREF fractions between 70 °C and 110 °C are shown in this plot. This was done by using a matrix to replace the x-axis of conventional graphs with a 3-D plot, and presenting the data of three variables. This graph was plotted using the normalized, baseline corrected and unweighted prep-TREF fractions and the DSC melting curves. The colour scales in all the plots are identical and therefore each plot can be directly compared with the darker colour showing a large endothermic DSC melt peak. This type of plot allows for the easy visual representation of the heterogeneity with respect to the TREF and DSC data.

The DSC melting peak data showed a large conical distribution between the 70 °C and 80 °C TREF fractions and a smaller distribution at higher and lower temperatures. The 3-D DSC crystallization map in Figure 4.31 clearly shows the melting peaks the area in between, where we expect some co-crystallization, where HDPE with the highest melting peak is able to co-crystallize with LLLPE to some extent.
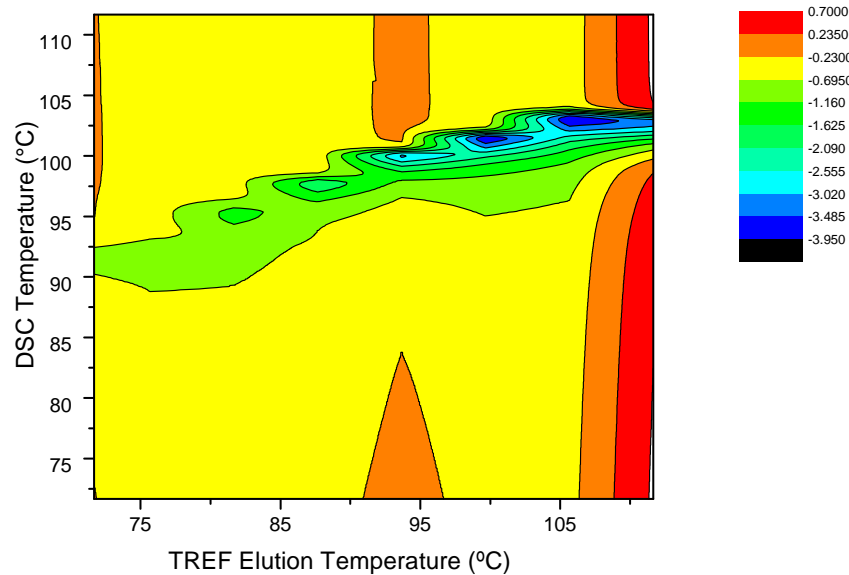

Figure 4.31 3D DSC-TREF for a HDPE-LLDPE blend obtained at a slow cooling rate (0.1 °C/h).

4.3.2.2 DSC results for the unfractionated polymers and fractionated blends from quench TREF

Figure 4.32 displays the quench TREF fractions for a HDPE-LLDPE blend. Results show that there is an increase in the melting temperature as the TREF fractionation temperature increases, which confirms the results from normal TREF. However, it shows the separation in the melting peaks much more clearly than normal TREF does. It also shows two endothermic peaks, observed for the co-crystal material, and which seem to be associated with linear and branched polyethylene. The linear component appears to melt at a somewhat lower temperature than regular HDPE does, and the branched material melts at a higher temperature than normal

LLDPE. These results are in agreement with the findings of Morgan and Hamilec [10], namely that the rapid cooling rate is favourable for co-crystallization behaviour.
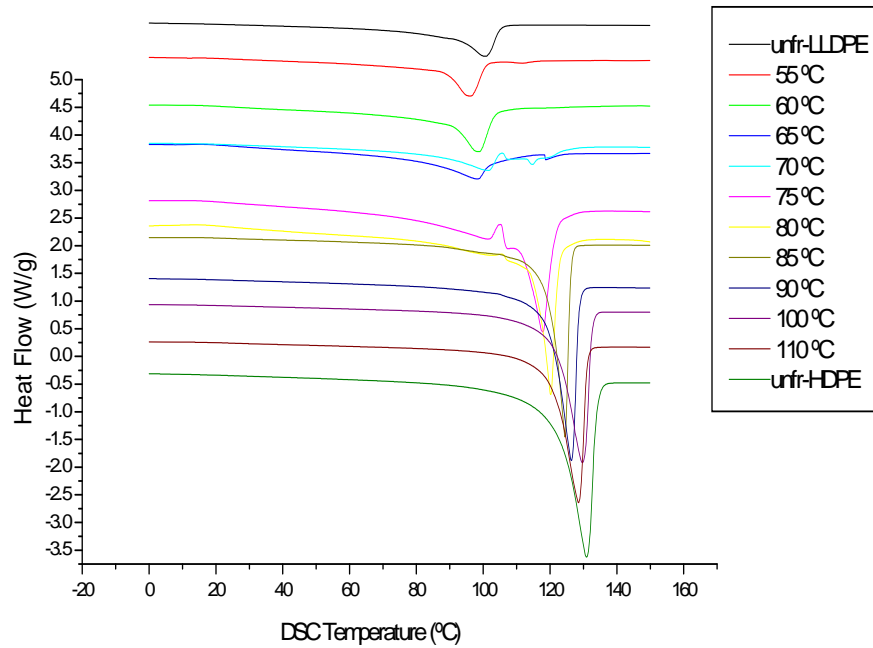

Figure 4.32 DSC melting peaks for the unfractionated polymers and fractionated HDPE-LLDPE blend, quench prep-TREF traces at profile A.

The DSC crystallization map for the quench TREF-DSC of HDPE-LLDPE is presented in Figure 4.33. Upon comparing this figure to Figure 4.31, it can be seen that by changing the profile from normal to quench TREF the crystallization temperature was shifted to lower temperature as observed by the lower temperature region on the TREF axis in Figure 4.33. This shift confirms the results in section 4.2.3 where the crystallization fractions shifted to a lower temperature on the TREF axis for the quench cooled sample.

As was done for Table 4.4, the percentage crystallinity in each fraction was calculated using the heat of fusion for 100% crystallinity for polyethylene and the observed heats of fusion in DSC. Table 4.5 tabulates the percentage crystallinty in each fraction in the HDPE-LLDPE blend.
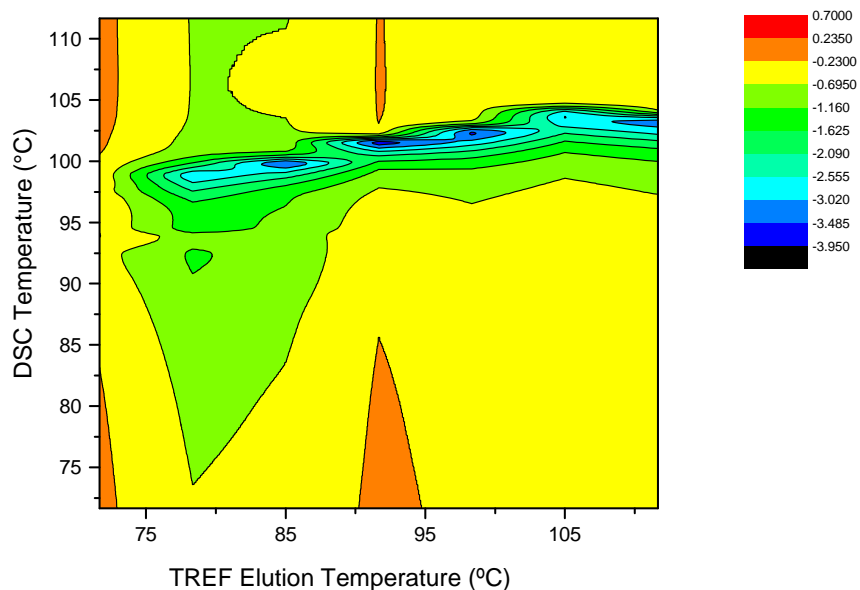
Figure 4.33 3D DSC-TREF for HDPE-LLDPE blend at quench cooling rate (DSC crystallization map).

Table 4.5: Percentage crystallinty present in each quench-TREF fraction for the HDPE-LLDPE blend

Fraction temperature (ºC)	T_m (ºC)	T_c (ºC)	ΔH_m (J/g)	% Crystallinty
60	98.72	83.6	88.7	30.2
70	101.59	89.2	72.9	24.8
75	117.74	107.5	96.7	33.0
80	120.18	110.3	122.2	41.6
85	124.48	113.3	129.4	44.1
90	126.4	113.1	142.0	48.4

Once again, a linear relationship between the percentage crystallinty and the TREF fractionation temperature is seen in the case of HDPE-LLDPE blend (Figure 4.34). In order to investigate the effect of changing the profile on the melting behaviour of the blend fractions, isothermal time was applied above the crystallization temperature to give the chains more time to arrange. It was also done to determine the effect on the co-crystallization region.
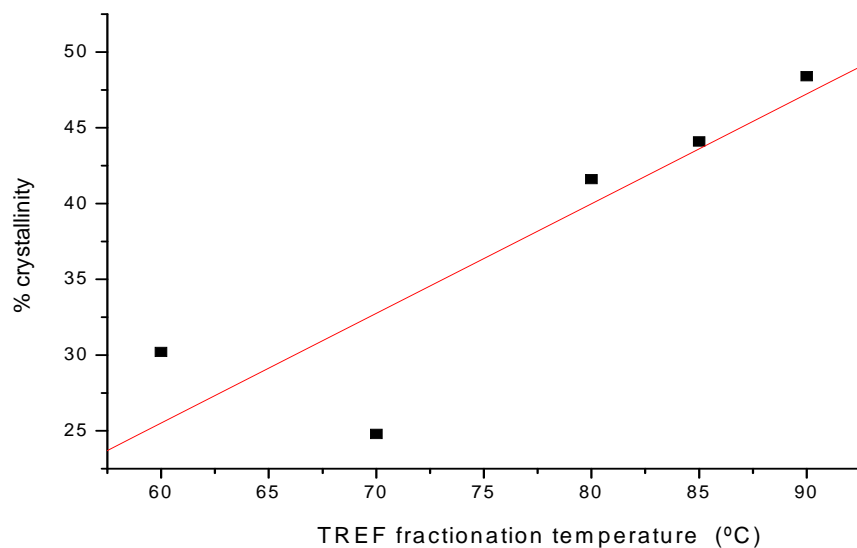
Figure 4.34 Percentage crystallinty present in quench-TREF fraction for the HDPE-LLDPE blend.

4.3.3 DSC results for the unfractionated polymers and fractionated blends at profile B

DSC was carried out for all the fractions in the following cases: normal TREF fractions at 'profile B', and quench TREF fractions at 'profile B'.

4.3.3.1 DSC results for the unfractionated polymers and fractionated blends from normal TREF

Figure 4.35 shows the DSC melting peaks for the unfractionated and fractionated HDPE-LLDPE blend at profile B. This figure shows similar results to those recorded for profile A; for the blend there is an increase in the T_m (DSC melting peak maxima) with an increase in the prep-TREF elution temperature. However, in profile B the results clearly show a growing new peak, especially in fraction 75 ºC. This may suggest the development of a miscible phase that arises from the co-crystallization between the molecules. The separation may also indicate that the two polymers are still immiscible in the crystal state, as confirmed by the presence of two melting peaks.
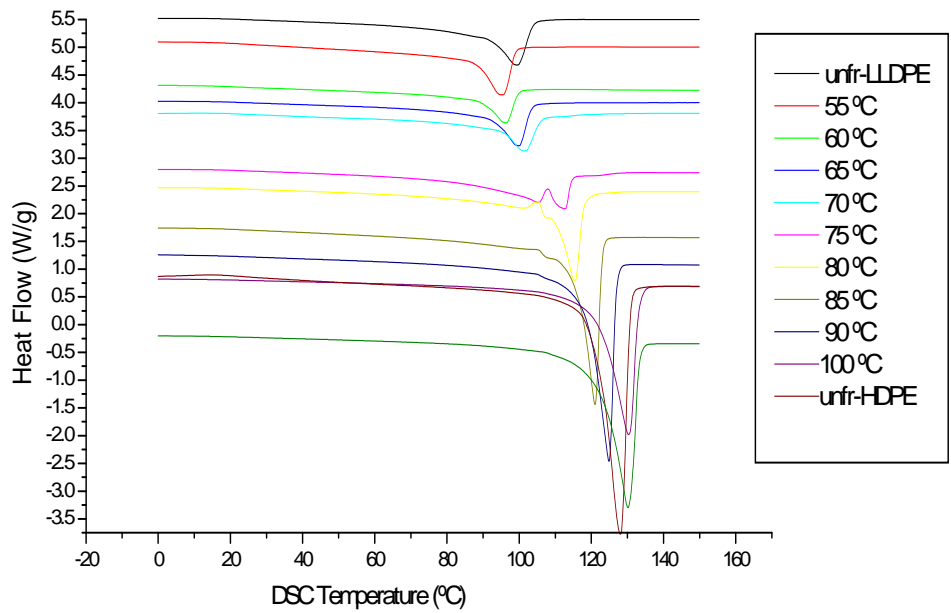
75

Figure 4.35 DSC melting peaks for the unfractionated HDPE and LLDPE, and fractionated HDPE-LLDPE blend, prep-TREF traces at profile B.
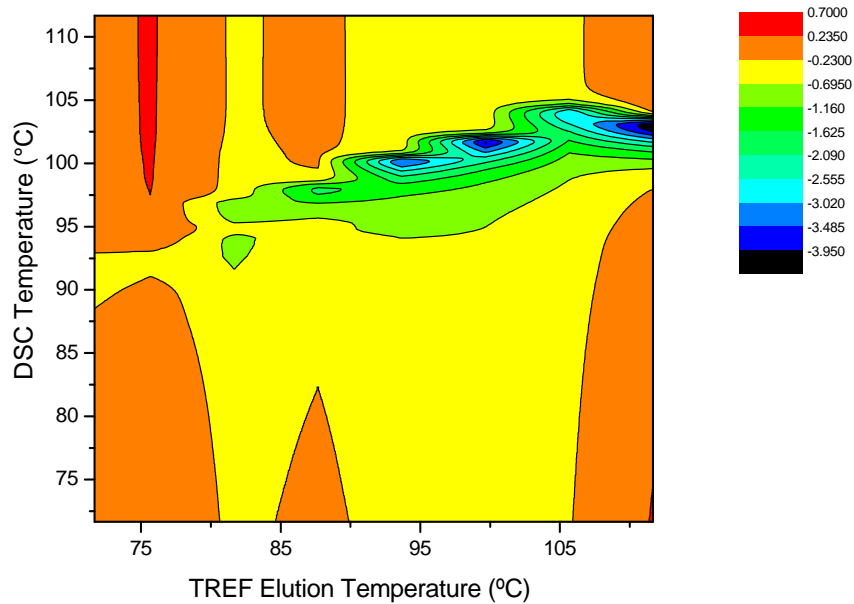

Figure 4.36 3D DSC-TREF for HDPE-LLDPE blend at isothermal profile B (DSC crystallization map).

By plotting Figure 4.35 in 3-D with TREF fractions it is possible to indicate much more clearly both the main melting peaks which correspond to HDPE and LLDPE, as now shown in Figure 4.36. Again it is noticed that by changing the profile we change the behaviour of the blend.

4.3.3.2 DSC results for the unfractionated polymers and fractionated blends from quench TREF

Figure 4.37 shows the DSC melting peaks for the unfractionated polymers and fractionated HDPE-LLDPE blend quench Prep-TREF traces at profile B.

On comparing this figure with Figure 4.32 we see that wide distribution curves are obtained and the presence of peaks associated with the middle fractions (65 ºC-75 ºC) in quench TREF. These may be due to crystalline linear chains at lower temperature because of co-crystallization behaviour.

Figure 4.38 displays 3D DSC-quench TREF for the HDPE-LLDPE blend. When we compare this figure with Figure 4.31 we can conclude that changing the profile will affect the crystallization temperature as well as the co-crystallization region.
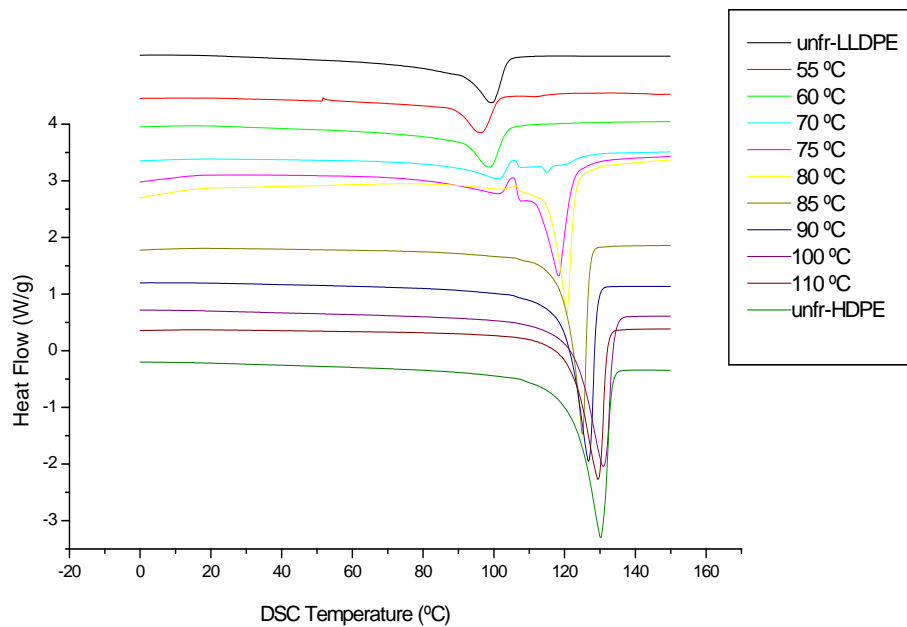

Figure 4.37 DSC melting peaks for the unfractionated polymers and fractionated HDPE-LLDPE blend, quench prep-TREF traces at profile B.
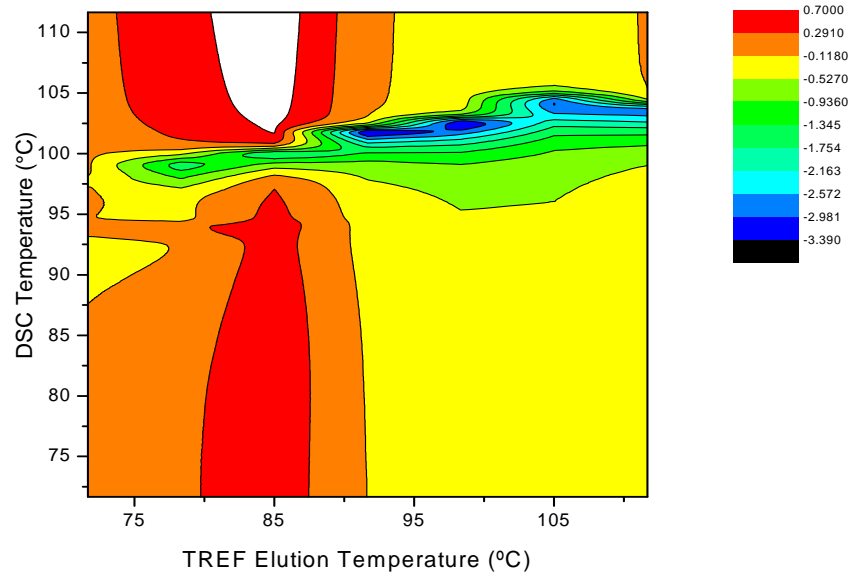
Figure 4.38 3D DSC-quench TREF for the HDPE-LLDPE blend at isothermal profile B (DSC crystallization map).

4.3.4 DSC results of the fractionated blends at profile C (first heating)

Figure 4.39 shows the DSC results for the fractionated HDPE-LLDPE blend - first heating, after cooling at a rate of 1 ℃ /h. Upon comparison of this figure to Figure 4.29 the results indicate that there is a clear change in the melting peaks, where this figure shows significant separation in the melting peak, especially at both fractions 75 ℃ and 80 ℃.

A similar result was found in the case of the HDPE-LDPE blend, as shown in Figure 4.40. There is a slight separation in the melting peak, especially at the middle fractions, and broadness in the melting peaks of fractions 75 ℃ and 80 ℃. However, it becomes very narrow as the temperature increases.
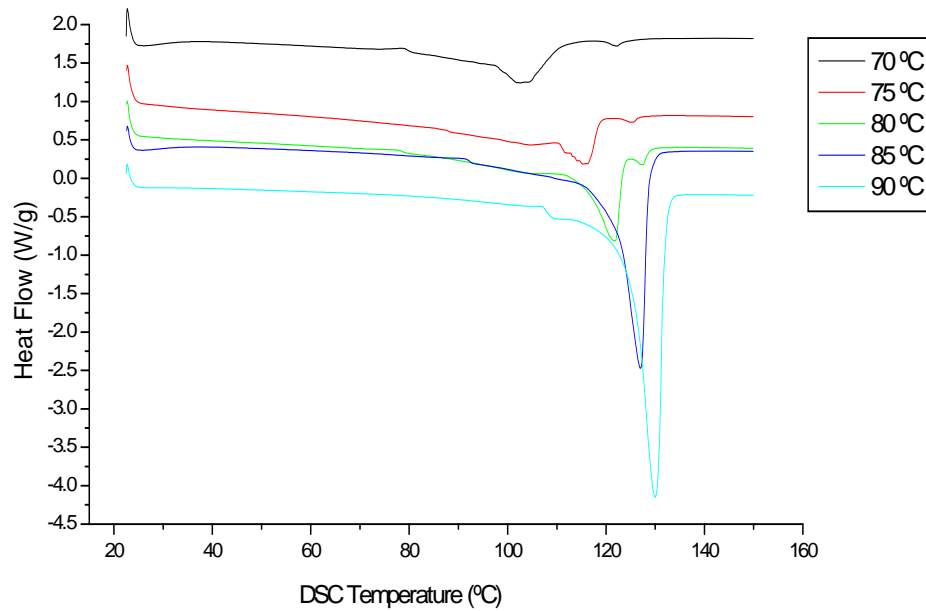
Figure 4.39 DSC for the fractionated HDPE-LLDPE blend at profile C (first heating).
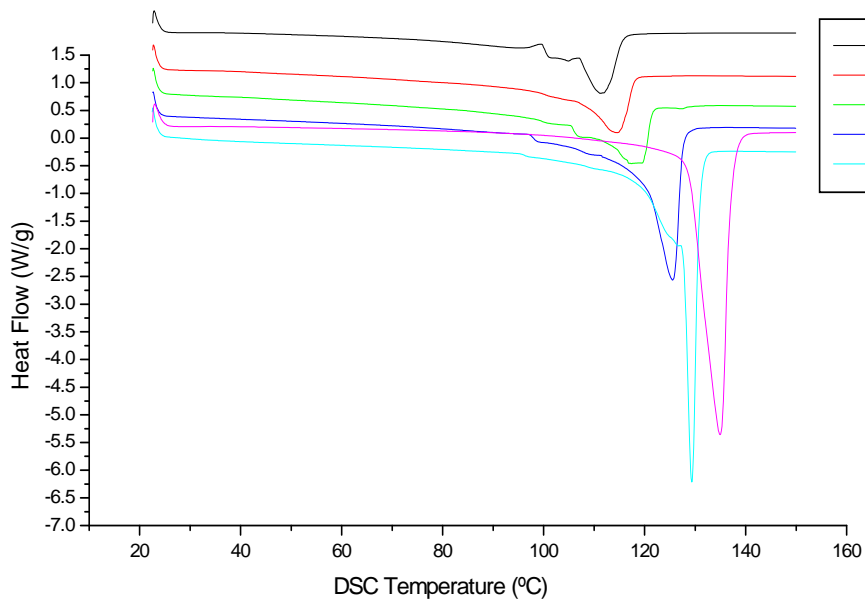
Figure 4.40 DSC for the fractionated HDPE-LDPE blend at profile C (first heating).

DSC results generally show an increase in the T_m(DSC melting peak maxima) with an increase in the prep-TREF fraction temperature. The results are, therefore, consistent with the presence of a relatively small degree of co-crystallization between the linear and the branched polyethylene that takes place in this interval of crystallization temperatures. This leads to broad melting (or

separation) peaks after the fractions are cooled at this very slow cooling rate since the individual compounds can crystallize on their own.

In order to investigate the effect of changing the profile on this co-crystallization phenomenon, Figures 4.41 and 4.42 are presented to show the effect of the profile on the those fractions. Figure 4.41 shows very clearly the effect of changing the profile on the 75 ºC fraction, where we can see a broad peak in the case of normal TREF at profile A. However as we change the profile to isothermal (profile B) we get a very clear separation for the melting peak.
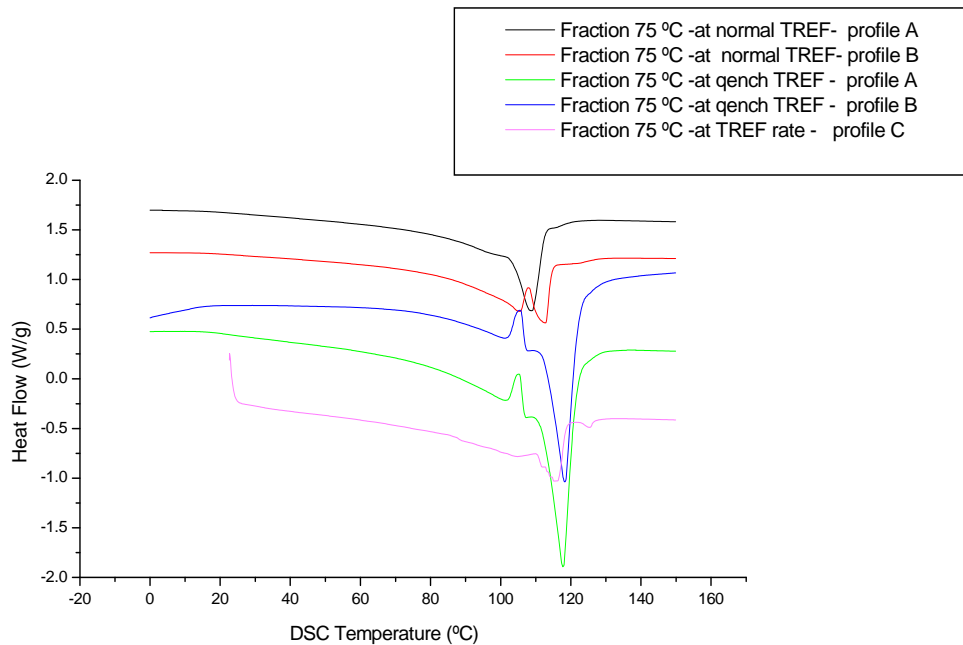
Figure 4.41 DSC for 75 ºC fraction of HDPE-LLDPE blend at different profiles.

A similar result was found in the case of the HDPE-LDPE blend, as shown in Figure 4.42; there is a narrow peak with a slight shoulder in the case of normal TREF at profile A, but the profile is changed to isothermal (profile B) we get a very clear separation with a very narrow melting peak. Also in the case of profile C we get a melting peak with a shoulder on the lower temperature side possibly due to separate crystallization of the components in this fraction.

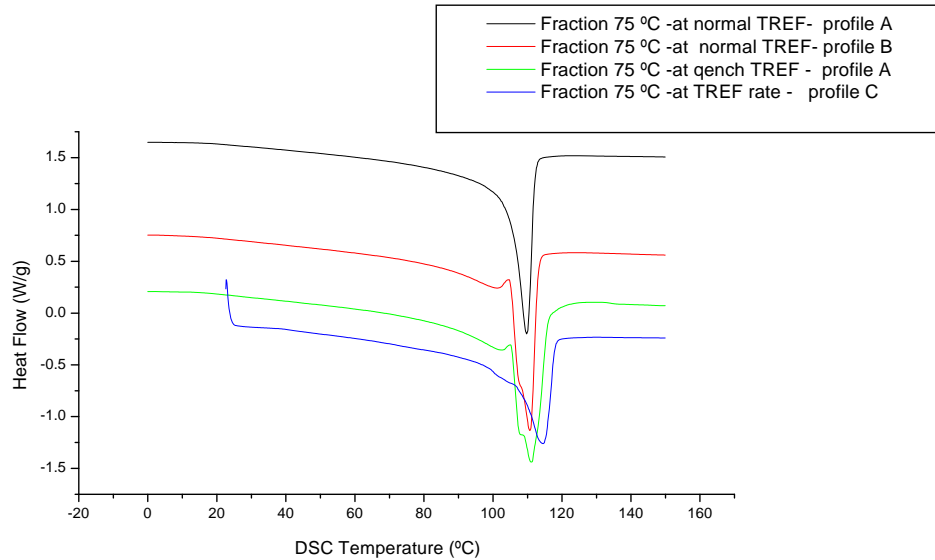**Figure 4.42 DSC for 75 ºC fraction of HDPE-LDPE blend at different profiles.**

4.3.5 DSC results for the unfractionated blends at profile D

Figure 4.43 presents DSC results for the unfractionated HDPE-LDPE blend at profile D. This profile is equivalent to the pre-TREF cooling profile where the polymer is crystallized out of solution as opposed to crystallization in the solid state as in profile C. There are clearly two melting peaks, at 100 ºC and 126 ºC respectively. The first peak corresponds to the melting temperature of LDPE (where the chains melt at lower temperature), because of a high amount of chain branching. The second peak corresponds to the melting temperature of HDPE. This figure shows understandable separation in the melting peaks, due to the crystallization period, where the chains have time to arrange and build the crystal structure.

Figure 4.44 shows DSC results for the unfractionated HDPE-LLDPE blend at profile D. The results indicate two melting peaks, at 109 ºC and 128 ºC respectively. The first peak corresponds to LLDPE and the second peak corresponds to HDPE.
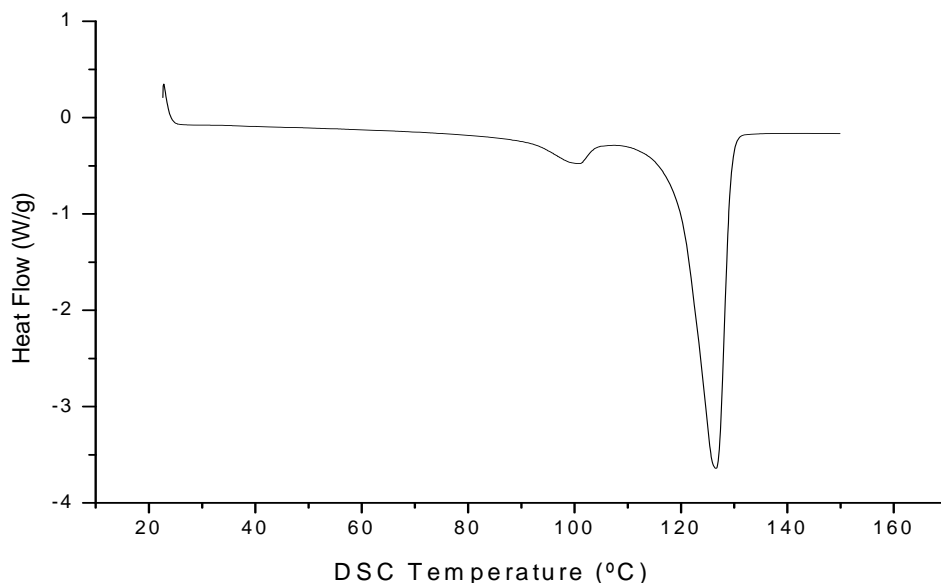
Figure 4.43 DSC for the unfractionated HDPE-LDPE blend at profile D (first heating).
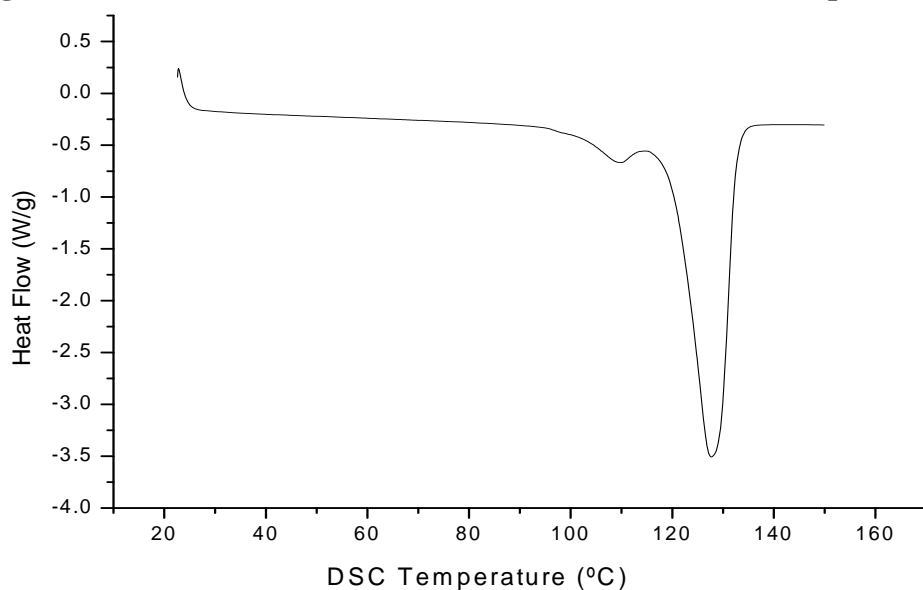
Figure 4.44 DSC for the unfractionated HDPE-LLDPE blend at profile D (first heating).

A comparison between DSC results for unfractionated HDPE-LLDPE at profile A and at profile D is shown in Figure 4.45. The figure illustrates that, evidently, by changing the profile and crystallization condition we can change the behaviour of the blend. There is just one melting peak for the blend in the case of profile A but two melting peaks in the case of profile D. This indicates that the chains have more time to organize in the second profile than in the first profile and

clearly shows the difference between crystallization out of solution (profile D) where the two components give separate peaks in the DSC melting curves and crystallization in the solid state where only one melt peak is observed.
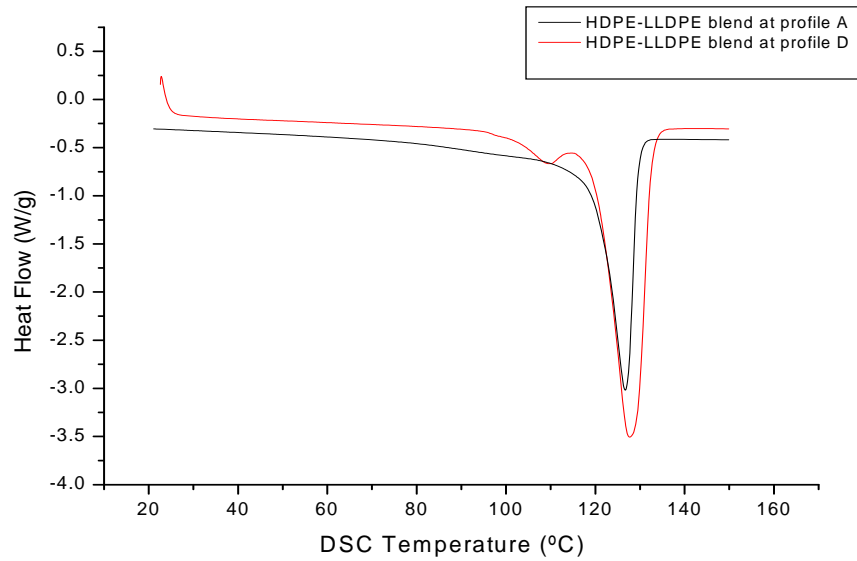
Figure 4.45 DSC results for unfractionated HDPE-LLDPE blend at profiles A and D.
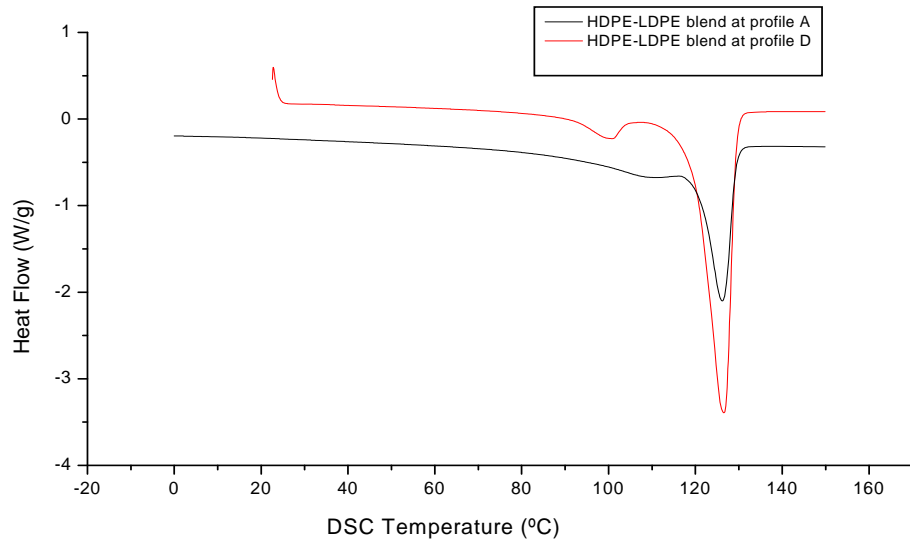
Figure 4.46 DSC results for unfractionated HDPE-LDPE blend at profiles A and D.

Similar results were found in the case of the HDPE-LDPE blend. Figure 4.46 shows just one melting peak for the blend in the case of profile A, however, it shows two melting peaks in the case of profile D.

4.4   References

1.   L. Britto, J. Soares and A. Penlidis. Journal of Polymer Science: Part B: Polymer Physics, 1999, 37, 553-560.

2.   C. Gabriela and D. Lilgeb. Polymer, 2001, 42, 297-303.

3.   J. Nieto, T. Oswald, G. Blanco and J. Soares. Journal of Polymer Science: Part B: Polymer Physics, 2001, 39, 1616-1628.

4.   S. Anantawaraskul, J. Soares and P. Wood-Adams. Journal of Polymer Science: Part B, 2003, 41, 1762-1778.

5.   F. Chiu, Q. Fu, Y. Peng and H. Shih. Journal of Polymer Science: Part B: Polymer Physics, 2002, 40, 325-337.

6.   A. Krumme, A. Lehtinen and A. Viikna. European Polymer Journal, 2004, 40, 371-378.

7.   S. Hosoda. Polymer, 1988, 20, 383.

8.   M. Mirabella. Journal of Applied Polymer Science, 2001, 39, 2819.

9.   J. Soares and A. Hamielec. Polymer 1995, 36, 1639-1654.

10.   R. Morgan, M. Hill and P. Barham. Polymer, 1999, 40, 337-348.

Chapter 5

Conclusions and recommendations

The co-crystallization in blends of linear and branched polyethylenes was studied under different crystallization conditions.

The main conclusions of this research are the following:

1) Preparative temperature rising elution fractionation was successfully used to fractionate several polyethylene blends, in order to isolate any potential co-crystallization fractions. Preparative fractionation of blends that were "quenched" was carried out in order to force co-crystallization. Each of the TREF fractions was studied using both DSC and CRYSTAF to determine whether the respective fractions contained both types of materials.

2) It was found that the combination of different crystallization analysis techniques formed a pair of valuable analytical tools that complement each other well in studying many areas of polymer crystallinty, where the understanding of polymer structure-property relationship is of central importance.

3) The morphology of polymer blends is dependent on crystallization conditions such as cooling rate and temperature profile.

4) Thermal studies contributed to a better understanding of the overall blend morphology.

5) The data could be presented in unique 3-dimensional plots, which clearly show the co-crystallization effect and give a "crystallization map" of the blends.

6) By varying the heating and cooling rate profiles in DSC the co-crystallization fractions appeared as a single fraction or as two separate fractions. It was also successfully demonstrated how the co-crystallization area can be illustrated using a 3-dimensional plot where the data from the prepTREF fractionation and the DSC and CRYSTAF are combined.

7) Changing the cooling rate of CRYSTAF has a significant effect on the crystallization temperature, as well as the broadness of the crystallization peaks. At the faster cooling rate the polymer appears to crystallize over a large temperature range, leading to peak broadening; this is due to less time for each polymer to crystallize at a different temperature. Significantly, results obtained with the blends used in this study showed that although the cooling rate affect the broadness of each of the peaks in the blend, these peaks still appear as separate peaks.

8) It has successfully been shown that by utilizing the difference in the crystallization fractionation mechanism between TREF, CRYSTAF and DSC, co-crystallization effects in polyolefin blends can be illustrated and studied.

Recommendations for future work

1) The techniques developed in this study could be applied to study co-crystallization effects in other polyolefin blends such as polypropylene and poly (propylene -1-pentene) copolymers.

2) Effects of co-crystallization in the absence of a support as apposed to crystallization onto support (as used in this study) in prep-TREF should be investigated as this may impact on the co-crystallization where there is non-nucleated versus nucleated crystallization.

Appendix A

The raw data of TREF fractions

Table A.1: Raw data of the LDPE obtained after TREF fractionation (profile A)

Temperature (ºC)	Mass (g)	W_i	W_i (%)	$\Sigma W_i\%$	ΔT (ºC)	$W_i\%/\Delta T$
35	0.11	0.06	5.59	5.59	35	-
40	0.03	0.02	1.55	7.13	5	0.31
50	0.06	0.03	3.24	10.37	10	0.32
55	0.04	0.02	2.01	12.37	5	0.40
60	0.07	0.03	3.45	15.82	5	0.69
65	0.18	0.08	8.46	24.27	5	1.69
70	0.22	0.11	10.61	34.87	5	2.12
75	0.47	0.22	21.99	56.86	5	4.40
80	0.49	0.23	23.23	80.09	5	4.65
85	0.19	0.09	8.84	88.93	5	1.77
90	0.05	0.03	2.46	91.38	5	0.49
100	0.18	0.08	8.22	99.60	10	0.82
110	0.01	0.01	0.41	100	10	0.04

Table A.2: Raw data of the LLDPE obtained after TREF fractionation (profile A)

Temperature (ºC)	Mass (g)	W_i	W_i (%)	$\Sigma W_i\%$	ΔT (ºC)	$W_i\%/\Delta T$
25	0.01	0.01	0.53	0.53	n/a	-
35	0.01	0.01	0.63	1.17	10	0.06
45	0.07	0.03	3.75	4.92	10	0.37
50	0.07	0.04	4.06	8.98	5	0.81
55	0.11	0.06	5.98	14.97	5	1.19
60	0.28	0.15	15.16	30.13	5	3.03
65	0.39	0.21	21.03	51.17	5	4.20
70	0.40	0.21	21.27	72.45	5	4.25
75	0.22	0.11	11.86	84.31	5	2.37
80	0.10	0.05	5.57	89.88	5	1.11
90	0.13	0.07	7.23	97.12	10	0.72
100	0.04	0.02	2.40	99.52	10	0.24
110	0.01	0.01	0.47	100	10	0.04

Table A.3: Raw data of the HDPE-LDPE blend obtained after TREF fractionation (profile A)

Temperature (ºC)	Mass (g)	W_i	W_i (%)	ΣW_i%	ΔT (ºC)	W_i%/ΔT
35	0.29	0.17	17.18	17.18	n/a	-
40	0.02	0.01	1.01	18.20	5	0.21
50	0.02	0.01	1.09	19.29	10	0.10
55	0.031	0.01	1.53	20.82	5	0.31
60	0.02	0.01	1.12	21.95	5	0.23
65	0.02	0.01	1.59	23.55	5	0.32
70	0.06	0.03	3.24	26.80	5	0.65
75	0.15	0.08	8.61	35.41	5	1.72
80	0.07	0.04	4.54	39.96	5	0.91
85	0.09	0.05	5.25	45.21	5	1.05
90	0.13	0.08	7.95	53.16	5	1.59
95	0.47	0.28	27.86	81.02	5	5.57
100	0.26	0.15	15.66	96.69	5	3.13
110	0.05	0.03	3.30	100	10	0.33

Table A.4: Raw data of the HDPE-LLDPE blend obtained after TREF fractionation (profile A)

Temperature (ºC)	Mass (g)	W_i	W_i (%)	ΣW_i%	ΔT (ºC)	W_i%/ΔT
30	0.10	0.08	7.60	7.61	30	-
40	0.02	0.01	1.11	8.72	10	0.11
45	0.01	0.01	0.55	9.27	5	0.14
50	0.01	0.01	0.68	9.95	5	0.48
55	0.07	0.02	2.39	12.35	5	1.34
60	0.09	0.08	6.72	19.06	5	1.18
65	0.07	0.06	5.88	24.95	5	1.38
70	0.08	0.07	6.90	31.85	5	1.14
75	0.07	0.06	5.68	37.53	5	1.06
80	0.09	0.05	5.29	42.82	5	0.22
85	0.10	0.01	1.13	43.95	5	1.71
90	0.11	0.09	8.57	52.52	5	4.51
100	0.54	0.45	45.05	97.57	10	0.24
110	0.03	0.03	2.43	100	10	0.11

Table A.5: Raw data of the LDPE-LLDPE blend obtained after TREF fractionation (profile A)

Temperature (ºC)	Mass (g)	W_i	W_i (%)	$\Sigma W_i\%$	ΔT (ºC)	$W_i\%/\Delta T$
25	0.01	0.01	0.74	0.74	n/a	-
35	0.01	0.01	0.04	0.79	10	0.01
45	0.05	0.02	2.55	3.35	10	0.25
50	0.05	0.02	2.57	5.92	5	0.51
55	0.10	0.05	5.10	11.03	5	1.02
60	0.20	0.10	10.13	21.17	5	2.02
65	0.33	0.16	16.49	37.66	5	3.29
70	0.27	0.13	13.52	51.19	5	2.70
75	0.27	0.13	13.75	64.94	5	2.75
80	0.29	0.14	14.41	79.35	5	2.88
85	0.18	0.09	9.07	88.43	5	1.81
90	0.18	0.09	9.10	97.53	5	1.82
100	0.03	0.01	1.95	99.49	10	0.19
110	0.01	0.01	0.50	100	10	0.05

Table A.6: Raw data of the HDPE-LDPE obtained after TREF fractionation (profile B)

Temperature (ºC)	Mass (g)	W_i	W_i (%)	$\Sigma W_i\%$	ΔT (ºC)	$W_i\%/\Delta T$
50	0.03	0.02	1.58	20.28	n/a	-
55	0.02	0.01	1.25	21.82	5	0.25
60	0.03	0.02	1.70	24.45	5	0.34
65	0.02	0.01	1.20	26.24	5	0.24
70	0.14	0.07	6.95	33.99	5	1.39
75	0.10	0.05	5.01	38.40	5	1.01
80	0.06	0.03	3.02	44.95	5	0.66
85	0.18	0.09	9.25	51.21	5	1.86
90	0.22	0.11	11.35	59.16	5	2.27
95	0.50	0.25	25.10	86.38	5	5.02
100	0.28	0.14	14.25	96.69	5	2.84
110	0.05	0.03	2.90	100	10	0.29

Table A.7: Raw data of the HDPE-LLDPE obtained after TREF fractionation (profile B)

Temperature (ºC)	Mass (g)	W_i	W_i (%)	$\Sigma W_i\%$	ΔT (ºC)	$W_i\%/\Delta T$
25	0.11	0.10	10.10	10.10	n/a	-
40	0.03	0.03	2.65	12.75	15	0.18
50	0.04	0.04	3.45	16.20	10	0.35
55	0.03	0.03	2.80	19.01	5	0.56
60	0.07	0.06	6.15	25.16	5	1.23
65	0.08	0.08	7.51	32.67	5	1.50
70	0.05	0.04	4.19	36.86	5	0.84
75	0.04	0.03	3.21	40.07	5	0.64
80	0.03	0.02	2.23	42.31	5	0.45
85	0.09	0.07	7.36	49.67	5	1.47
90	0.11	0.10	9.57	59.26	5	1.92
100	0.39	0.35	34.64	93.90	10	3.47
110	0.07	0.06	6.09	100	10	0.61

Table A.8: Raw data of the LDPE-LLDPE blend obtained after TREF fractionation (profile B)

Temperature (ºC)	Mass (g)	W_i	W_i (%)	$\Sigma W_i\%$	ΔT (ºC)	$W_i\%/\Delta T$
25	0.07	0.03	3.40	3.40	n/a	-
35	0.05	0.02	2.62	6.02	10	0.26
45	0.05	0.02	2.39	8.41	10	0.23
50	0.08	0.04	3.96	12.38	5	0.79
55	0.07	0.03	3.36	15.74	5	0.67
60	0.22	0.10	10.39	26.13	5	2.07
65	0.21	0.10	10.27	36.41	5	2.05
70	0.37	0.17	17.29	53.70	5	3.45
75	0.53	0.24	24.85	78.55	5	4.97
80	0.22	0.10	10.65	89.21	5	2.13
85	0.07	0.03	3.43	92.65	5	0.68
90	0.05	0.02	2.40	95.05	5	0.48
100	0.04	0.02	2.01	97.06	10	0.20
110	0.04	0.02	2.15	99.21	10	0.21
120	0.01	0.01	0.78	100	10	0.07

Appendix B

CRYSTAF traces
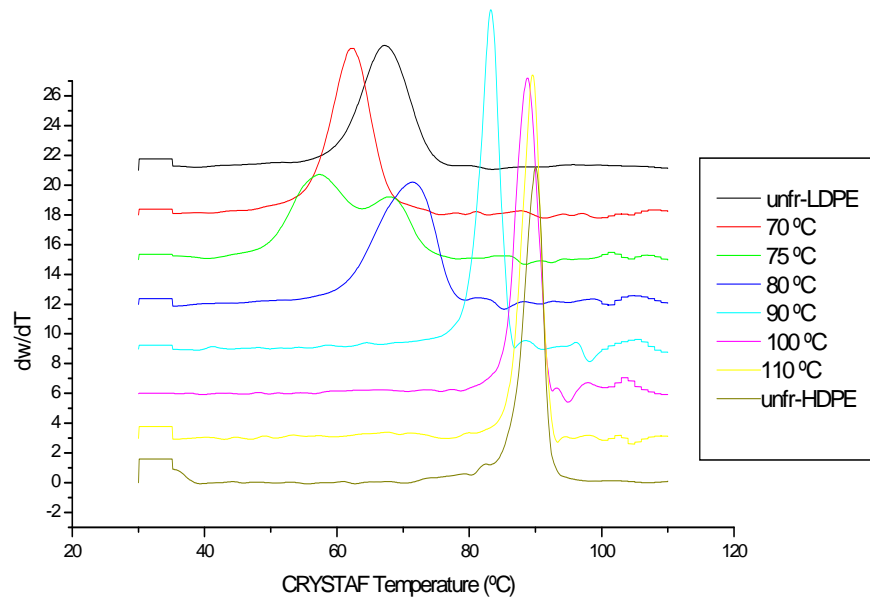
Figure B.1: The fractionated HDPE-LDPE blend CRYSTAF trace, and unfractionated HDPE and unfractionated LDPE CRYSTAF traces.
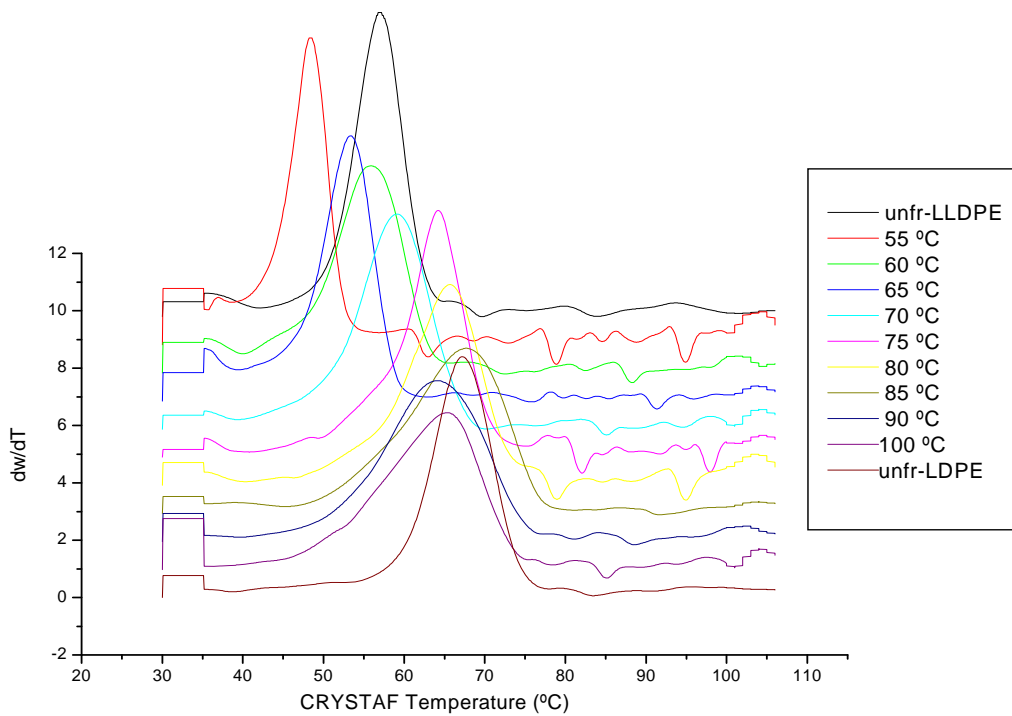

Figure B.2: The fractionated LDPE-LLDPE blend CRYSTAF trace, and unfractionated LLDPE and unfractionated LDPE CRYSTAF traces.
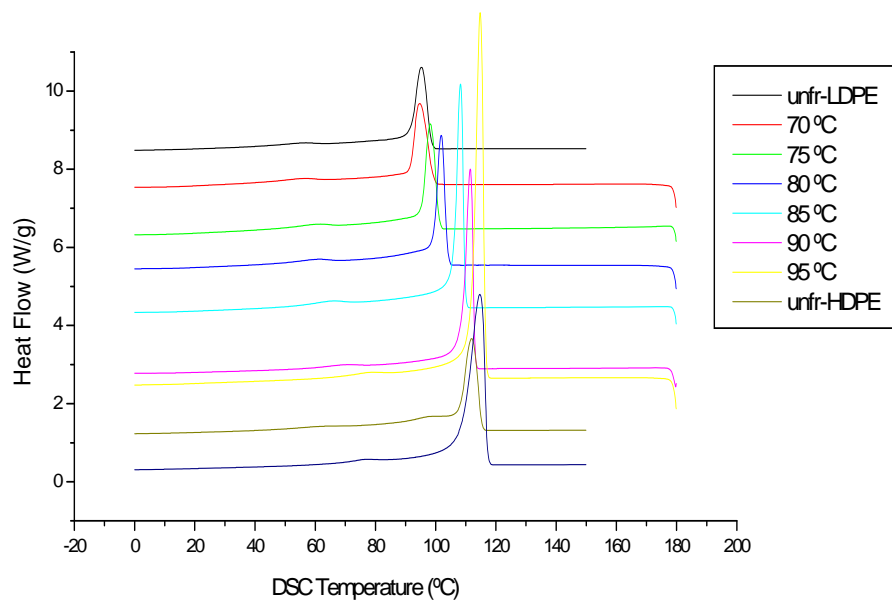
Appendix C

DSC curves

Figure C.1: DSC crystallization peaks for the unfractionated polymers and fractionated HDPE-LDPE blend, normal prep-TREF traces at profile A.
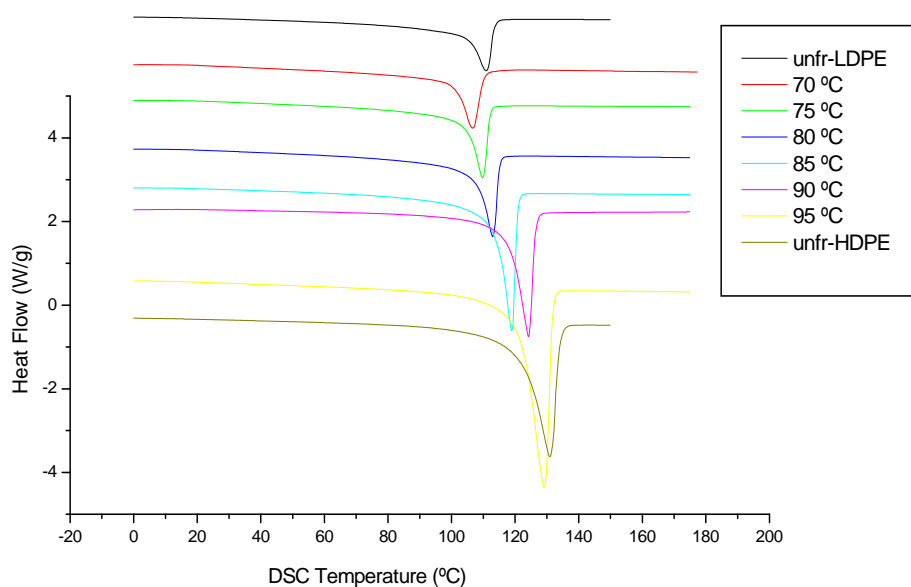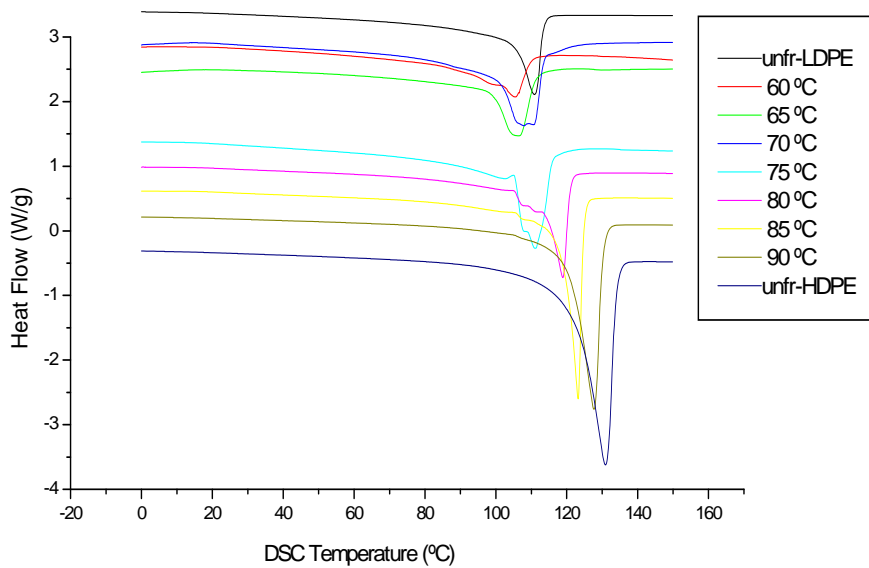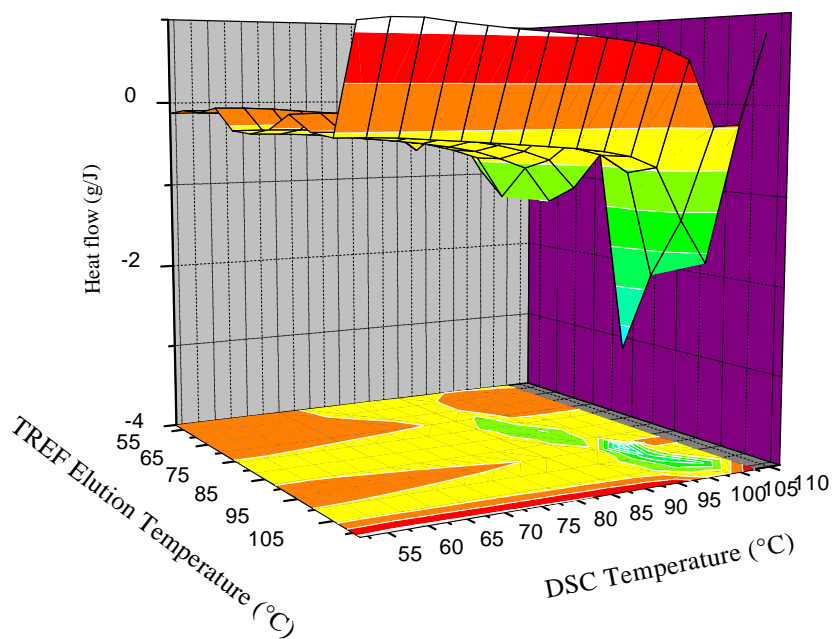

Figure C.2: DSC melting peaks for the unfractionated polymers and fractionated HDPE-LDPE blend, normal prep-TREF traces at profile A.

Figure C.3: DSC melting peaks for the unfractionated polymers and fractionated HDPE-LDPE blend, quench prep-TREF traces at profile A.

Figure C.4: 3D DSC-TREF for HDPE-LLDPE blend at slow cooling rate of 0.1 °C/h.
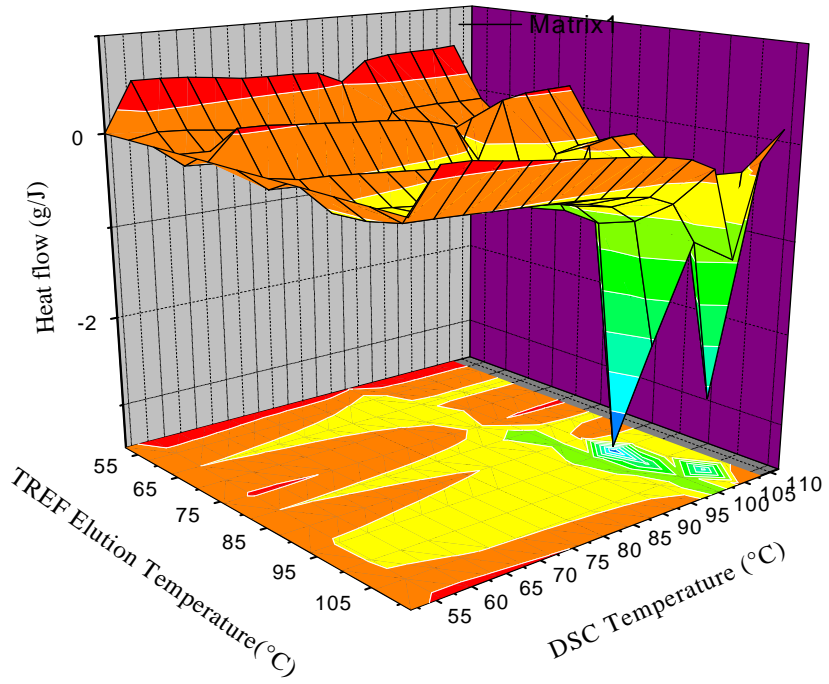
Figure C.5: 3D DSC-TREF for HDPE-LLDPE blend at isothermal profile B.
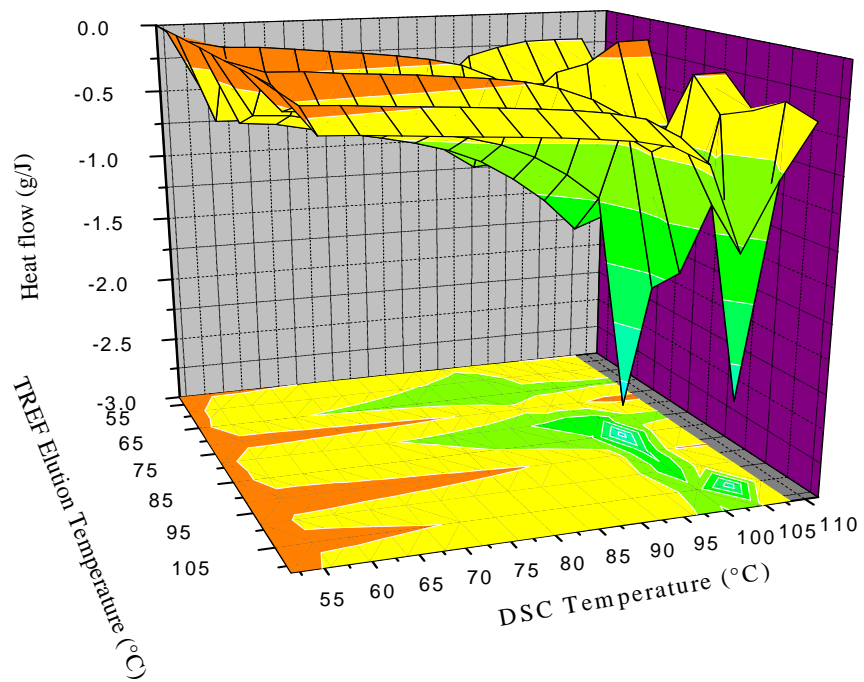
Figure C.6: 3D DSC-TREF for HDPE-LLDPE blend at quench cooling rate.
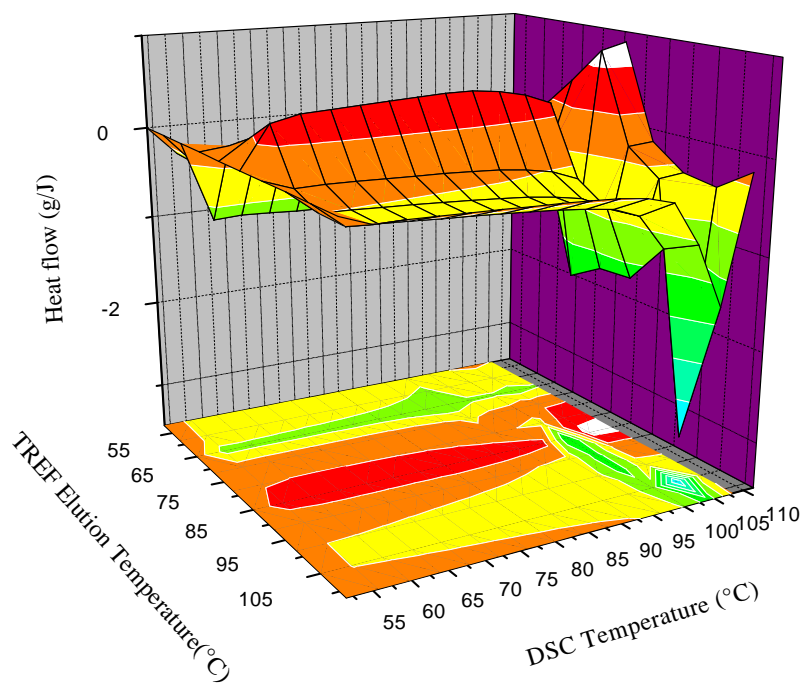
Figure C.7: 3D DSC-quench TREF for HDPE-LLDPE blend at isothermal profile B.

Appendix D

HT-SEC

Mn	Mw	PD
91364	278755	3.05104
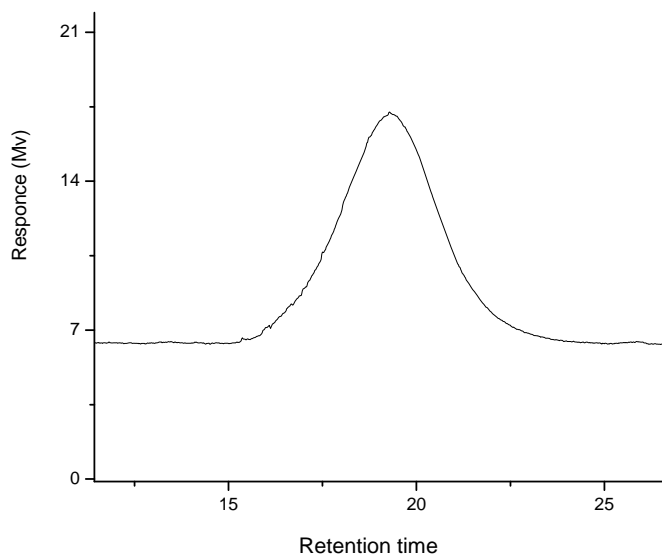
Figure D.1: The HT-SEC for the HDPE

Mn	Mw	PD
49473	236568	4.78176
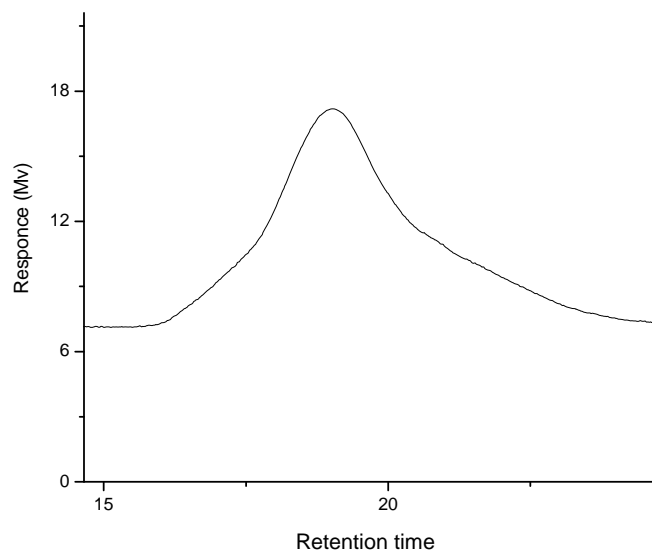
Figure D.2: The HT-SEC for the LDPE

Mn	Mw	PD
96721	196447	2.03107
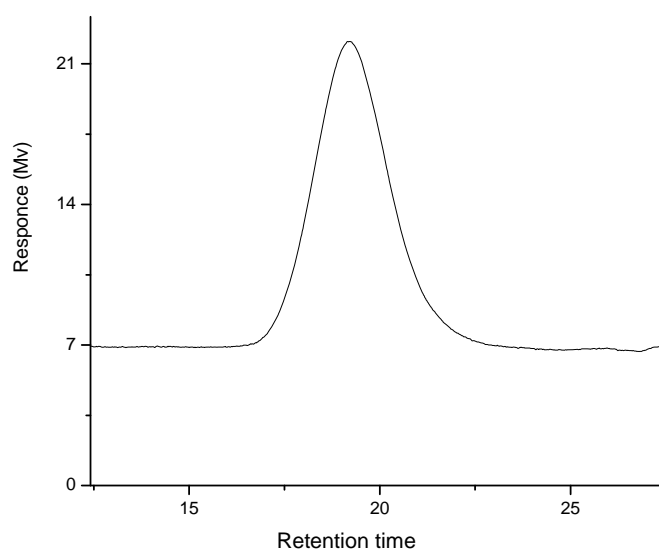
Figure D.3: The HT-SEC for the LLDPE

Appendix E

NMR
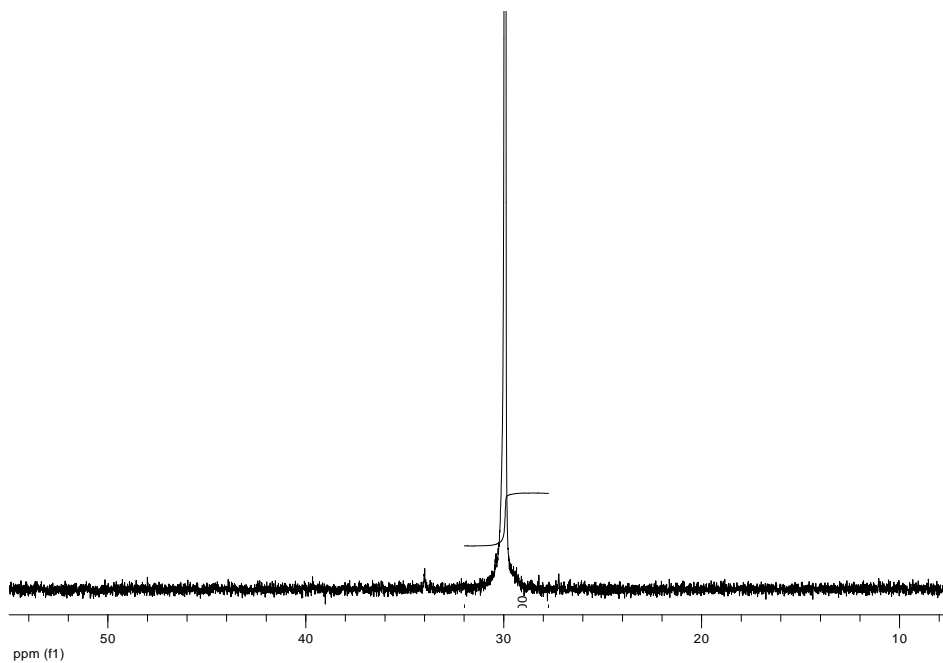
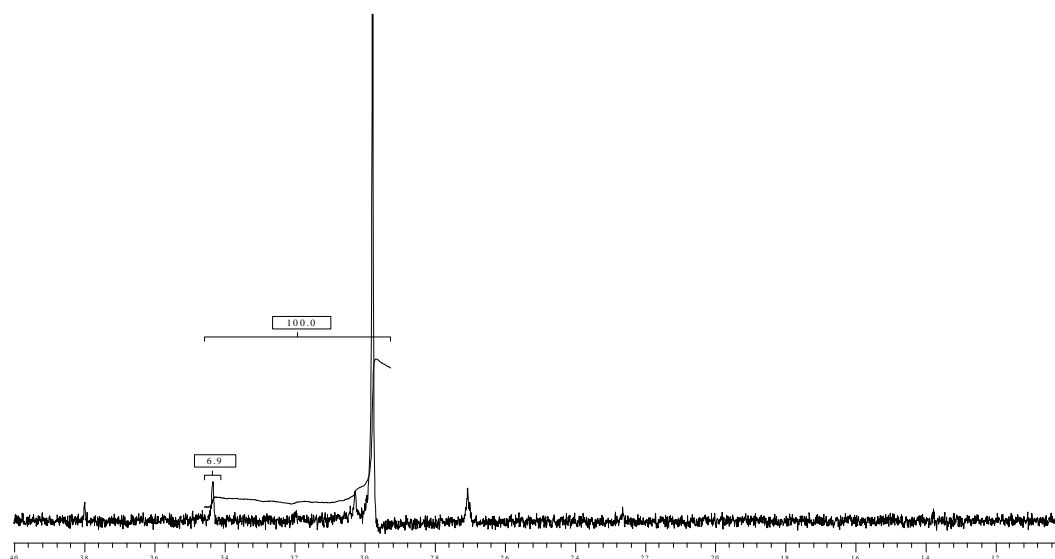**Figure E.1: The Carbon[13] NMR showing the unfractionated HDPE**
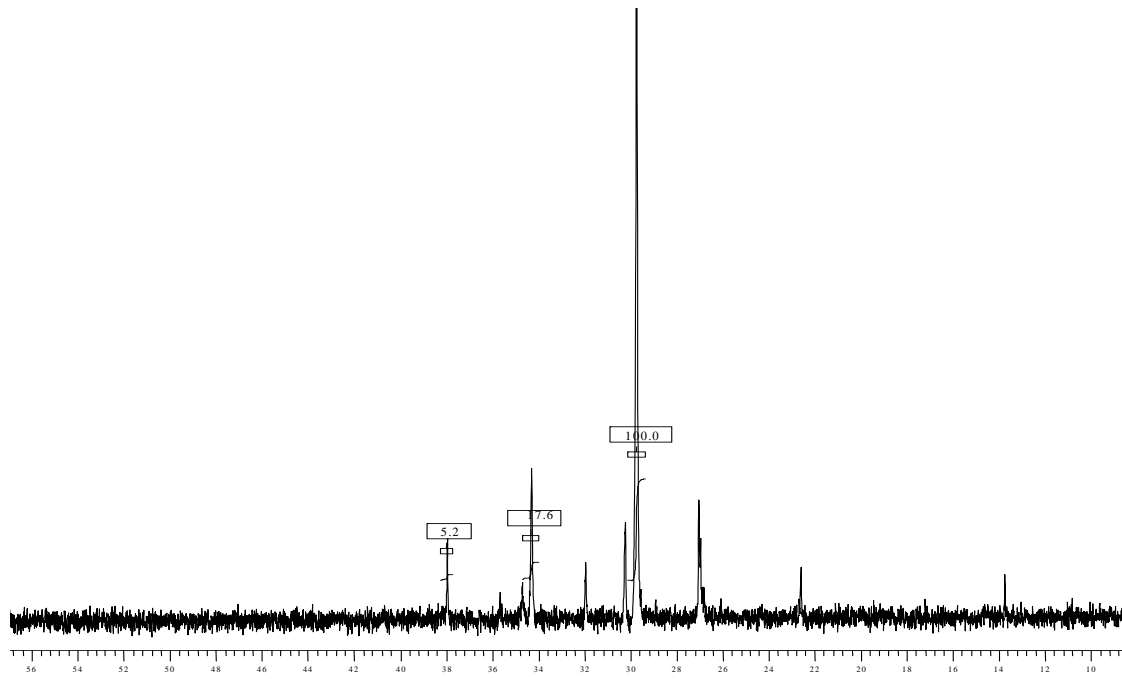

Figure E.2: The Carbon[13] NMR showing the unfractionated LDPE

Figure E.3: The C^{13} NMR for the unfractionated of LLDPE.